Modélisation du fonctionnement de la Prothèse Totale de Hanche Double Mobilité - Compréhension des comportements biomécanique et tribologique.

Bertrand Boyer

NNT : 2014 EMSE 0762

THÈSE

présentée par

Berrand BOYER

pour obtenir le grade de
Docteur de l'École Nationale Supérieure des Mines de Saint-Étienne

Spécialité : Sciences et Génie des Matériaux

Modélisation du fonctionnement de la Prothèse Totale de Hanche Double Mobilité - Compréhension des comportements biomécanique et tribologique.

soutenue à Saint-Etienne, le 30 octobre 2014

Membres du jury

Président :	Prénom NOM	Grade, Établissement, Ville
Rapporteurs :	Philippe Kapsa	Directeur de Recherche, Ecole Centrale Lyon, Ecully
	Michel-Henry Fessy	PU-PH, Hospices Civils de Lyon, Lyon
Examinateur(s) :	Dominique Saragaglia	PU-PH, CHU Grenoble, Grenoble
	Patrick Chabrand	Professeur, Université Aix-Marseille,
Directeur(s) de thèse :	Frédéric Farizon	PU-PH, CHU Saint-Etienne, Saint-Etienne
Co-Directeur de thèse	Jean Geringer	Maître Assistant, ENSM-SE, Saint-Etienne
Invité(s) éventuel(s):	Prénom NOM	Grade, Établissement, Ville

Spécialités doctorales :	Responsables :
SCIENCES ET GENIE DES MATERIAUX	K. Wolski Directeur de recherche
MECANIQUE ET INGENIERIE	S. Drapier, professeur
GENIE DES PROCEDES	F. Gruy, Maître de recherche
SCIENCES DE LA TERRE	B. Guy, Directeur de recherche
SCIENCES ET GENIE DE L'ENVIRONNEMENT	D. Graillot, Directeur de recherche
MATHEMATIQUES APPLIQUEES	O. Roustant, Maître-assistant
INFORMATIQUE	O. Boissier, Professeur
IMAGE, VISION, SIGNAL	JC. Pinoli, Professeur
GENIE INDUSTRIEL	A. Dolgui, Professeur
MICROELECTRONIQUE	

EMSE : Enseignants-chercheurs et chercheurs autorisés à diriger des thèses de doctorat (titulaires d'un doctorat d'État ou d'une HDR)

AVRIL	Stéphane	PR2	Mécanique et ingénierie	CIS
BATTON-HUBERT	Mireille	PR2	Sciences et génie de l'environnement	FAYOL
BENABEN	Patrick	PR1	Sciences et génie des matériaux	CMP
BERNACHE-ASSOLLANT	Didier	PR0	Génie des Procédés	CIS
BIGOT	Jean Pierre	MR(DR2)	Génie des Procédés	SPIN
BILAL	Essaid	DR	Sciences de la Terre	SPIN
BOISSIER	Olivier	PR1	Informatique	FAYOL
BORBELY	Andras	MR(DR2)	Sciences et génie de l'environnement	SMS
BOUCHER	Xavier	PR2	Génie Industriel	FAYOL
BRODHAG	Christian	DR	Sciences et génie de l'environnement	FAYOL
BURLAT	Patrick	PR2	Génie Industriel	FAYOL
COLLOT	Michel	PR0	Génie des Procédés	DIR
DARRIEULAT	Michel	IGM	Sciences et génie des matériaux	SMS
DAUZERE-PERES	Stéphane	PR1	Génie Industriel	CMP
DEBAYLE	Johan	CR	Image Vision Signal	CIS
DELAFOSSE	David	PR1	Sciences et génie des matériaux	SMS
DESRAYAUD	Christophe	PR2	Mécanique et ingénierie	SMS
DOLGUI	Alexandre	PR0	Génie Industriel	FAYOL
DRAPIER	Sylvain	PR1	Mécanique et ingénierie	SMS
FEILLET	Dominique	PR2	Génie Industriel	CMP
FOREST	Bernard	PR1	Sciences et génie des matériaux	CIS
FORMISYN	Pascal	PR0	Sciences et génie de l'environnement	DIR
FRACZKIEWICZ	Anna	DR	Sciences et génie des matériaux	SMS
GARCIA	Daniel	MR(DR2)	Génie des Procédés	SPIN
GERINCIER	Jean	MA(MDC)	Sciences et génie des matériaux	CIS
GIRARDOT	Jean-jacques	MR(DR2)	Informatique	FAYOL
GOEURIOT	Dominique	DR	Sciences et génie des matériaux	SMS
GRAILLOT	Didier	DR	Sciences et génie de l'environnement	SPIN
GROSSEAU	Philippe	DR	Génie des Procédés	SPIN
GRUY	Frédéric	PR1	Génie des Procédés	SPIN
GUY	Bernard	DR	Sciences de la Terre	SPIN
GUYONNET	René	DR	Génie des Procédés	SPIN
HAN	Woo-Suck	CR	Mécanique et ingénierie	SMS
HERRI	Jean Michel	PR1	Génie des Procédés	SPIN
INAL	Karim	PR2	Microélectronique	CMP
KERMOUCHE	Guillaume	PR2	Mécanique et Ingénierie	SMS
KLOCKER	Helmut	DR	Sciences et génie des matériaux	SMS
LAFOREST	Valérie	MR(DR2)	Sciences et génie de l'environnement	FAYOL
LERICHE	Rodolphe	CR	Mécanique et ingénierie	FAYOL
LI	Jean Michel		Microélectronique	CMP
MALLIARAS	Georges	PR1	Microélectronique	CMP
MOLIMARD	Jérôme	PR2	Mécanique et ingénierie	CIS
MONTHEILLET	Franck	DR	Sciences et génie des matériaux	SMS
PERIER-CAMBY	Laurent	PR2	Génie des Procédés	DFG
PIJOLAT	Christophe	PR0	Génie des Procédés	SPIN
PIJOLAT	Michèle	PR1	Génie des Procédés	SPIN
PINOLI	Jean Charles	PR0	Image Vision Signal	CIS
POURCHEZ	Jérémy	CR	Génie des Procédés	CIS
ROUSTANT	Olivier	MA(MDC)		FAYOL
STOLARZ	Jacques	CR	Sciences et génie des matériaux	SMS
SZAFNICKI	Konrad	MR(DR2)	Sciences et génie de l'environnement	CMP
TRIA	Assia		Microélectronique	CMP
VALDEVIESO	François	MA(MDC)	Sciences et génie des matériaux	SMS
VIRICELLE	Jean Paul	MR(DR2)	Génie des Procédés	SPIN
WOLSKI	Krzysztof	DR	Sciences et génie des matériaux	SMS
XIE	Xiaolan	PR1	Informatique	CIS

ENISE : Enseignants-chercheurs et chercheurs autorisés à diriger des thèses de doctorat (titulaires d'un doctorat d'État ou d'une HDR)

BERGHEAU	Jean-Michel	PU	Mécanique et Ingénierie	ENISE
BERTRAND	Philippe	MCF	Génie des procédés	ENISE
DUBUJET	Philippe	PU	Mécanique et Ingénierie	ENISE
FORTUNIER	Roland	PR	Sciences et Génie des matériaux	ENISE
GUSSAROV	Andrey	Enseignant contractuel	Génie des procédés	ENISE
HAMDI	Hédi	MCF	Mécanique et Ingénierie	ENISE
LYONNET	Patrick	PU	Mécanique et Ingénierie	ENISE
RECH	Joël	MCF	Mécanique et Ingénierie	ENISE
SMUROV	Igor	PU	Mécanique et Ingénierie	ENISE
TOSCANO	Rosario	MCF	Mécanique et Ingénierie	ENISE
ZAHOUANI	Hassan	PU	Mécanique et Ingénierie	ENISE

Mise à jour : 07/04/2013

PR 0	Professeur classe exceptionnelle
PR 1	Professeur 1ère classe
PR 2	Professeur 2ème classe
PU	Professeur des Universités
MA (MDC)	Maître assistant
DR	Directeur de recherche

Ing.	Ingénieur
MCF	Maître de conférences
MR (DR2)	Maître de recherche
CR	Chargé de recherche
EC	Enseignant-chercheur
IGM	Ingénieur général des mines

SMS	Sciences des Matériaux et des Structures
SPIN	Sciences des Processus Industriels et Naturels
FAYOL	Institut Henri Fayol
CMP	Centre de Microélectronique de Provence
CIS	Centre Ingénierie et Santé

NNT :

Bertrand BOYER

Modeling the functioning of Dual Mobility Total Hip Arthroplasty – Comprehension of biomechanical and tribological behaviors

Keywords : Dual Mobility, Total Hip Arthroplasty, Wear, Tribology, Intra Prosthetic Dislocation

Abstract :

Introduction: Dual Mobility Total Hip Arthroplasty (DM-THA) was invented by Professor Bousquet and André Rambert to combine the low wear of the concept of low friction from Charnley while providing the solution to the problem of dislocation of PTH. The concept has undergone several changes in almost forty years.

Ultra High Molecular Weight Polyethylene (UHMWPE) has some features that have been the subject of various studies and there are also other wear phenomena involved in the survival of the arthroplasty.

Dual Mobility has different components and indications are diverse.

A clinical long-term study of a PTH-DM first line has identified the benefits and failures of this concept. A specific complication is Intra Prosthetic Dislocation (IPD) or wear of the collar retaining the polyethylene liner. Different types of IPD can be encountered.

The main objective of our work was to understand the functioning of the Dual Mobility, that is to say, the respective roles of the two mobilities and retention and their wear profiles.

Secondary objectives were to understand the failures, loosening of the cup and intra-prosthetic dislocation and define an optimization of wear.

Material and Methods:

Several wear analysis techniques at different scales have been developed. Mechanical profilometry was used to study the surface roughness, the scanning electron microscopy researched the mechanisms of wear. Coordinate Measuring Machine Mapping (CMM) allowed us to understand the shape and waviness parameters. We suggested a new technique using a heat color scale to increase the qualitative analysis of wear. The finite element analysis would complete these means, which were applied to the explants from a library of more than 450 implants removed for various reasons. 3 groups of explants, formed by the liners having functioned for over 15 years without IPD, IPD and more recent liners, the design and material of the insert having been changed.

Results:

The three groups were compared. IPD has been identified as related to wear of the rim, with a threshold at 32%. This wear was mainly composed by the wear of the outer side of the rim, which was itself related to the properties of the neck of the femoral stem.

Explants over 15 years showed wear about 45 mm^3/year, which was at least comparable, if not lower, to standard Charnley-type metal on polyethylene implants. Standard wear analytical methods such as x-rays linear penetration rate could not be applied to the analysis of DM-THA.

The dimensions of the metal back and characteristics of the prosthetic femoral neck were the only factors affecting the incidence of IPD.

Discussion:

A schematic model of the functioning of DM-THA has been given based on the data of the explants. The second mobility, through its role as a reserve of mobility, reduces the overall wear and should be encouraged. The retentive rim is also a key point in the design and has a role in the implant survival.

The wear data were still incomplete and there will be further work to improve our work at the statistical level. Further investigations were defined to further the ultimate modeling goal for design optimization and expansion of the indications of DM-THA to a younger population.

NNT :

Bertrand BOYER

Modélisation du fonctionnement de la Prothèse Totale de Hanche Double Mobilité - Compréhension des comportements biomécanique et tribologique

Spécialité: Science et Génie des Matériaux

Mots clefs : Double Mobilité, Prothèse Totale de Hanche, usure, tribologie, Luxation Intra Prothétique

Résumé :

Introduction : La Prothèse Totale de Hanche Double Mobilité (PTH-DM) a été inventée par le Pr Bousquet et André Rambert pour conjuguer l'usure faible du concept de *low friction* de Charnley tout en proposant la solution au problème de la luxation de PTH. Le concept a fait l'objet de plusieurs modifications en presque quarante ans.

Le PolyEthylène à Ultra Haut Poids Moléculaire (UHMWPE) présente certaines caractéristiques qui ont fait l'objet d'études variées et il existe également d'autres phénomènes que l'usure jouant sur la survie d'une arthroplastie.

La Double Mobilité présente différentes composantes et ses indications sont diverses.

Une étude clinique à long terme d'une PTH-DM en première intention a permis de définir les avantages et échecs de ce concept. Une complication spécifique est la Luxation Intra Prothétique (LIP) ou usure de la collerette de rétention de l'insert en polyéthylène. Différentes formes peuvent être rencontrées.

L'objectif principal de notre travail était de comprendre le fonctionnement de la Double Mobilité, c'est-à-dire le rôle respectif des 2 mobilités et de la collerette ainsi que leurs profils d'usure.

Les objectifs secondaires étaient de comprendre les échecs, le descellement de cupule et la luxation intra-prothétique et de définir des pistes d'optimisation de l'usure.

Matériel et Méthodes :

Plusieurs techniques d'analyse d'usure, à différentes échelles ont été élaborées. La profilométrie mécanique permet d'étudier la rugosité de surface, la microscopie électronique à balayage recherche les mécanismes d'usure. La cartographie *Coordinate Measuring Machine* (CMM) permet d'appréhender les paramètres de forme et d'ondulation. Nous proposons une nouvelle technique de caractérisation par échelle de chaleur pour augmenter l'analyse qualitative de l'usure. L'analyse par éléments finis complète ces moyens, qui ont été appliquées sur des explants issus d'une banque de plus de 450 prothèses retirées pour des causes diverses. 3 groupes d'explants, constitués par les inserts ayant fonctionnés plus de 15 ans sans LIP, les inserts issus de LIP et les inserts récents, le dessin et le matériau de l'insert ayant été modifiés.

Résultats :

Les trois groupes ont été comparés. La LIP a pu être identifiée comme liée à l'usure de la collerette avec un seuil critique à 32 %. Cette usure est majoritairement composée par l'usure externe de la collerette, elle-même liée aux propriétés du col de la tige fémorale.

Les explants de plus de 15 ans ont présenté une usure d'environ 45 mm^3/an, ce qui est comparable aux implants standard à couple métal-polyéthylène de type Charnley. Les méthodes standard d'analyse d'usure radiographique ne peuvent pas être appliquées à l'analyse des PTH-DM.

Les dimensions de la cupule métallique et les caractéristiques du col fémoral prothétique étaient les seuls facteurs influant sur l'incidence de LIP.

Discussion :

Une ébauche de modélisation de fonctionnement de la PTH-DM a pu être proposée en se basant sur les données des explants. La deuxième mobilité, par son rôle de réserve de mobilité, permet de diminuer l'usure globale et doit être encouragée. La collerette de rétention constitue également un point clé du concept et possède un rôle dans la survie.

Les données d'usure étaient néanmoins incomplètes et feront l'objet de travaux ultérieurs pour en augmenter la valeur au niveau statistique. Des pistes de poursuite des investigations furent définies pour poursuivre l'objectif final étant la modélisation du fonctionnement permettant l'optimisation du concept et l'extension des indications à une population de plus en plus jeune.

Chapitre I. RESUME ETENDU

L'objectif de ce travail s'est axé sur le sujet de référence de l'équipe de Chirurgie Orthopédique et Traumatologie du CHU Saint-Etienne, dirigé par le Pr. Frédéric Farizon : la prothèse totale de hanche Double Mobilité.

Le concepteur de la Double Mobilité a été le Pr. Gilles Bousquet, chef de service au début des années 1970. Les inventeurs ont été Pr. G. Bousquet & M. A. Rambert. Le concept était à l'époque complètement révolutionnaire, *i.e*. en dehors des standards en vigueur auprès de la communauté des chirurgiens orthopédiques. Le développement du concept a ainsi été quasi exclusivement stéphanois jusqu'à la fin du brevet en 1996. Ce point est important car, en plus des problèmes de jeunesse de fabrication, il est un des éléments pour expliquer la durée nécessaire d'étude. Dans le domaine des implants orthopédiques, il est important de prendre conscience que l'appareil locomoteur peut être considéré comme un organe mécanique, sur le principe, mais l'influence du corps humain ne peut être occultée, avec tous les domaines scientifiques que cela implique : du comportement biologique à la corrosion des matériaux. Au début, l'idée de la prothèse Double Mobilité ne prenait pas en compte la complexité de la problématique.

Ainsi la démarche de recherche pourrait être traduite en une première question qui est celle d'ailleurs posée par les responsables des sociétés savantes américaines en orthopédie : comment la prothèse de Double Mobilité fonctionne-t-elle par rapport au *gold standard*, la prothèse de Charnley ? Il est proposé de répondre à cette question en détaillant chacun des points d'investigation entrepris dans ce travail de doctorat.

Six étapes majeures peuvent être extraites de ce travail, correspondant au plan :

1- Le suivi clinique, recul de 22 ans, de 240 prothèses de Double Mobilité et l'étude épidémiologique de 450 explants
2- La mesure de l'usure d'explants Double Mobilité, correspondance entre les données cliniques et les données tribologiques,
3- L'étude méthodologique critique des données d'usure et des faciès d'usure : expériences et modélisation,
4- Une nouvelle approche de la description de l'usure,

5- L'étude spécifique d'une complication du concept de double mobilité, la luxation intra-prothétique et ses données cliniques,
6- L'étude focalisée sur l'usure des explants double mobilité : influence du *design* de la collerette sur la luxation intra prothétique et l'usure.

Le document maître, ainsi que les articles, apporteront tous les détails. Dans ce document qui se veut suffisant pour la compréhension des points clefs, le lecteur trouvera les conclusions majeures mises en évidence dans les six points clefs décrits ci-dessus. Avant de décrire ces derniers, en préambule, un travail bibliographique spécifique a été mené sur le matériau constituant l'insert en polymère, *Ultra High Molecular Weight PolyEthylene* (UHMWPE), Figure 1.

Cet élément constitutif de la prothèse totale de hanche Double Mobilité est fabriqué en polymère. La maîtrise de la fabrication matériau est détaillée plus précisément dans ce document. La première étape est de fabriquer de longues chaînes de polymère, comme un plat de spaghettis, qui vont s'entremêler pour former un matériau solide. Les évolutions du processus de réticulation montrent qu'il y a toujours eu itération entre les propriétés physiques-mécaniques et tribologiques. Dans ce chapitre II.A, toutes les propriétés sont décrites. Il est intéressant de noter qu'elles ont été déterminées depuis moins d'une dizaine d'années (cristallinité et réticulation notamment). A l'heure actuelle, ce matériau basé sur l'UHMWPE offre des perspectives très encourageantes, en termes de constitution massive.

L'usure, quoiqu'il arrive, ne pourra pas être évitée étant donné que la durée de vie d'implantation augmente. Le polyethylène hautement réticulé est une voie intéressante. Cependant diminuer l'usure se fait aux dépens des propriétés mécaniques du polymère, qui dans le cas de la Double Mobilité peut être inacceptable. L'ajout de vitamine E est une perspective qui a été explorée depuis quelque temps, elle fait toujours l'objet de recherche. Il apparaît intéressant de noter que le type d'usure, comme certaines conditions spécifiques notamment l'*edge loading*, seraient à étudier spécifiquement. L'influence du *design* de l'insert est, dans cette problématique, un élément clef. Des investigations supplémentaires seront menées en collaboration avec le fabricant historique de l'insert Double Mobilité.

Figure 1 : Image avec un insert en UHMWPE et un *metal back* Novae®, www. Serf-dediennesante.com

Une étude bibliographique qui se veut exhaustive sur les presque 40 ans de développement de la cupule Double Mobilité est ensuite proposée. Le document propose un historique. Nous détaillerons dans ce paragraphe principalement l'ouverture à la communauté internationale. Le brevet de la société fondatrice est tombé dans le domaine public en 1996. Il est intéressant de noter que de nombreuses écoles ont testé ce type d'implants et la confrontation des résultats s'avère bénéfique car les méthodes de détermination du volume d'usure ont évolué dans le sens de la robustesse des résultats avec une étude comprenant l'incertitude de mesure.

Ce travail se situe donc dans cette perspective : améliorer la robustesse des résultats déjà obtenus avec une analyse critique et la focalisation sur des mécanismes d'endommagement particuliers de cet implant Double Mobilité.

1- Etude clinique à long terme d'un implant Double Mobilité (d'après Boyer et al, Primary THA with Dual Mobility socket to prevent dislocation - An average 22 year follow-up of 240 hips, Int Orthop 2012)

Cette étude clinique est basée sur 240 explants de prothèse totale de hanche double mobilité. Elle porte sur le couple tige PF™ et cupule/insert original, surnommé tripode (CHIM-3P). Du point de vue chirurgical, une étude épidémiologique complète a été menée : voies d'abord, score d'activité du patient, etc. Le premier résultat marquant est la courbe de survie. A 20 ans, la survie globale est de 74% avec un IC95 à 7%. Ce dernier chiffre s'avère tout à fait comparable aux prothèses « simple mobilité », standard, implantées depuis le début des années 1980. Le deuxième résultat est qu'aucune luxation n'a été constatée dans

cette série. Cette intuition du Pr. Gilles Bousquet se confirme grâce à cette étude. Il est intéressant de noter que la nuance de polyéthylène était du Cestilène®, pas encore les dernières nuances performantes d'UHMWPE. La perspective de cette étude réside dans l'indication d'une PTH Double Mobilité. Les résultats présentés dans cette étude montrent qu'une population de patients de plus de 65 ans s'avère la plus adéquate en termes d'efficacité. La pratique chirurgicale du service a fait évoluer l'indication de la pose de tels implants pour une population de plus de 50 ans, le taux de reprise n'étant pas plus élevé entre 50 et 65 ans. L'expérience chirurgicale s'avère confirmer ces premiers résultats expérimentaux. Il est à noter qu'il reste à comprendre la luxation intra-prothétique car cette occurrence se produit, pour cet implant typique et d'autres séries, à hauteur de 4 % environ. S'arrêter à ces conclusions n'est pas suffisant même si elles sont très encourageantes car les couples prothétiques datent des années 80 et les progrès n'ont pas cessé d'améliorer les performances.

> Etude épidémiologique de 450 explants et analyse dimensionnelle de la surface externe d'inserts de PTH à double mobilité (d'après 400 Dual Mobility Hip Retrievals: Research of risk factors for revision – A. Di Iorio, B. Boyer, J. Geringer, R. Philippot, F. Farizon – en cours)

Cette deuxième étude reprend le plan de la précédente. L'objectif a été d'étendre le nombre d'explants pour obtenir la plus grande et la plus significative série d'explants de Double Mobilité et une des séries de la littérature les plus conséquentes. Il est important de noter qu'en voulant augmenter la population, un premier biais est apparu : la combinaison des types de tige et de *design* d'insert, par exemple, s'est avéré un facteur de confusion important. Cette étude d'explants donne des résultats conformes à la science des matériaux et de la biomécanique, par exemple les tiges PRO associées aux *metal backs* Ti6Al4V au dessin et aux matériaux les plus délétères présentant un taux de Luxation Intra-Prothétique le plus important. Le facteur épidémiologique principal, statistiquement relié à une augmentation de la durée de vie des implants était le petit diamètre de tête, la Double Mobilité rejoignant ainsi la théorie de *low friction* de Charnley.

2- Développement de techniques d'analyse d'usure d'inserts Double Mobilité (d'après Understanding the Dual mobility concept for total hip arthroplasty. Investigations on a multiscale analysis - Highlighting the role of arthrofibrosis - J. Geringer, B. Boyer, F. Farizon dans Wear 2011)

Toutes les mesures du service, jusqu'en 2007, étaient basées sur des mesures radiologiques qui permettaient de déterminer une usure linéaire de l'insert. Sur le plan de la comparaison, il était possible de classer les différents types d'explants avec un coefficient de corrélation des données proches de 0,2, évidemment trop éloigné de 1. Le point 0 de cette étude a été basé sur les 450 explants cités dans la partie précédente. Le premier travail a consisté au tri des explants pour aboutir à ceux dont l'origine de l'explantation n'était que l'usure de l'insert. Finalement 12 explants ont été sélectionnés avec un 13ème qui a été un implant des années 1990 issu de la même série de fabrication des explants de cette étude. Ce dernier a servi de référence. Trois techniques expérimentales avaient été étudiées dans cette étude :

- La profilométrie 3D avec comme objectif de caractériser par des paramètres de rugosité les surfaces usées, presque 9 heures de mesures continues pour un explant ;
- La CMM, *Coordinate Measuring Machine*, pour avoir accès au volume d'usure ;
- La Microscopie Electronique à Balayage pour obtenir des informations qualitatives sur le type d'endommagement.

Il s'agissait de la première fois que de tels outils étaient utilisés pour l'analyse d'explants Double Mobilité. Cette méthode est maintenant utilisée en routine dans plusieurs laboratoires, spécifiquement le fameux HSS de New York.

Le taux d'usure, *i.e.* la quantité de matière totale enlevée, a été évaluée à environ 50 mm^3/an. Ce résultat a permis de répondre à la question qu'une grande partie de la communauté des chirurgiens orthopédiques se posait : est-ce-que deux surfaces qui frottent entraînent deux fois plus d'usure ? Pour certains il était acquis que l'usure était pénalisante pour cet implant double mobilité. En comparant avec des cupules simple mobilité, ce taux d'usure est comparable à quelques mm^3 près. Les paramètres de rugosité ont pu être mesurés de manière exhaustive et le résultat fondamental a été le choix des paramètres clef pour mettre en évidence spécifiquement les zones usées. Des bandes caractéristiques ont

ainsi été mises en évidence permettant de comprendre le fonctionnement de la cupule double mobilité in vivo. A 45° environ, en partant du pôle de chacune des cupules, se trouve la bande usée. Elle correspond à l'application de la charge cyclique durant la marche humaine. Le cupule est inclinée et tourne sur elle-même. Ce résultat a été vérifié dans le cadre d'un essai de simulateur de marche avec une cupule Double Mobilité. Les *metal back* en titane ont été étudiés et mettent en évidence un blocage de la seconde mobilité. Il est intéressant de noter que ce métal a été proscrit car ses performances tribologiques sont mauvaises et dans le but de diminuer les débris d'usure il a été supprimé dans toutes parties frottantes d'une prothèse totale de hanche. Il se trouve ainsi que dans le cadre de la prothèse Double Mobilité, probablement par des phénomènes d'adhérence, le *metal back* en titane bloque la seconde mobilité, ce qui présente un désavantage en termes de cône de mobilité, principal avantage mis en avant par rapport à la simple mobilité. Cependant de nombreuses limites ont été mises en évidence dans l'utilisation des méthodes qualitatives, profilométrie 3D mécanique, et quantitatives, CMM.

3- Comparaison de différentes mesures de type qualitatives, profilométrie 3D, et quantitatives, mesure de forme à 3 dimensions (d'après Wear analysis of hip explants, dual mobility concept : Comparison of quantitative and qualitative analyses Proc IMechE Part J : J Engineering Tribology 226(10) 838-853 et Computational Modeling of Biomechanics and Biotribology in the Musculoskeletal- Computational modeling of hip implants Ed. Zhongmin Jin, Woodhead publishing series in Biomaterials, pp. 389-416)

Cette partie vise à répondre à la question : quelle est la meilleure méthode d'imagerie de surface, profilométrie 3D mécanique ou optique, pour obtenir les paramètres de rugosité les plus pertinents pour mettre en avant les zones usées sur les explants de cupule double mobilité ? La deuxième interrogation concerne la méthode de traitement des données issues de la CMM. De nombreux algorithmes peuvent être utilisés et l'objectif est le choix de celui qui présente les résultats les plus robustes. De plus la troisième question relève de l'opportunité d'utiliser la modélisation par éléments finis. Comme présenté dans le

manuscrit complet le choix de la méthode d'imagerie de surface ne s'est pas conclu par un choix ferme et définitif. Les deux techniques ont leur point fort et leur faiblesse. Il se trouve que le profilomètre mécanique présente des avantages lorsque la zone de matériau usée est très endommagée. Certains laboratoires de tribologie ont choisi d'utiliser les deux techniques et il semble, d'après cette étude, que ce choix s'avère le plus judicieux. Ensuite le post traitement des mesures de CMM s'avère un point important pour déterminer les valeurs les plus justes. Cinq algorithmes de traitement ont été testés pour aboutir à un '*home made*' qui n'est pas celui utilisé en routine avec un logiciel répandu dans l'industrie, Méthode 1a. Ce travail sur les méthodes de mesure a permis de trouver des paramètres de rugosité et des mesures de volume d'usure les plus robustes, dans la mesure du possible. Au final les paramètres de rugosité permettent d'établir la cartographie des zones usées et les mesures de CMM de se rendre compte du volume d'usure des éléments prothétiques en UHMWPE, i.e. l'insert.

Les travaux de modélisation ont été abordés dans la cadre de cet assemblage spécifique qu'est la prothèse totale de hanche double mobilité. Les questions de design et de convergence, à partir du code d'éléments finis Abaqus®, ont été abordées pour trouver les conditions les plus stables. Le résultat principal a été la répartition des contraintes lors de l'application du maximum de la force normale durant la marche. Cet endroit correspond au placement de la bande d'usure isolée dans la deuxième partie. La notion d'asphéricité a été abordée sur la répartition des contraintes. Un léger bénéfice a été mis en évidence. Un écart subsiste néanmoins avec les objectifs initiaux. Il était prévu de pouvoir prédire, grâce au coefficient de frottement, les conditions de glissement entre la cupule double mobilité et la tête et le *metal back*. Malheureusement cet objectif n'a pas été atteint dans le cadre de ce travail. Au niveau de la méthode, les étapes clef ont été isolées mais les capacités de calcul n'ont pas été à disposition pour aboutir à des résultats exploitables.

4- Développement d'une technique d'analyse qualitative de l'usure de l'insert avec échelle de chaleur (d'après Understanding the Intra Prosthetic Dislocation in Dual Mobility Total Hip Arthroplasty - Explant wear patterns - B. Boyer, J. Geringer, R. Philippot, R. Ballas, F. Farizon - review en cours)

L'objectif de ce travail a été de créer une image 3D, munie d'un code couleur pour l'altitude, à partir des données brutes de CMM. Cette analyse de l'usure est une analyse qualitative et non plus quantitative. Elle a pour but de mettre en évidence des processus de fonctionnement, ou *patterns*. Cette analyse complète donc l'analyse quantitative classique qui a montré ses limites dans le point 2. Cette présentation pourrait conduire à la conclusion d'un travail très technique, certes de bon niveau, mais qui reste très appliqué. En plus de la mise en évidence très claire et très didactique de la bande d'usure externe, les premiers résultats ont montré que l'usure interne était différente suivant le type de *metal back*. Un effet mèche a été mis en évidence c'est-à-dire que la tête fémorale a creusé dans l'insert en polyéthylène suivant un effet qui a été nommé 'effet mèche' ou '*Drill Effect*'. Le point le plus important est le lien statistiquement fait entre le paramètre clinique qu'est la présence de fibrose articulaire et l'usure de la cupule Double Mobilité en raison de cet effet mèche de la tête dans l'insert. La Double Mobilité utilise un ROM, *Range of Motion*, ou cône de mobilité, plus important que la PTH simple mobilité. Il est important de noter que la population étudiée a été celle évoquée dans la partie III.I. Ce travail a été entrepris à la suite.

Les parties 5. Et 6. étaient particulièrement focalisées sur la complication observée cliniquement : la Luxation Intra-Prothétique. Ce travail est issu de discussions et de questions émanant de membres de la communauté des chirurgiens orthopédiques.

5- Définition des formes de Luxation Intra Prothétique et de ses causes (d'après Intra Prosthetic Dislocation, a specific complication of the Dual Mobility system, R. Philippot, B. Boyer, F. Farizon, Clinical Orthopedics and Related Research 2013)

La luxation intra prothétique, LIP, a été observée comme une complication spécifique de l'implant particulier double mobilité. 80 cas ont été isolés sur les 1960 arthroplasties effectuées dans le service entre 1985 et 1998. Trois classes de LIP ont pu être mises en évidence :

- type I : la grande articulation se trouve bloquée par des facteurs cliniques ;
- Type II : métallose importante ;
- Type III : l'usure de la rétentivité s'est produite et la réduction de la grande mobilité n'a pas été observée.

Deux facteurs ont été isolés statistiquement comme liés à une LIP : le jeune âge et la grande taille du *metal back*. Cette étude permet de définir les conditions épidémiologiques de survenue de la LIP. De plus il est important de noter le tryptique : matériau (type d'UHMWPE)-métal de la tête fémorale et *design* de la cupule et plus spécifiquement celui de la collerette de rétentivité. De nos jours, les efforts portent principalement sur le *design* de la cupule qui est fabricant dépendant. Après cette mise en évidence il apparaît que la rétentivité est bien un paramètre clef pour la luxation intra prothétique et ainsi la durée de vie globale de l'implant orthopédique Double Mobilité.

6- Luxations Intra-Prothétiques : Evaluation de l'usure de la rétention et de la part de celle-ci dans l'usure et le fonctionnement de l'insert dans sa globalité (d'après T.Neri, B. Boyer, A. Di Iorio, J. Geringer, R. Philippot, F. Farizon, en cours et 2 autres études en cours.

Le point de cette dernière partie se focalise sur le rôle de la rétentivité, *i.e.* la collerette, sur l'usure totale de l'insert en UHMWPE. L'usure a d'ailleurs été séparée en deux composantes : une interne et l'autre externe. Une corrélation existe entre l'usure totale de la collerette et le risque de faire une LIP. Le résultat le plus important est que lorsque la collerette est usée à plus de 32 % de son volume initial, le risque de faire une LIP est de 100 %. Le type d'usure a aussi une importance dans la luxation intra prothétique. Trois mécanismes ont pu être isolés dans ce cadre. Le premier correspond à une usure qualifiée harmonieuse, c'est-à-dire homogène sur toute la surface de cette dernière. Le deuxième cas correspond à un blocage de la grande mobilité dû à une ankylose ou une fibrose articulaire.

Dans ce cas l'effet mèche isolé et décrit dans la partie IV. était à l'origine d'une usure asymétrique. Dans ce cas, l'usure asymétrique peut être aussi due aux particules d'usure provenant de combinaison de matériaux spécifiques à chaque type d'implants, ce qui ne ressort pas de manière statistiquement significative. Le troisième type correspond à une LIP associée à un descellement aseptique. On soupçonne un effet des débris, ou effet troisième corps, sur l'usure de la collerette.

De façon à déterminer des facteurs influençant l'usure de la Double Mobilité et déterminer l'influence des modifications de l'insert sur l'usure, trois populations ont été définies. La première correspond à des explants de plus de 15 ans, la seconde correspond à la population de LIP, la troisième est une population d'inserts récents. La comparaison des 3 populations est encore en cours d'analyse. Cependant une mesure plus affinée de l'usure de l'insert a d'ores et déjà pu être déterminée. Le volume médian a été déterminé à 45 mm^3, ce qui est dans la fourchette basse de l'usure du couple métal-polyéthylène. Ce volume est composé pour moitié de l'usure interne, celle-ci étant souvent sphérique et multidirectionnelle, ce qui n'est pas le cas du concept de *low friction* de Charnley. Plusieurs études ayant confirmé que l'usure unidirectionnelle était la raison du succès de la prothèse de Charnley, il est probable que la réserve de mobilité offerte par la seconde mobilité explique les faibles volumes d'usure d'une configuration interne peu favorable.

L'autre moitié de l'usure globale est répartie entre l'usure externe et la rétention.

Pour conclure, ce résumé étendu risque de poser autant de questions qu'il n'apporte de réponses, signe que la démarche de recherche a porté ses fruits. Il est à noter que d'autres travaux ont déjà commencés à être abordés. Les inserts ont été modifiés au fil du temps. Le premier sujet correspond à l'étude de l'influence de la rétentivité sur l'usure. Le deuxième est relatif à l'influence du design de la collerette sur l'usure interne et externe.

A ce stade, les résultats ont été obtenus et le plus important devient l'évocation des perspectives à envisager à la suite de ce travail. Cinq domaines ont été isolés comme des points clef à envisager dans les années à venir :

- Les analyses d'usure sur les trois groupes d'explants seront affinées.
- L'idée de mesurer la répartition des contraintes lors d'un cycle de marche sur la cupule double mobilité est apparue au cours de ce travail de thèse. La concavité posait des problèmes importants techniques en 2009 mais, de nos jours, il apparaît possible d'effectuer des mesures correctement.

- Des premiers travaux ont été entrepris sur la cinématique de l'insert double mobilité, en direct, sur un simulateur de marche.
- Le développement de la méthode par éléments finis est aussi une piste sérieuse de perspectives.
- La poursuite du travail d'Ola Ahmad. Son travail de thèse visait à établir un modèle prédictif de l'usure d'un insert en UHMWPE à partir de mesures profilométriques. Ce travail pourra être consulté sur demande.
- La dernière perspective est l'optimisation des dessins pour éviter les problèmes de fonctionnement de cet implant double mobilité pour lequel les indications et le nombre de pays concernés ne vont qu'en croissant.

Chapitre II. **REMERCIEMENTS**

Nous souhaitons remercier dans le cadre de ce travail :

- L'ENISE : M. DURSAPT et H. ZAHOUANI
- La société SERF : F. BLION, M. DARMEDRU, P. MARMONNIER, C. MANIN, P. MOLLIER, S. MICHELON et J.-L. AURELLE
- L'Ecole Nationale Supérieure des Mines –Saint Etienne : C. DESRAYAUD
- Le laboratoire ABBOU, ayant permis les analyses Zfx: Messieurs ABBOU

Chapitre III. BIBLIOGRAPHIE

1. Charnley, J., Kamangar, A. & Longfield, M. D. The optimum size of prosthetic heads in relation to the wear of plastic sockets in total replacement of the hip. *Med. Biol. Eng.* **7,** 31–39 (1969).
2. Charnley, J. The long-term results of low-friction arthroplasty of the hip performed as a primary intervention. *J. Bone Joint Surg. Br.* **54,** 61–76 (1972).
3. Philippot, R., Camilleri, J. P., Boyer, B., Adam, P. & Farizon, F. The use of a dual-articulation acetabular cup system to prevent dislocation after primary total hip arthroplasty: analysis of 384 cases at a mean follow-up of 15 years. *Int. Orthop.* **33,** 927–932 (2009).
4. Bousquet, G. & Grammont, P. [Experimental study of the longevity of hip prostheses from the mechanical viewpoint]. *Acta Orthop. Belg.* **38 Suppl 1,** 123–143 (1972).

5. Schmalzried, T. P., Szuszczewicz, E. S., Akizuki, K. H., Petersen, T. D. & Amstutz, H. C. Factors correlating with long term survival of McKee-Farrar total hip prostheses. *Clin. Orthop.* S48–59 (1996).
6. Jäger, M., Küsswetter, W., Rütt, J., Ungethüm, M. & Burkhardt, R. [Losening of acetabular prosthesis with various methods of implantation used in cadaver-hipjoints (author's transl)]. *Z. Für Orthop. Ihre Grenzgeb.* **112,** 34–44 (1974).
7. Gómez-Barrena, E., Medel, F. & Puértolas, J. A. Polyethylene oxidation in total hip arthroplasty: evolution and new advances. *Open Orthop. J.* **3,** 115–120 (2009).
8. Lewis, G., Fencl, R. M., Carroll, M. & Collins, T. The relative influence of five variables on the in vitro wear rate of uncrosslinked UHMWPE acetabular cup liners. *Biomaterials* **24,** 1925–1935 (2003).
9. Edidin, A. A. *et al.* Plasticity-induced damage layer is a precursor to wear in radiation-cross-linked UHMWPE acetabular components for total hip replacement. Ultra-high-molecular-weight polyethylene. *J. Arthroplasty* **14,** 616–627 (1999).
10. Lewis, G. Properties of crosslinked ultra-high-molecular-weight polyethylene. *Biomaterials* **22,** 371–401 (2001).
11. Kurtz, S. M., Muratoglu, O. K., Evans, M. & Edidin, A. A. Advances in the processing, sterilization, and crosslinking of ultra-high molecular weight polyethylene for total joint arthroplasty. *Biomaterials* **20,** 1659–1688 (1999).
12. Huddleston, J. I., Harris, A. H. S., Atienza, C. A. & Woolson, S. T. Hylamer vs conventional polyethylene in primary total hip arthroplasty: a long-term case-control study of wear rates and osteolysis. *J. Arthroplasty* **25,** 203–207 (2010).
13. Ho, S. P., Joseph, P. F., Drews, M. J., Boland, T. & LaBerge, M. Experimental and numerical modeling of variable friction between nanoregions in coventional and crosslinked UHMWPE. *J. Biomech. Eng.* **126,** 111–119 (2004).
14. Gul, R. M. The effects of peroxide content on the wear behavior, microstructure and mechanical properties of peroxide crosslinked ultra-high molecular weight polyethylene used in total hip replacement. *J. Mater. Sci. Mater. Med.* **19,** 2427–2435 (2008).
15. Rimnac, C. & Pruitt, L. How do material properties influence wear and fracture mechanisms? *J. Am. Acad. Orthop. Surg.* **16 Suppl 1,** S94–100 (2008).
16. Gomoll, A., Wanich, T. & Bellare, A. J-integral fracture toughness and tearing modulus measurement of radiation cross-linked UHMWPE. *J. Orthop. Res.* **20,** 1152–1156 (2002).
17. Pruitt, L. A. Deformation, yielding, fracture and fatigue behavior of conventional and highly cross-linked ultra high molecular weight polyethylene. *Biomaterials* **26,** 905–915 (2005).
18. Bradford, L., Baker, D., Ries, M. D. & Pruitt, L. A. Fatigue crack propagation resistance of highly crosslinked polyethylene. *Clin. Orthop.* 68–72 (2004).
19. Ries, M. D. & Pruitt, L. Effect of cross-linking on the microstructure and mechanical properties of ultra-high molecular weight polyethylene. *Clin. Orthop.* **440,** 149 (2005).
20. Oral, E., Godleski-Beckos, C., Ghali, B. W., Lozynsky, A. J. & Muratoglu, O. K. Effect of cross-link density on the high pressure crystallization of UHMWPE. *J. Biomed. Mater. Res. B Appl. Biomater.* **90,** 720–729 (2009).
21. Muratoglu, O. K., Bragdon, C. R., O'connor, D. O., Jasty, M. & Harris, W. H. A novel method of cross-linking ultra-high-molecular-weight polyethylene to improve wear, reduce oxidation, and retain mechanical properties. Recipient of the 1999 HAP Paul Award. *J. Arthroplasty* **16,** 149 (2001).

22. Muratoglu, O. K. *et al.* Gradient crosslinking of UHMWPE using irradiation in molten state for total joint arthroplasty. *Biomaterials* **23,** 717–724 (2002).
23. Kurtz, S. M. *et al.* In vivo degradation of polyethylene liners after gamma sterilization in air. *J. Bone Joint Surg. Am.* **87,** 815–823 (2005).
24. Dumbleton, J. H., D'Antonio, J. A., Manley, M. T., Capello, W. N. & Wang, A. The basis for a second-generation highly cross-linked UHMWPE. *Clin. Orthop.* **453,** 265–271 (2006).
25. Barrack, R. L., Lavernia, C., Szuszczewicz, E. S. & Sawhney, J. Radiographic wear measurements in a cementless metal-backed modular cobalt-chromium acetabular component. *J. Arthroplasty* **16,** 820–828 (2001).
26. Devane, P. A., Horne, J. G., Martin, K., Coldham, G. & Krause, B. Three-dimensional polyethylene wear of a press-fit titanium prosthesis. Factors influencing generation of polyethylene debris. *J. Arthroplasty* **12,** 256–266 (1997).
27. Wu, J. S.-S., Hsu, S.-L. & Chen, J.-H. Evaluating the accuracy of wear formulae for acetabular cup liners. *Med. Biol. Eng. Comput.* **48,** 157–165 (2010).
28. Ilchmann, T., Mjöberg, B. & Wingstrand, H. Measurement accuracy in acetabular cup wear. Three retrospective methods compared with Roentgen stereophotogrammetry. *J. Arthroplasty* **10,** 636–642 (1995).
29. Ilchmann, T., Reimold, M. & Müller-Schauenburg, W. Estimation of the wear volume after total hip replacement. A simple access to geometrical concepts. *Med. Eng. Phys.* **30,** 373–379 (2008).
30. Chen, J.-H. & Shih-Shyn Wu, J. Measurement of polyethylene wear - a new three-dimensional methodology. *Comput. Methods Programs Biomed.* **68,** 117–127 (2002).
31. Beksaç, B., Salas, A., González Della Valle, A. & Salvati, E. A. Wear is reduced in THA performed with highly cross-linked polyethylene. *Clin. Orthop.* **467,** 1765–1772 (2009).
32. Bitsch, R. G., Loidolt, T., Heisel, C., Ball, S. & Schmalzried, T. P. Reduction of osteolysis with use of Marathon cross-linked polyethylene. A concise follow-up, at a minimum of five years, of a previous report. *J. Bone Joint Surg. Am.* **90,** 1487–1491 (2008).
33. Campbell, D. G., Field, J. R. & Callary, S. A. Second-generation Highly Cross-linked X3 Polyethylene Wear: A Preliminary Radiostereometric Analysis Study. *Clin. Orthop.* (2010). doi:10.1007/s11999-010-1259-y
34. Glyn-Jones, S. *et al.* Does highly cross-linked polyethylene wear less than conventional polyethylene in total hip arthroplasty? A double-blind, randomized, and controlled trial using roentgen stereophotogrammetric analysis. *J. Arthroplasty* **23,** 337–343 (2008).
35. Heisel, C., Silva, M. & Schmalzried, T. P. In vivo wear of bilateral total hip replacements: conventional versus crosslinked polyethylene. *Arch. Orthop. Trauma Surg.* **125,** 555–557 (2005).
36. Hopper, R. H., Young, A. M., Orishimo, K. F. & McAuley, J. P. Correlation between early and late wear rates in total hip arthroplasty with application to the performance of marathon cross-linked polyethylene liners. *J. Arthroplasty* **18,** 60–67 (2003).
37. McCalden, R. W. *et al.* Wear rate of highly cross-linked polyethylene in total hip arthroplasty. A randomized controlled trial. *J. Bone Joint Surg. Am.* **91,** 773–782 (2009).
38. Mu, Z., Tian, J., Wu, T., Yang, J. & Pei, F. A systematic review of radiological outcomes of highly cross-linked polyethylene versus conventional polyethylene in total hip arthroplasty. *Int. Orthop.* **33,** 599–604 (2009).

39. Shia, D. S., Clohisy, J. C., Schinsky, M. F., Martell, J. M. & Maloney, W. J. THA with highly cross-linked polyethylene in patients 50 years or younger. *Clin. Orthop.* **467,** 2059–2065 (2009).
40. Wroblewski, B. M., Siney, P. D. & Fleming, P. A. The principle of low frictional torque in the Charnley total hip replacement. *J. Bone Joint Surg. Br.* **91,** 855–858 (2009).
41. Maxian, T. A., Brown, T. D., Pedersen, D. R. & Callaghan, J. J. Adaptive finite element modeling of long-term polyethylene wear in total hip arthroplasty. *J. Orthop. Res. Off. Publ. Orthop. Res. Soc.* **14,** 668–675 (1996).
42. Maxian, T. A., Brown, T. D., Pedersen, D. R. & Callaghan, J. J. The Frank Stinchfield Award. 3-Dimensional sliding/contact computational simulation of total hip wear. *Clin. Orthop.* 41–50 (1996).
43. Lombardi, A. V. *et al.* An in vivo determination of total hip arthroplasty pistoning during activity. *J. Arthroplasty* **15,** 702–709 (2000).
44. Stewart, T., Tipper, J., Streicher, R., Ingham, E. & Fisher, J. Long-term wear of HIPed alumina on alumina bearings for THR under microseparation conditions. *J. Mater. Sci. Mater. Med.* **12,** 1053–1056 (2001).
45. Williams, S. *et al.* Wear and deformation of ceramic-on-polyethylene total hip replacements with joint laxity and swing phase microseparation. *Proc. Inst. Mech. Eng. [H]* **217,** 147–153 (2003).
46. Fialho, J. C., Fernandes, P. R., Eça, L. & Folgado, J. Computational hip joint simulator for wear and heat generation. *J. Biomech.* **40,** 2358–2366 (2007).
47. Affatato, S. *et al.* The performance of gamma- and EtO-sterilised UHMWPE acetabular cups tested under severe simulator conditions. Part 2: wear particle characteristics with isolation protocols. *Biomaterials* **24,** 4045–4055 (2003).
48. Affatato, S. *et al.* The predictive power of surface profile parameters on the amount of wear measured in vitro on metal-on-polyethylene artificial hip joints. *Proc. Inst. Mech. Eng. [H]* **220,** 457–464 (2006).
49. Affatato, S., Emiliani, D., Bersaglia, G., Traina, F. & Toni, A. An easy technique to digest and isolate UHMWPE wear particles from a hip joint simulator. *Int. J. Artif. Organs* **27,** 424–432 (2004).
50. Affatato, S. *et al.* Wear behaviour of cross-linked polyethylene assessed in vitro under severe conditions. *Biomaterials* **26,** 3259–3267 (2005).
51. Bragdon, C. R., Jasty, M., Muratoglu, O. K. & Harris, W. H. Third-body wear testing of a highly cross-linked acetabular liner: the effect of large femoral head size in the presence of particulate poly(methyl-methacrylate) debris. *J. Arthroplasty* **20,** 379–385 (2005).
52. Schneider, L., Philippot, R., Boyer, B. & Farizon, F. Revision total hip arthroplasty using a reconstruction cage device and a cemented dual mobility cup. *Orthop. Traumatol. Surg. Res.* **97,** 807–813 (2011).
53. Burroughs, B. R., Hallstrom, B., Golladay, G. J., Hoeffel, D. & Harris, W. H. Range of motion and stability in total hip arthroplasty with 28-, 32-, 38-, and 44-mm femoral head sizes. *J. Arthroplasty* **20,** 11–19 (2005).
54. Lachiewicz, P. F. & Watters, T. S. The Use of Dual-mobility Components in Total Hip Arthroplasty. *J. Am. Acad. Orthop. Surg.* **20,** 481–486 (2012).
55. Kelly, N. H., Rajadhyaksha, A. D., Wright, T. M., Maher, S. A. & Westrich, G. H. High stress conditions do not increase wear of thin highly crosslinked UHMWPE. *Clin. Orthop.* **468,** 418–423 (2010).

56. Bradford, L. *et al.* Wear and surface cracking in early retrieved highly cross-linked polyethylene acetabular liners. *J. Bone Joint Surg. Am.* **86-A,** 1271–1282 (2004).
57. Bourne, R. B., Barrack, R., Rorabeck, C. H., Salehi, A. & Good, V. Arthroplasty options for the young patient: Oxinium on cross-linked polyethylene. *Clin. Orthop.* **441,** 159–167 (2005).
58. Sakoda, H. *et al.* A comparison of the wear and physical properties of silane cross-linked polyethylene and ultra-high molecular weight polyethylene. *J. Arthroplasty* **16,** 1018–1023 (2001).
59. Simis, K. S., Bistolfi, A., Bellare, A. & Pruitt, L. A. The combined effects of crosslinking and high crystallinity on the microstructural and mechanical properties of ultra high molecular weight polyethylene. *Biomaterials* **27,** 1688–1694 (2006).
60. Teeter, M. G. *et al.* Regional measurements of surface deviation volume in worn polyethylene joint replacement components. *J. Long. Term Eff. Med. Implants* **20,** 49–56 (2010).
61. Teeter, M. G., Naudie, D. D. R., Charron, K. D. & Holdsworth, D. W. Highly cross-linked polyethylene acetabular liners retrieved four to five years after revision surgery: a report of two cases. *J. Mech. Behav. Biomed. Mater.* **3,** 464–469 (2010).
62. Birman, M. V., Noble, P. C., Conditt, M. A., Li, S. & Mathis, K. B. Cracking and impingement in ultra-high-molecular-weight polyethylene acetabular liners. *J. Arthroplasty* **20,** 87–92 (2005).
63. Scott, D. L., Campbell, P. A., McClung, C. D. & Schmalzried, T. P. Factors contributing to rapid wear and osteolysis in hips with modular acetabular bearings made of hylamer. *J. Arthroplasty* **15,** 35–46 (2000).
64. Berzins, A., Sumner, D. R. & Galante, J. O. Dimensional characteristics of uncomplicated autopsy-retrieved acetabular polyethylene liners by ultrasound. *J. Biomed. Mater. Res.* **39,** 120–129 (1998).
65. Bevill, S. L., Bevill, G. R., Penmetsa, J. R., Petrella, A. J. & Rullkoetter, P. J. Finite element simulation of early creep and wear in total hip arthroplasty. *J. Biomech.* **38,** 2365–2374 (2005).
66. Penmetsa, J. R., Laz, P. J., Petrella, A. J. & Rullkoetter, P. J. Influence of polyethylene creep behavior on wear in total hip arthroplasty. *J. Orthop. Res. Off. Publ. Orthop. Res. Soc.* **24,** 422–427 (2006).
67. Martell, J. M., Leopold, S. S. & Liu, X. The effect of joint loading on acetabular wear measurement in total hip arthroplasty. *J. Arthroplasty* **15,** 512–518 (2000).
68. Bennett, D. *et al.* Wear paths produced by individual hip-replacement patients--a large-scale, long-term follow-up study. *J. Biomech.* **41,** 2474–2482 (2008).
69. Bennett, D. *et al.* The influence of wear paths produced by hip replacement patients during normal walking on wear rates. *J. Orthop. Res. Off. Publ. Orthop. Res. Soc.* **26,** 1210–1217 (2008).
70. Davey, S. M., Orr, J. F., Buchanan, F. J., Nixon, J. R. & Bennett, D. The effect of patient gait on the material properties of UHMWPE in hip replacements. *Biomaterials* **26,** 4993–5001 (2005).
71. Kurtz, S. M., Ochoa, J. A., Hovey, C. B. & White, C. V. Simulation of initial frontside and backside wear rates in a modular acetabular component with multiple screw holes. *J. Biomech.* **32,** 967–976 (1999).

72. Akbari, A., Roy, M. E., Whiteside, L. A., Katerberg, B. J. & Schnettgoecke, D. J. Minimal Backside Surface Changes Observed in Retrieved Acetabular Liners. *J. Arthroplasty* (2010). doi:10.1016/j.arth.2010.07.012
73. Krieg, A. H., Speth, B. M. & Ochsner, P. E. Backside volumetric change in the polyethylene of uncemented acetabular components. *J. Bone Joint Surg. Br.* **91,** 1037–1043 (2009).
74. Romero, F., Amirouche, F., Aram, L. & Gonzalez, M. H. Experimental and analytical validation of a modular acetabular prosthesis in total hip arthroplasty. *J. Orthop. Surg.* **2,** 7 (2007).
75. Ong, K. L. *et al.* Biomechanical modeling of acetabular component polyethylene stresses, fracture risk, and wear rate following press-fit implantation. *J. Orthop. Res. Off. Publ. Orthop. Res. Soc.* **27,** 1467–1472 (2009).
76. Wang, Y., Dai, K. & Zhang, P. [Polyethylene wear in periprosthetic tissue of failed cemented total hip arthroplasties]. *Zhonghua Wai Ke Za Zhi* **35,** 459–461 (1997).
77. Coultrup, O. J., Hunt, C., Wroblewski, B. M. & Taylor, M. Computational assessment of the effect of polyethylene wear rate, mantle thickness, and porosity on the mechanical failure of the acetabular cement mantle. *J. Orthop. Res. Off. Publ. Orthop. Res. Soc.* **28,** 565–570 (2010).
78. Bhatt, H. & Goswami, T. Implant wear mechanisms--basic approach. *Biomed. Mater. Bristol Engl.* **3,** 042001 (2008).
79. Jaffe, W. L., Strauss, E. J., Cardinale, M., Herrera, L. & Kummer, F. J. Surface oxidized zirconium total hip arthroplasty head damage due to closed reduction effects on polyethylene wear. *J. Arthroplasty* **24,** 898–902 (2009).
80. Mimnaugh, K. D. *et al.* The effect of entrapped bone particles on the surface morphology and wear of polyethylene. *J. Arthroplasty* **24,** 303–309 (2009).
81. Greenbaum, E. S., Burroughs, B. B., Harris, W. H. & Muratoglu, O. K. Effect of lipid absorption on wear and compressive properties of unirradiated and highly crosslinked UHMWPE: an in vitro experimental model. *Biomaterials* **25,** 4479–4484 (2004).
82. Scholes, S. C. & Unsworth, A. The effects of proteins on the friction and lubrication of artificial joints. *Proc. Inst. Mech. Eng. [H]* **220,** 687–693 (2006).
83. Korhonen, R. K., Koistinen, A., Konttinen, Y. T., Santavirta, S. S. & Lappalainen, R. The effect of geometry and abduction angle on the stresses in cemented UHMWPE acetabular cups--finite element simulations and experimental tests. *Biomed. Eng. Online* **4,** 32 (2005).
84. Lombardi, A. V., Jr *et al.* An in vivo determination of total hip arthroplasty pistoning during activity. *J. Arthroplasty* **15,** 702–709 (2000).
85. Markel, D. C. *et al.* The effect of neutron radiation on conventional and highly cross-linked ultrahigh-molecular-weight polyethylene wear. *J. Arthroplasty* **23,** 732–735 (2008).
86. Kang, L., Galvin, A. L., Fisher, J. & Jin, Z. Enhanced computational prediction of polyethylene wear in hip joints by incorporating cross-shear and contact pressure in additional to load and sliding distance: effect of head diameter. *J. Biomech.* **42,** 912–918 (2009).
87. Matsoukas, G. & Kim, I. Y. Design optimization of a total hip prosthesis for wear reduction. *J. Biomech. Eng.* **131,** 051003 (2009).

88. Matsoukas, G., Willing, R. & Kim, I. Y. Total hip wear assessment: a comparison between computational and in vitro wear assessment techniques using ISO 14242 loading and kinematics. *J. Biomech. Eng.* **131,** 041011 (2009).
89. Goosen, J. H. M., Verheyen, C. C. P. M., Kollen, B. J. & Tulp, N. J. A. In vivo wear reduction of argon compared to air sterilized UHMW-polyethylene liners. *Arch. Orthop. Trauma Surg.* **129,** 879–885 (2009).
90. Hopper, R. H., Young, A. M., Orishimo, K. F. & Engh, C. A. Effect of terminal sterilization with gas plasma or gamma radiation on wear of polyethylene liners. *J. Bone Joint Surg. Am.* **85-A,** 464–468 (2003).
91. Viano, A. M. *et al.* Structural and chemical changes in ultra-high-molecular-weight polyethylene due to gamma radiation-induced crosslinking and annealing in air. *Biomed. Mater. Eng.* **17,** 257–268 (2007).
92. Kurtz, S. M., Dumbleton, J., Siskey, R. S., Wang, A. & Manley, M. Trace concentrations of vitamin E protect radiation crosslinked UHMWPE from oxidative degradation. *J. Biomed. Mater. Res. A* **90,** 549–563 (2009).
93. Kurtz, S. M. *et al.* Thermomechanical behavior of virgin and highly crosslinked ultra-high molecular weight polyethylene used in total joint replacements. *Biomaterials* **23,** 3681–3697 (2002).
94. Kurtz, S. M. *et al.* Mechanical properties, oxidation, and clinical performance of retrieved highly cross-linked Crossfire liners after intermediate-term implantation. *J. Arthroplasty* **25,** 614–623.e1–2 (2010).
95. Kurtz, S. M. *et al.* Degradation of mechanical properties of UHMWPE acetabular liners following long-term implantation. *J. Arthroplasty* **18,** 68–78 (2003).
96. Jacob, R. J. *et al.* Time- and depth-dependent changes in crosslinking and oxidation of shelf-aged polyethylene acetabular liners. *J. Biomed. Mater. Res.* **56,** 168–176 (2001).
97. Pezzotti, G. *et al.* Confocal Raman spectroscopic analysis of cross-linked ultra-high molecular weight polyethylene for application in artificial hip joints. *J. Biomed. Opt.* **12,** 014011 (2007).
98. Knahr, K., Pospischill, M., Köttig, P., Schneider, W. & Plenk, H. Retrieval analyses of highly cross-linked polyethylene acetabular liners four and five years after implantation. *J. Bone Joint Surg. Br.* **89,** 1036–1041 (2007).
99. Wannomae, K. K. *et al.* In vivo oxidation of retrieved cross-linked ultra-high-molecular-weight polyethylene acetabular components with residual free radicals. *J. Arthroplasty* **21,** 1005–1011 (2006).
100. Currier, B. H., Van Citters, D. W., Currier, J. H. & Collier, J. P. In vivo oxidation in remelted highly cross-linked retrievals. *J. Bone Joint Surg. Am.* **92,** 2409–2418 (2010).
101. Patten, E. W. *et al.* Delamination of a highly cross-linked polyethylene liner associated with titanium deposits on the cobalt-chromium modular femoral head following dislocation. *J. Bone Joint Surg. Br.* **92,** 1306–1311 (2010).
102. Oral, E., Christensen, S. D., Malhi, A. S., Wannomae, K. K. & Muratoglu, O. K. Wear resistance and mechanical properties of highly cross-linked, ultrahigh-molecular weight polyethylene doped with vitamin E. *J. Arthroplasty* **21,** 580–591 (2006).
103. Oral, E. & Muratoglu, O. K. Vitamin E diffused, highly crosslinked UHMWPE: a review. *Int. Orthop.* (2010). doi:10.1007/s00264-010-1161-y
104. Oral, E., Wannomae, K. K., Rowell, S. L. & Muratoglu, O. K. Diffusion of vitamin E in ultra-high molecular weight polyethylene. *Biomaterials* **28,** 5225–5237 (2007).

105. Oral, E., Wannomae, K. K., Rowell, S. L. & Muratoglu, O. K. Migration stability of alpha-tocopherol in irradiated UHMWPE. *Biomaterials* **27,** 2434–2439 (2006).
106. Renò, F. & Cannas, M. UHMWPE and vitamin E bioactivity: an emerging perspective. *Biomaterials* **27,** 3039–3043 (2006).
107. Smith, R. A., Maghsoodpour, A. & Hallab, N. J. In vivo response to cross-linked polyethylene and polycarbonate-urethane particles. *J. Biomed. Mater. Res. A* **93,** 227–234 (2010).
108. Kane, S. R., Ashby, P. D. & Pruitt, L. A. Characterization and tribology of PEG-like coatings on UHMWPE for total hip replacements. *J. Biomed. Mater. Res. A* **92,** 1500–1509 (2010).
109. Kyomoto, M. *et al.* Enhanced wear resistance of modified cross-linked polyethylene by grafting with poly(2-methacryloyloxyethyl phosphorylcholine). *J. Biomed. Mater. Res. A* **82,** 10–17 (2007).
110. Xie, X. L. *et al.* Wear performance of ultrahigh molecular weight polyethylene/quartz composites. *Biomaterials* **24,** 1889–1896 (2003).
111. Scott, M., Morrison, M., Mishra, S. R. & Jani, S. Particle analysis for the determination of UHMWPE wear. *J. Biomed. Mater. Res. B Appl. Biomater.* **73,** 325–337 (2005).
112. Zolotarevova, E. *et al.* Distribution of polyethylene wear particles and bone fragments in periprosthetic tissue around total hip joint replacements. *Acta Biomater.* **6,** 3595–3600 (2010).
113. Yue, H. *et al.* Particle size affects the cellular response in macrophages. *Eur. J. Pharm. Sci. Off. J. Eur. Fed. Pharm. Sci.* (2010). doi:10.1016/j.ejps.2010.09.006
114. Pokorný, D. *et al.* [New metod for quantification of UHMWPE wear particles around joint replacements]. *Acta Chir. Orthop. Traumatol. Cech.* **76,** 374–381 (2009).
115. Tipper, J. L. *et al.* Isolation and characterization of UHMWPE wear particles down to ten nanometers in size from in vitro hip and knee joint simulators. *J. Biomed. Mater. Res. A* **78,** 473–480 (2006).
116. Jasty, M. *et al.* Etiology of osteolysis around porous-coated cementless total hip arthroplasties. *Clin. Orthop.* 111–126 (1994).
117. Dumbleton, J. H., Manley, M. T. & Edidin, A. A. A literature review of the association between wear rate and osteolysis in total hip arthroplasty. *J. Arthroplasty* **17,** 649–661 (2002).
118. Restrepo, C. *et al.* Isolated polyethylene exchange versus acetabular revision for polyethylene wear. *Clin. Orthop.* **467,** 194–198 (2009).
119. Olivier, V., Duval, J. L., Hindié, M., Pouletaut, P. & Nagel, M. D. Comparative particle-induced cytotoxicity toward macrophages and fibroblasts. *Cell Biol. Toxicol.* **19,** 145–159 (2003).
120. Catelas, I. *et al.* Induction of macrophage apoptosis by ceramic and polyethylene particles in vitro. *Biomaterials* **20,** 625–630 (1999).
121. Sethi, R. K., Neavyn, M. J., Rubash, H. E. & Shanbhag, A. S. Macrophage response to cross-linked and conventional UHMWPE. *Biomaterials* **24,** 2561–2573 (2003).
122. Kaufman, A. M., Alabre, C. I., Rubash, H. E. & Shanbhag, A. S. Human macrophage response to UHMWPE, TiAlV, CoCr, and alumina particles: analysis of multiple cytokines using protein arrays. *J. Biomed. Mater. Res. A* **84,** 464–474 (2008).
123. Goodman, S. B. Wear particles, periprosthetic osteolysis and the immune system. *Biomaterials* **28,** 5044–5048 (2007).

124. Hatton, A., Nevelos, J. E., Matthews, J. B., Fisher, J. & Ingham, E. Effects of clinically relevant alumina ceramic wear particles on TNF-alpha production by human peripheral blood mononuclear phagocytes. *Biomaterials* **24,** 1193–1204 (2003).
125. Ingham, E. & Fisher, J. The role of macrophages in osteolysis of total joint replacement. *Biomaterials* **26,** 1271–1286 (2005).
126. Daniels, A. U., Barnes, F. H., Charlebois, S. J. & Smith, R. A. Macrophage cytokine response to particles and lipopolysaccharide in vitro. *J. Biomed. Mater. Res.* **49,** 469–478 (2000).
127. Baxter, R. M., Ianuzzi, A., Freeman, T. A., Kurtz, S. M. & Steinbeck, M. J. Distinct immunohistomorphologic changes in periprosthetic hip tissues from historical and highly crosslinked UHMWPE implant retrievals. *J. Biomed. Mater. Res. A* **95,** 68–78 (2010).
128. Endo, M. *et al.* Comparison of wear, wear debris and functional biological activity of moderately crosslinked and non-crosslinked polyethylenes in hip prostheses. *Proc. Inst. Mech. Eng. [H]* **216,** 111–122 (2002).
129. Péoc'h, M., Pasquier, D. & Pasquier, B. Polyethylene debris in lymph nodes. *J. Bone Joint Surg. Am.* **78,** 1784 (1996).
130. Mabrey, J. D. *et al.* Comparison of UHMWPE particles in synovial fluid and tissues from failed THA. *J. Biomed. Mater. Res.* **58,** 196–202 (2001).
131. Iwakiri, K. *et al.* In vivo comparison of wear particles between highly crosslinked polyethylene and conventional polyethylene in the same design of total knee arthroplasties. *J. Biomed. Mater. Res. B Appl. Biomater.* **91,** 799–804 (2009).
132. Sumner, D. R., Turner, T. M., Urban, R. M. & Galante, J. O. Experimental studies of bone remodeling in total hip arthroplasty. *Clin. Orthop.* 83–90 (1992).
133. Behrens, B.-A., Nolte, I., Wefstaedt, P., Stukenborg-Colsman, C. & Bouguecha, A. Numerical investigations on the strain-adaptive bone remodelling in the periprosthetic femur: influence of the boundary conditions. *Biomed. Eng. Online* **8,** 7 (2009).
134. Jonkers, I. *et al.* Relation between subject-specific hip joint loading, stress distribution in the proximal femur and bone mineral density changes after total hip replacement. *J. Biomech.* **41,** 3405–3413 (2008).
135. Lennon, A. B. *et al.* Predicting revision risk for aseptic loosening of femoral components in total hip arthroplasty in individual patients--a finite element study. *J. Orthop. Res. Off. Publ. Orthop. Res. Soc.* **25,** 779–788 (2007).
136. Boyer, B., Philippot, R., Geringer, J. & Farizon, F. Primary total hip arthroplasty with dual mobility socket to prevent dislocation: a 22-year follow-up of 240 hips. *Int. Orthop.* **36,** 511–518 (2012).
137. Tai, C.-L. *et al.* Finite element analysis of the cervico-trochanteric stemless femoral prosthesis. *Clin. Biomech. Bristol Avon* **18,** S53–58 (2003).
138. Yamada, H. *et al.* Cementless total hip replacement: past, present, and future. *J. Orthop. Sci. Off. J. Jpn. Orthop. Assoc.* **14,** 228–241 (2009).
139. Geringer, J., Boyer, B. & Farizon, F. Understanding the dual mobility concept for total hip arthroplasty. Investigations on a multiscale analysis-highlighting the role of arthrofibrosis. *Wear* **271,** 2379–2385 (2011).
140. Bryant, M. *et al.* Characterisation of the surface topography, tomography and chemistry of fretting corrosion product found on retrieved polished femoral stems. *J. Mech. Behav. Biomed. Mater.* **32,** 321–334 (2014).

141. Hara, K., Kaku, N., Tsumura, H. & Torisu, T. Analysis of wear and oxidation on retrieved bipolar polyethylene liner. *J. Orthop. Sci. Off. J. Jpn. Orthop. Assoc.* **13,** 366–370 (2008).
142. Nadzadi, M. E., Pedersen, D. R., Yack, H. J., Callaghan, J. J. & Brown, T. D. Kinematics, kinetics, and finite element analysis of commonplace maneuvers at risk for total hip dislocation. *J. Biomech.* **36,** 577–591 (2003).
143. Navarro, M., Michiardi, A., Castaño, O. & Planell, J. . Biomaterials in orthopaedics. *J R Soc Interface* **5,** 1137–1158 (2008).
144. Walter, W. L., Insley, G. M., Walter, W. K. & Tuke, M. A. Edge loading in third generation alumina ceramic-on-ceramic bearings: stripe wear. *J. Arthroplasty* **19,** 402–413 (2004).
145. Tower, S. S. *et al.* Rim cracking of the cross-linked longevity polyethylene acetabular liner after total hip arthroplasty. *J. Bone Joint Surg. Am.* **89,** 2212–2217 (2007).
146. Philippot, R., Adam, P., Farizon, F., Fessy, M. H. & Bousquet, G. [Survival of cementless dual mobility sockets: ten-year follow-up]. *Rev. Chir. Orthopédique Réparatrice Appar. Mot.* **92,** 326–331 (2006).
147. McKee, G. K. & Chen, S. C. The statistics of the McKee-Farrar method of total hip replacement. *Clin. Orthop.* 26–33 (1973).
148. Sudmann, E., Ramstad, K. R. & Engesæter, L. B. Christiansen's artificial hip joints--what went wrong? *Tidsskr. Den Nor. Lægeforen. Tidsskr. Prakt. Med. Ny Række* **133,** 2513–2518 (2013).
149. Farizon, F., de Lavison, R., Azoulai, J. J. & Bousquet, G. Results with a cementless alumina-coated cup with dual mobility. A twelve-year follow-up study. *Int. Orthop.* **22,** 219–224 (1998).
150. Aubriot, J. H., Lesimple, P. & Leclercq, S. [Study of Bousquet's non-cemented acetabular implant in 100 hybrid total hip prostheses (Charnley type cemented femoral component). Average 5-year follow-up]. *Acta Orthop. Belg.* **59 Suppl 1,** 267–271 (1993).
151. Kerboull, M., Hamadouche, M. & Kerboull, L. The Kerboull acetabular reinforcement device in major acetabular reconstructions. *Clin. Orthop.* 155–168 (2000).
152. Gill, T. J., Sledge, J. B. & Müller, M. E. The Bürch-Schneider anti-protrusio cage in revision total hip arthroplasty: indications, principles and long-term results. *J. Bone Joint Surg. Br.* **80,** 946–953 (1998).
153. Paprosky, W. G., Perona, P. G. & Lawrence, J. M. Acetabular defect classification and surgical reconstruction in revision arthroplasty. A 6-year follow-up evaluation. *J. Arthroplasty* **9,** 33–44 (1994).
154. Nevelos, J. *et al.* What Factors Affect Posterior Dislocation Distance in THA? *Clin. Orthop. Relat. Res.* **471,** 519–526 (2013).
155. Philippot, R. *et al.* Survival of cementless dual mobility socket with a mean 17 years follow-up. *Rev. Chir. Orthopédique Réparatrice Appar. Mot.* **94,** e23–27 (2008).
156. Philippot, R., Meucci, J. F., Boyer, B. & Farizon, F. Modern dual-mobility cup implanted with an uncemented stem: about 100 cases with 12-year follow-up. *Surg. Technol. Int.* **23,** 208–212 (2013).
157. Lautridou, C., Lebel, B., Burdin, G. & Vielpeau, C. [Survival of the cementless Bousquet dual mobility cup: Minimum 15-year follow-up of 437 total hip arthroplasties]. *Rev. Chir. Orthopédique Réparatrice Appar. Mot.* **94,** 731–739 (2008).
158. Vielpeau, C., Lebel, B., Ardouin, L., Burdin, G. & Lautridou, C. The dual mobility socket concept: experience with 668 cases. *Int. Orthop.* **35,** 225–230 (2011).
159. Bauchu, P. *et al.* The dual-mobility POLARCUP: first results from a multicenter study. *Orthopedics* **31,** (2008).

160. Leclercq, S. *et al.* Evora® chromium-cobalt dual mobility socket: results at a minimum 10 years' follow-up. *Orthop. Traumatol. Surg. Res. OTSR* **99,** 923–928 (2013).
161. Epinette, J.-A., Béracassat, R., Tracol, P., Pagazani, G. & Vandenbussche, E. Are Modern Dual Mobility Cups a Valuable Option in Reducing Instability After Primary Hip Arthroplasty, Even in Younger Patients? *J. Arthroplasty* (2013). doi:10.1016/j.arth.2013.12.011
162. Prudhon, J.-L., Ferreira, A. & Verdier, R. Dual mobility cup: dislocation rate and survivorship at ten years of follow-up. *Int. Orthop.* **37,** 2345–2350 (2013).
163. Guyen, O. *et al.* Unconstrained tripolar implants for primary total hip arthroplasty in patients at risk for dislocation. *J. Arthroplasty* **22,** 849–858 (2007).
164. Fessy, M.-H. La double mobilité. *Rev. Chir. Orthopédique Traumatol.* **96,** 891–898 (2010).
165. Combes, A., Migaud, H., Girard, J., Duhamel, A. & Fessy, M. H. Low rate of dislocation of dual-mobility cups in primary total hip arthroplasty. *Clin. Orthop.* **471,** 3891–3900 (2013).
166. Bouchet, R., Mercier, N. & Saragaglia, D. Posterior approach and dislocation rate: a 213 total hip replacements case-control study comparing the dual mobility cup with a conventional 28-mm metal head/polyethylene prosthesis. *Orthop. Traumatol. Surg. Res. OTSR* **97,** 2–7 (2011).
167. Adam, P., Hardy, M., Philippot, R. & Farizon, F. [Total hip arthroplasty in patients younger than 30-years-old with stiff hip]. *Rev. Chir. Orthopédique Réparatrice Appar. Mot.* **94 Suppl,** S170–172 (2008).
168. Guyen, O., Béjui-Hugues, J. & Carret, J.-P. [Total hip arthroplasty in patients younger than 30-years-old who are not able to walk]. *Rev. Chir. Orthopédique Réparatrice Appar. Mot.* **94 Suppl,** S177–179 (2008).
169. Hamadouche, M., Arnould, H. & Bouxin, B. Is a cementless dual mobility socket in primary THA a reasonable option? *Clin. Orthop.* **470,** 3048–3053 (2012).
170. Caton, J. H., Prudhon, J. L., Ferreira, A., Aslanian, T. & Verdier, R. A comparative and retrospective study of three hundred and twenty primary Charnley type hip replacements with a minimum follow up of ten years to assess wether a dual mobility cup has a decreased dislocation risk. *Int. Orthop.* (2014). doi:10.1007/s00264-014-2313-2
171. Gregory, R. J., Gibson, M. J. & Moran, C. G. Dislocation after primary arthroplasty for subcapital fracture of the hip. Wide range of movement is a risk factor. *J. Bone Joint Surg. Br.* **73,** 11–12 (1991).
172. Adam, P. *et al.* Dual mobility cups hip arthroplasty as a treatment for displaced fracture of the femoral neck in the elderly. A prospective, systematic, multicenter study with specific focus on postoperative dislocation. *Orthop. Traumatol. Surg. Res. OTSR* **98,** 296–300 (2012).
173. Bensen, A. S., Jakobsen, T. & Krarup, N. Dual mobility cup reduces dislocation and re-operation when used to treat displaced femoral neck fractures. *Int. Orthop.* (2014). doi:10.1007/s00264-013-2276-8
174. Tarasevicius, S., Busevicius, M., Robertsson, O. & Wingstrand, H. Dual mobility cup reduces dislocation rate after arthroplasty for femoral neck fracture. *BMC Musculoskelet. Disord.* **11,** 175 (2010).

175. Bousquet, G. *et al.* [Recovery after aseptic loosening of cemented total hip arthroplasties with Bousquet's cementless prosthesis. Apropos of 136 cases]. *Rev. Chir. Orthopédique Réparatrice Appar. Mot.* **72 Suppl 2,** 70–74 (1986).
176. Wegrzyn, J. *et al.* Acetabular Reconstruction Using a Kerboull Cross-Plate, Structural Allograft and Cemented Dual-Mobility Cup in Revision THA at a Minimum 5-Year Follow-Up. *J. Arthroplasty* (2013). doi:10.1016/j.arth.2013.05.030
177. Civinini, R., Carulli, C., Matassi, F., Nistri, L. & Innocenti, M. A dual-mobility cup reduces risk of dislocation in isolated acetabular revisions. *Clin. Orthop.* **470,** 3542–3548 (2012).
178. Massin, P. & Besnier, L. Acetabular revision using a press-fit dual mobility cup. *Orthop. Traumatol. Surg. Res. OTSR* **96,** 9–13 (2010).
179. Guyen, O., Pibarot, V., Vaz, G., Chevillotte, C. & Béjui-Hugues, J. Use of a dual mobility socket to manage total hip arthroplasty instability. *Clin. Orthop.* **467,** 465–472 (2009).
180. Leclercq, S., el Blidi, S. & Aubriot, J. H. [Bousquet's device in the treatment of recurrent dislocation of a total hip prosthesis. Apropos of 13 cases]. *Rev. Chir. Orthopédique Réparatrice Appar. Mot.* **81,** 389–394 (1995).
181. Hamadouche, M., Biau, D. J., Huten, D., Musset, T. & Gaucher, F. The use of a cemented dual mobility socket to treat recurrent dislocation. *Clin. Orthop.* **468,** 3248–3254 (2010).
182. Leiber-Wackenheim, F., Brunschweiler, B., Ehlinger, M., Gabrion, A. & Mertl, P. Treatment of recurrent THR dislocation using of a cementless dual-mobility cup: a 59 cases series with a mean 8 years' follow-up. *Orthop. Traumatol. Surg. Res. OTSR* **97,** 8–13 (2011).
183. Saragaglia, D., Ruatti, S. & Refaie, R. Relevance of a press-fit dual mobility cup to deal with recurrent dislocation of conventional total hip arthroplasty: a 29-case series. *Eur. J. Orthop. Surg. Traumatol. Orthopédie Traumatol.* **23,** 431–436 (2013).
184. Mertl, P. *et al.* Recurrence of dislocation following total hip arthroplasty revision using dual mobility cups was rare in 180 hips followed over 7 years. *HSS J. Musculoskelet. J. Hosp. Spec. Surg.* **8,** 251–256 (2012).
185. Philippeau, J.-M. *et al.* Dual mobility design use in preventing total hip replacement dislocation following tumor resection. *Orthop. Traumatol. Surg. Res. OTSR* **96,** 2–8 (2010).
186. Langlais, F., Lambotte, J. C., Collin, P. & Thomazeau, H. Long-term results of allograft composite total hip prostheses for tumors. *Clin. Orthop.* 197–211 (2003). doi:10.1097/01.blo.0000079270.91782.23
187. Lecuire, F., Benareau, I., Rubini, J. & Basso, M. [Intra-prosthetic dislocation of the Bousquet dual mobility socket]. *Rev. Chir. Orthopédique Réparatrice Appar. Mot.* **90,** 249–255 (2004).
188. Goyal, N., Tripathy, M. S. & Parvizi, J. Modern Dual Mobility Cups for Total Hip Arthroplasty. *Surg. Technol. Int.* **XXI,** 227–232 (2012).
189. Grazioli, A., Ek, E. T. H. & Rüdiger, H. A. Biomechanical concept and clinical outcome of dual mobility cups. *Int. Orthop.* (2012). doi:10.1007/s00264-012-1678-3
190. Plummer, D. R., Haughom, B. D. & Della Valle, C. J. Dual mobility in total hip arthroplasty. *Orthop. Clin. North Am.* **45,** 1–8 (2014).
191. Stulberg, S. D. Dual mobility for chronic hip instability: a solution option. *Orthopedics* **33,** 637 (2010).
192. Hailer, N. P., Weiss, R. J., Stark, A. & Kärrholm, J. Dual-mobility cups for revision due to instability are associated with a low rate of re-revisions due to dislocation. *Acta Orthop.* (2012). doi:10.3109/17453674.2012.742395

193. Mont, M. A. *et al.* The Use of Dual-Mobility Bearings in Difficult Hip Arthroplasty Reconstructive Cases. *Surg. Technol. Int.* **XXI,** 234–240 (2012).
194. Pattyn, C. & Audenaert, E. Early complications after revision total hip arthroplasty with cemented dual-mobility socket and reinforcement ring. *Acta Orthop. Belg.* **78,** 357–361 (2012).
195. Sanders, R. J. M., Swierstra, B. A. & Goosen, J. H. M. The use of a dual-mobility concept in total hip arthroplasty patients with spastic disorders : No dislocations in a series of ten cases at midterm follow-up. *Arch. Orthop. Trauma Surg.* (2013). doi:10.1007/s00402-013-1759-9
196. Griffin, X. L., McArthur, J., Achten, J., Parsons, N. & Costa, M. L. The Warwick Hip Trauma Evaluation Two -an abridged protocol for the WHiTE Two Study: An embedded randomised trial comparing the Dual-Mobility withpolyethylene cups in hip arthroplasty for fracture. *Bone Jt. Res.* **2,** 210–213 (2013).
197. Stulberg, S. D. Dual poly liner mobility optimizes wear and stability in THA: affirms. *Orthopedics* **34,** e445–448 (2011).
198. Stulberg, S. D. Dual Mobility for Chronic Instability. *Semin. Arthroplasty* **22,** 90–94 (2011).
199. Pritchett, J. W. One-component revision of failed hip resurfacing from adverse reaction to metal wear debris. *J. Arthroplasty* **29,** 219–224 (2014).
200. Banzhof, J. A., Robbins, C. E., Ven, A. van der, Talmo, C. T. & Bono, J. V. Femoral head dislodgement complicating use of a dual mobility prosthesis for recurrent instability. *J. Arthroplasty* **28,** 543.e1–3 (2013).
201. Mohammed, R. & Cnudde, P. Severe Metallosis Owing to Intraprosthetic Dislocation in a Failed Dual-Mobility Cup Primary Total Hip Arthroplasty. *J. Arthroplasty* (2011). doi:10.1016/j.arth.2010.11.019
202. Klingenstein, G. G., Yeager, A. M., Lipman, J. D. & Westrich, G. H. Computerized Range of Motion Analysis Following Dual Mobility Total Hip Arthroplasty, Traditional Total Hip Arthroplasty, and Hip Resurfacing. *J. Arthroplasty* (2013). doi:10.1016/j.arth.2012.08.017
203. Chen, Q. *et al.* Technical note: validation of a motion analysis system for measuring the relative motion of the intermediate component of a tripolar total hip arthroplasty prosthesis. *Med. Eng. Phys.* **27,** 505–512 (2005).
204. Pineau, V., Lebel, B., Gouzy, S., Dutheil, J.-J. & Vielpeau, C. Dual mobility hip arthroplasty wear measurement: Experimental accuracy assessment using radiostereometric analysis (RSA). *Orthop. Traumatol. Surg. Res. OTSR* (2010). doi:10.1016/j.otsr.2010.04.007
205. Loving, L., Lee, R. K., Herrera, L., Essner, A. P. & Nevelos, J. E. Wear Performance Evaluation of a Contemporary Dual Mobility Hip Bearing Using Multiple Hip Simulator Testing Conditions. *J. Arthroplasty* (2013). doi:10.1016/j.arth.2012.09.011
206. Nakata, K. *et al.* Acetabular osteolysis and migration in bipolar arthroplasty of the hip: five- to 13-year follow-up study. *J. Bone Joint Surg. Br.* **79,** 258–264 (1997).
207. Yoshimine, F. The safe-zones for combined cup and neck anteversions that fulfill the essential range of motion and their optimum combination in total hip replacements. *J. Biomech.* **39,** 1315–1323 (2006).
208. Yoshimine, F. The influence of the oscillation angle and the neck anteversion of the prosthesis on the cup safe-zone that fulfills the criteria for range of motion in total hip

replacements. The required oscillation angle for an acceptable cup safe-zone. *J. Biomech.* **38,** 125–132 (2005).
209. Yoshimine, F. & Ginbayashi, K. A mathematical formula to calculate the theoretical range of motion for total hip replacement. *J. Biomech.* **35,** 989–993 (2002).
210. Yoshimine, F., Latta, L. L. & Milne, E. L. Sliding characteristics of compression hip screws in the intertrochanteric fracture: a clinical study. *J. Orthop. Trauma* **7,** 348–353 (1993).
211. Widmer, K.-H. & Majewski, M. The impact of the CCD-angle on range of motion and cup positioning in total hip arthroplasty. *Clin. Biomech. Bristol Avon* **20,** 723–728 (2005).
212. Widmer, K.-H. & Zurfluh, B. Compliant positioning of total hip components for optimal range of motion. *J. Orthop. Res. Off. Publ. Orthop. Res. Soc.* **22,** 815–821 (2004).
213. Widmer, K.-H. Containment versus impingement: finding a compromise for cup placement in total hip arthroplasty. *Int. Orthop.* **31 Suppl 1,** S29–33 (2007).
214. Widmer, K.-H. & Grützner, P. A. Joint replacement-total hip replacement with CT-based navigation. *Injury* **35 Suppl 1,** S–A84–89 (2004).
215. Widmer, K.-H. Comment on 'A mathematical formula to calculate the theoretical range of motion for total hip arthroplasty'. *J. Biomech.* **36,** 615; author reply 617–618 (2003).
216. Widmer, K.-H. A simplified method to determine acetabular cup anteversion from plain radiographs. *J. Arthroplasty* **19,** 387–390 (2004).
217. Mcbride, E. D. Doorknob hip-joint endoprosthesis. *Med. Radiogr. Photogr.* **31,** 124–125 (1955).
218. Von Knoch, M., Berry, D. J., Harmsen, W. S. & Morrey, B. F. Late dislocation after total hip arthroplasty. *J. Bone Joint Surg. Am.* **84-A,** 1949–1953 (2002).
219. MERLE D'AUBIGNE, R. & POSTEL, M. [Treatment of failures in arthroplasty.]. *Acta Orthop. Belg.* **21,** 565–578; discussion, 578–584 (1955).
220. Sedel, L. Long-term results of cemented total hip arthroplasty in patients 45 years old or younger: a 16-year follow-up study. *J. Arthroplasty* **10,** 255–256 (1995).
221. Dorey, F. & Amstutz, H. C. The validity of survivorship analysis in total joint arthroplasty. *J. Bone Joint Surg. Am.* **71,** 544–548 (1989).
222. Gruen, T. A., McNeice, G. M. & Amstutz, H. C. 'Modes of failure' of cemented stem-type femoral components: a radiographic analysis of loosening. *Clin. Orthop.* 17–27 (1979).
223. DeLee, J. G. & Charnley, J. Radiological demarcation of cemented sockets in total hip replacement. *Clin. Orthop.* 20–32 (1976).
224. Brooker, A. F., Bowerman, J. W., Robinson, R. A. & Riley, L. H. Ectopic ossification following total hip replacement. Incidence and a method of classification. *J. Bone Joint Surg. Am.* **55,** 1629–1632 (1973).
225. Martínez de Aragón, J. S. & Keisu, K. S. 21-year results of the uncemented fully textured lord hip prosthesis. *Clin. Orthop.* **454,** 133–138 (2007).
226. Lord, G. A., Hardy, J. R. & Kummer, F. J. An uncemented total hip replacement: experimental study and review of 300 madreporique arthroplasties. *Clin. Orthop.* 2–16 (1979).
227. Gaffey, J. L. *et al.* Cementless acetabular fixation at fifteen years. A comparison with the same surgeon's results following acetabular fixation with cement. *J. Bone Joint Surg. Am.* **86-A,** 257–261 (2004).
228. Engh, C. A. & Massin, P. Cementless total hip arthroplasty using the anatomic medullary locking stem. Results using a survivorship analysis. *Clin. Orthop.* 141–158 (1989).

229. Grübl, A. *et al.* Cementless total hip arthroplasty with the rectangular titanium Zweymuller stem. A concise follow-up, at a minimum of fifteen years, of a previous report. *J. Bone Joint Surg. Am.* **88,** 2210–2215 (2006).
230. García-Rey, E. & García-Cimbrelo, E. Clinical and radiographic results and wear performance in different generations of a cementless porous-coated acetabular cup. *Int. Orthop.* **32,** 181–187 (2008).
231. Reigstad, O., Siewers, P., Røkkum, M. & Espehaug, B. Excellent long-term survival of an uncemented press-fit stem and screw cup in young patients: follow-up of 75 hips for 15-18 years. *Acta Orthop.* **79,** 194–202 (2008).
232. Yoon, T. R., Rowe, S.-M., Kim, M.-S., Cho, S.-G. & Seon, J.-K. Fifteen- to 20-year results of uncemented tapered fully porous-coated cobalt-chrome stems. *Int. Orthop.* **32,** 317–323 (2008).
233. Parvizi, J., Sullivan, T., Duffy, G. & Cabanela, M. E. Fifteen-year clinical survivorship of Harris-Galante total hip arthroplasty. *J. Arthroplasty* **19,** 672–677 (2004).
234. Hendrich, C., Sauer, U., Kirschner, S., Schmitz, H. & Martell, J. M. High long-term loosening rate of conical screw cups. *Acta Orthop.* **77,** 886–892 (2006).
235. Hallan, G., Lie, S. A. & Havelin, L. I. High wear rates and extensive osteolysis in 3 types of uncemented total hip arthroplasty: a review of the PCA, the Harris Galante and the Profile/Tri-Lock Plus arthroplasties with a minimum of 12 years median follow-up in 96 hips. *Acta Orthop.* **77,** 575–584 (2006).
236. Wangen, H., Lereim, P., Holm, I., Gunderson, R. & Reikerås, O. Hip arthroplasty in patients younger than 30 years: excellent ten to 16-year follow-up results with a HA-coated stem. *Int. Orthop.* **32,** 203–208 (2008).
237. Raj, D., Jaiswal, P. K., Sharma, B. L. & Fergusson, C. M. Long term results of the Corin C-Fit uncemented total hip arthroplasty in young patients. *Arch. Orthop. Trauma Surg.* **128,** 1391–1395 (2008).
238. Berend, M. E. *et al.* Long-term outcome and risk factors of proximal femoral fracture in uncemented and cemented total hip arthroplasty in 2551 hips. *J. Arthroplasty* **21,** 53–59 (2006).
239. Wessinghage, D. & Kisslinger, E. [Long-term results after cemented total hip arthroplasty in chronic polyarthritis]. *Orthop.* **27,** 381–391 (1998).
240. Rajaratnam, S. S. *et al.* Long-term results of a hydroxyapatite-coated femoral component in total hip replacement: a 15- to 21-year follow-up study. *J. Bone Joint Surg. Br.* **90,** 27–30 (2008).
241. Goosen, J. H. M., Castelein, R. M., Runne, W. C., Dartee, D. A. & Verheyen, C. C. P. M. Long-term results of a soft interface- (Proplast-) coated femoral stem. *Acta Orthop.* **77,** 585–590 (2006).
242. Eingartner, C., Heigele, T., Volkmann, R. & Weise, K. Long-term results of an uncemented straight femoral shaft prosthesis. *Hip Int. J. Clin. Exp. Res. Hip Pathol. Ther.* **16,** 23–32 (2006).
243. Kim, Y.-H. Long-term results of the cementless porous-coated anatomic total hip prosthesis. *J. Bone Joint Surg. Br.* **87,** 623–627 (2005).
244. Rozkydal, Z., Janícek, P., Tomás, T. & Florian, Z. [Long-term results of the CLS acetabular cup in primary total hip replacement]. *Acta Chir. Orthop. Traumatol. Cech.* **76,** 90–97 (2009).
245. Engh, C. A., Claus, A. M., Hopper, R. H. & Engh, C. A. Long-term results using the anatomic medullary locking hip prosthesis. *Clin. Orthop.* 137–146 (2001).

246. Andrew, T. A., Berridge, D., Thomas, A. & Duke, R. N. Long-term review of ring total hip arthroplasty. *Clin. Orthop.* 111–122 (1985).
247. Hallan, G. *et al.* Medium- and long-term performance of 11,516 uncemented primary femoral stems from the Norwegian arthroplasty register. *J. Bone Joint Surg. Br.* **89,** 1574–1580 (2007).
248. Della Valle, C. J. *et al.* Primary total hip arthroplasty with a porous-coated acetabular component. A concise follow-up, at a minimum of twenty years, of previous reports. *J. Bone Joint Surg. Am.* **91,** 1130–1135 (2009).
249. Bojescul, J. A., Xenos, J. S., Callaghan, J. J. & Savory, C. G. Results of porous-coated anatomic total hip arthroplasty without cement at fifteen years: a concise follow-up of a previous report. *J. Bone Joint Surg. Am.* **85-A,** 1079–1083 (2003).
250. Harris, W. H. Results of uncemented cups: a critical appraisal at 15 years. *Clin. Orthop.* 121–125 (2003). doi:10.1097/01.blo.0000096824.67494.aa
251. Ihle, M., Mai, S., Pfluger, D. & Siebert, W. The results of the titanium-coated RM acetabular component at 20 years: a long-term follow-up of an uncemented primary total hip replacement. *J. Bone Joint Surg. Br.* **90,** 1284–1290 (2008).
252. Dorey, F. & Amstutz, H. C. The validity of survivorship analysis in total joint arthroplasty. *J. Bone Joint Surg. Am.* **71,** 544–548 (1989).
253. Grant, P. & Nordsletten, L. Total hip arthroplasty with the Lord prosthesis. A long-term follow-up study. *J. Bone Joint Surg. Am.* **86-A,** 2636–2641 (2004).
254. Aldinger, P. R. *et al.* Uncemented grit-blasted straight tapered titanium stems in patients younger than fifty-five years of age. Fifteen to twenty-year results. *J. Bone Joint Surg. Am.* **91,** 1432–1439 (2009).
255. Han, C. D., Choe, W. S. & Yoo, J. H. Effect of polyethylene wear on osteolysis in cementless primary total hip arthroplasty: minimal 5-year follow-up study. *J. Arthroplasty* **14,** 714–723 (1999).
256. Williams, D. F. On the mechanisms of biocompatibility. *Biomaterials* **29,** 2941–2953 (2008).
257. Shirong Ge, S. W. Wear behavior and wear debris distribution of UHMWPE against Si3N4 ball in bi-directional sliding. *Wear* 571–578 (2008). doi:10.1016/j.wear.2007.05.001
258. Laheurte, R., Darnis, P., Darbois, N., Cahuc, O. & Neauport, J. Subsurface damage distribution characterization of ground surfaces using Abbott-Firestone curves. *Opt. Express* **20,** 13551–13559 (2012).
259. Blunt, L. & Jiang, X. Q. Three dimensional measurement of the surface topography of ceramic and metallic orthopaedic joint prostheses. *J. Mater. Sci. Mater. Med.* **11,** 235–246 (2000).
260. Buford, A. & Goswami, T. Review of wear mechanisms in hip implants: Paper I – General. *Mater. Des.* **25,** 385–393 (2004).
261. Pauwels, F. *Biomechanics of the Locomotor Apparatus: Contributions on the Functional Anatomy of the Locomotor Apparatus*. (Springer-Verlag, 1980).
262. Imbert, L., Geringer, J., Boyer, B. & Farizon, F. Wear analysis of hip explants, dual mobility concept: Comparison of quantitative and qualitative analyses. *Proc. Inst. Mech. Eng. Part J J. Eng. Tribol.* **226,** 838–853 (2012).
263. Jin, Z. *Computational Modelling of Biomechanics and Biotribology in the Musculoskeletal System: Biomaterials and Tissues*. (Elsevier, 2014).

264. Najjar, D., Bigerelle, M., Migaud, H. & Iost, A. Identification of scratch mechanisms on a retrieved metallic femoral head. *Wear* **258,** 240–250 (2005).
265. Peltonen, J. Topographical parameters for specifying a three-di...[Langmuir. 2004] -
266. Philippot, R., Boyer, B. & Farizon, F. Intraprosthetic Dislocation: A Specific Complication of the Dual-mobility System. *Clin. Orthop.* (2012).
267. Ola Ahmad, J.-C. P. On the linear combination of the Gaussian and student's t random field and the integral geometry of its excursion sets. *Stat. Amp Probab. Lett.* **38,** 559–567 (2013).
268. Ola Suleiman Ahmad, J.-C. P. Lipschitz-Killing curvatures of the Excursion Sets of Skew Student's t Random fields. *Stoch. Models* 273–289 (2013).

Chapitre IV. **ANNEXES**

Copie des articles correspondant au travail de Mme L. Imbert.

Original Article

Institution of MECHANICAL ENGINEERS
Journal of ENGINEERING TRIBOLOGY

Proc IMechE Part J:
J Engineering Tribology
226(10) 838–853

DOI: 10.1177/1350650112451211
pij.sagepub.com
SAGE

Wear analysis of hip explants, dual mobility concept: Comparison of quantitative and qualitative analyses

L Imbert[1], J Geringer[1,2], B Boyer[3] and F Farizon[3]

Abstract

Total hip replacement fails mainly because of wear. It is of interest to analyse wear to be able to increase the longevity of the hip implants. One way to achieve it is to use instruments on explants but the most suitable depends on the application. This article aims at comparing several methods of surface analysis in the particular application of wear determination in a series of dual mobility explants. Wear measurement could help understand the wear mechanism only partially known. A coordinate measuring machine is used to get three-dimensional points representing the explants, then Pro/Engineer® and Matlab® are used to calculate wear. A mechanical (SOMICRONIC®) and an optical profilometer (Bruker nanoscope Wyko® NT 9100, ex. Veeco) are used to access roughness parameters. The comparisons of the two software showed similar results for wear calculation except in a few cases where differences are due to the theoretical volumes calculation. The comparison of the two profiling techniques resulted in similar results particularly for Sa and Sdr. The comparison of the results showed that wear is present for four explants; it is relevant with the observed characteristics. The mechanical profilometer showed better accuracy than the optical one which enable to conclude that it must not be neglected for that particular application, even if measurements need more time.

Keywords

Total hip replacement, explants, dual mobility concept, wear measurements, surface roughness

Date received: 28 December 2011; accepted: 27 April 2012

Introduction

The hip joint, like every other joints, can suffer from a disease or a fracture and might need to be replaced. That surgery is one of the most common performed nowadays but it is likely to occur several times in a lifetime since a total hip replacement lasts 15 20 years at most.

The most common cause of premature failure of implanted joints is aseptic loosening, accounting for 75% of revision operations. Aseptic loosening can be attributed to macrophage (immune system) response to particulate debris generated by wear of the components and bone resorption due to stress shielding after prosthesis implantation.[1]

Wear of hip replacement can be studied by several ways such as numerical simulation,[2–5] tests performed on simulators[1,6–8] or explants analysis.[1,9–11] When analysing explants, i.e. implants removed from patients, one needs to look at the surface to get information on wear mechanisms. Quantitative and qualitative informations can be obtained using appropriate instruments. For instance, Geringer et al.[9] used a coordinate measuring machine (CMM) to calculate wear volumes and a mechanical profilometer to assess the surface roughness on a series of 12 dual mobility explants and a blank cup.

Quantification of wear can be carried out by roundness measurements or gravimetric methods. Gravimetric testing consists in weighing the implant before and after being used. This technique has some limits since the surfaces have been proved to change, for instance protein absorption may occur.[12] Besides, it seems possible only for in vitro studies given the initial implant weight is not known. Blunt et al.[1] seemed to think that a geometric method like CMM could overcome several problems linked to the gravimetric technique such as the surface absorption. However, the initial data are often unavailable as well but they overcame it using a similar implant or the no-wear zones as reference.[1] The principle of this

[1]Ecole Nationale Supérieure des Mines, CIS-EMSE, CNRS UMR5146, Saint-Etienne, France
[2]Penn State University, MSE/CEST, PA, USA
[3]Centre d'Orthopédie Traumatologie CHU, Saint-Etienne, France

Corresponding author:
J Geringer, Ecole Nationale Supérieure des Mines, CIS-EMSE, CNRS UMR5146, LCG, F-42023 Saint-Etienne de Saint-Etienne 42023, France.
Email: geringer@emse.fr

'Wear analysis of hip explants, dual mobility concept : Comparison of quantitative and qualitative analyses' Proc IMechE Part J : J Engineering Tribology 226(10) 838-853.

technique is to get the coordinates of many points on the implant surface. Morris et al. validated the use of a CMM for implant analysis and suggested it to be applicable for explants analysis as well. Moreover, they found a strong correlation between the CMM method and the gravimetric method and between the CMM method and the roundness measurement. Nevertheless, they recognized the limitations of the CMM method like the fact that the implant should not be damaged on the entire surface.[12]

Qualitative measurement of wear can be achieved by roughness measurement methods. They are classified as contact or non-contact techniques. Contact methods employ a mechanical stylus whereas non-contact ones are mostly optical such as laser profilometry, confocal measurement methods[13] or interferometry which has been used a lot for surface profiling.[14–16] The mechanical technique can damage the surface but it is cheaper. The optical method used in Geringer et al.[9] produce interferograms giving the height at each pixel. It is more expensive but faster as well. Moreover, previous works have been dedicated to compare contacting and non-contacting, profilometry and/or atomic force microscopy (AFM) related to the bio-engineering field[17] or not.[18] Stout and Blunt[17] used a phase shifting interferometer on hip implants to measure the topography but no comparison to a contact method is performed. Recently, hybrid profilometers combining contact and non-contact measurements have been emerging[19] because the two techniques may be complementary. Some other studies highlighted the interest of in-process measurement techniques[20] or portable devices.[21]

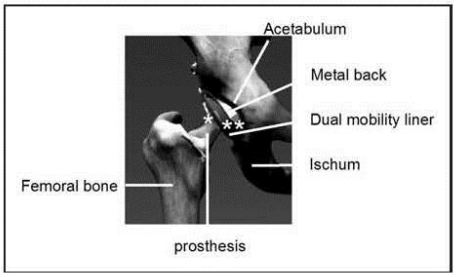

Figure 1. Schematic of a dual mobility implant.
*is related to the first mobility between head and cup and **corresponds to the second mobility between cup and metal-back. Two motions are possible.

The dual mobility concept is invented in the 1970s by Professor Gilles Bousquet. The dual mobility implant consists in a small metallic head moving within an acetabular cup in ultra high molecular weight polyethylene (UHMWPE). This latter is moving within a metal-back (Figure 1). It is of interest to measure the wear performance of this kind of implants to compare them to simple mobility implants. In a previous study,[9] the wear of the acetabular cup is assessed quantitatively and qualitatively using a CMM and profilometers.

The purpose of this article is to compare methods related to CMM and especially the accuracy of the post-treatment. Additionally, the roughness parameters from mechanical and optical three-dimensional (3D) profilometry are studied for understanding mechanisms of wear in the particular application of dual mobility concept of hip prosthesis, from explants analysis. From this study, one may expect to find wear volume with better accuracy. Moreover, the investigations about 3D profilometry should allow improving

Table 1. Table of the measurements performed on each implant.

MB type	Explants	Implant survival (years)	CMM on the inner surface	CMM on the outer surface	Mechanical profilometer	Optical profilometer
MB SS 316 L	I2	11.4	×	×	×	×
	I3	10.4	×	×	×	×
	I5	9.3	×	×	×	×
	I6	9.1		×	×	×
	I7	7.3	×	×	×	×
MB SS 316L AF	I4	10.3	×	×	×	×
	I8	6.3	×		×	×
MB SS 316L high brooker	I1	I2	×	×	×	×
MB Ti-6Al-4 V (AF)	T4	6.2	×	×	×	×
	T3	7.3	×	×	×	×
MB Ti-6Al-4V	T2	13.9	×	×	×	×
	T1	15.5	×	×	×	×
	Blank cup				×	×

CMM: coordinate measuring machine; AF: arthrofibrosis.

the best method dedicated to understand the wear mechanisms.

Materials and methods

This study presents the comparison of techniques used during the study performed in Geringer et al.[9] and other techniques used later on the same series of explants. Table 1 presents all the measurements performed on each implant. Dual mobility cups are in UHMWPE (SERF, Décines, France). Eight of them, called I1–I8, are in contact with a stainless steel back shell (metal-back, combination Novae®) whereas for the four others, T1–T4, it is Ti-6Al-4V. It is worth noting this metal-back, Ti-6Al-4V, is nowadays quite abandoned due to high wear related to corrosive medium. The implantation time goes from 74 to 186 months. Besides, I4, I8, T3 and T4 are cases for which fibrosis is observed and written down in the report. Also, an equatorial stripe is observed for I2, I3, I5, I6, I7 and T1. In that study, they used a CMM and the Pro/Engineer® software to calculate volumetric wear and a mechanical profilometer to access information about wear mechanisms. This article details the other techniques used for the same purposes and the comparison with the methods used in Geringer et al.[9]

Wear calculation

The volume of the part of the insert palpated by the CMM must be calculated and compared to the same part of the insert before implantation to calculate wear. The insert before implantation has a certain

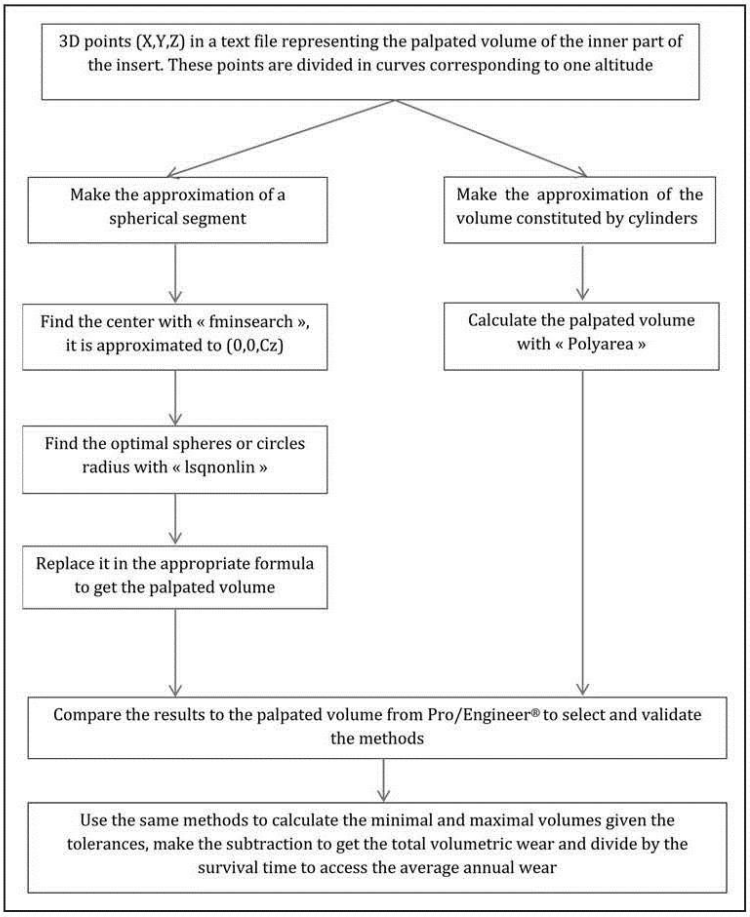

Figure 2. Algorithm for the palpated volumes and annual wear calculations. The methods are selected and validated for the inner part of the insert.

dimension comprised in the dimension range ordered by the manufacturer SERF, i.e. $22.2^{+0.3}_{+0.1}$ mm for eight explants, $26^{+0.3}_{+0.1}$ mm for two explants and $28^{+0.3}_{+0.1}$ mm for the last two. Therefore, the minimum volume is given by a diameter of 22.1, 26.1 or 28.1 mm and it will result in the maximum wear. The shape of samples did not change during the implantation time because dimensions are included in the manufacturing tolerances. If the shape of explants changed, the outliers, i.e. the dimensions are outside of the tolerances, are excluded from the analysed series. Figure 2 shows an algorithm of the volumes and wear calculation for the inner part of the inserts.

To calculate the volume within the palpated part of the insert, two strategies are envisaged. They are to be explained and then compared to select the best ones to make the wear calculations. A first strategy is to approximate the worn volume to a spherical segment, i.e. a portion of a sphere cut by two planes (Figure 3). The optimal radius R of this approximated sphere is found by optimization but the centre had to be determined first. One calculates the distances between an initial centre and all the points to find the centre. Then, using the Matlab® function 'fminsearch', one is looking for the minimal difference between the maximum and the minimum distances. The centres are approximated to be (0, 0, C_z) for simplification. The difference between the distance points centre and the radius is minimized to find the optimal radius. To do so, the Matlab®'s function 'lsqnonlin' is used. First, only the points from the CMM are used and then 15,300 points given by 'nrbmak', the constructor of the interpolation surface in a NURBS toolbox, Matlab®'s software. One also uses more than 35,000 points given by 'TriScatteredInterp', a Matlab® function used for interpolation. Once the optimal radius is known it is to replace in an appropriate formula to get the volume. The first three methods are called method 1a to 1c in the following according the number of points used for the radius calculation, first 840, then 15,300 and finally more than 35,000. The formula used is

$$V = \frac{\pi}{3} h^2 (3R - h) \tag{1}$$

for a spherical cap as we considered the worn volume as a sphere minus two spherical caps. In this formula, h is the height of the cap ($h1$ and $h2$), it is calculated from the radius R and from the height H that is used in the Pro/Engineer® method.

In a second method (called method 2 in the following), the formula used is the formula of a spherical segment

$$V = \frac{\pi}{2} h \left(r^2 + r'^2 + \frac{h^2}{3} \right) \tag{2}$$

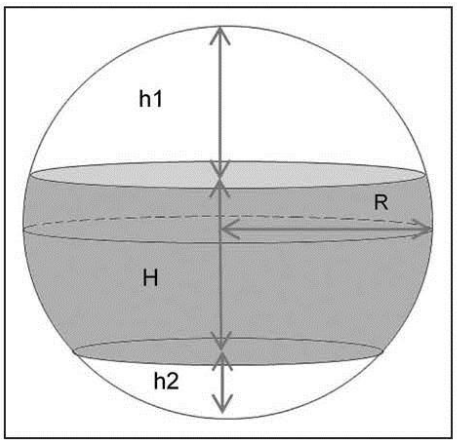

Figure 3. Spherical segment (coloured), its height is H. Two spherical caps of heights $h1$ and $h2$ complete the sphere of radius R. Its centre is approximated to be (0, 0, C_z).

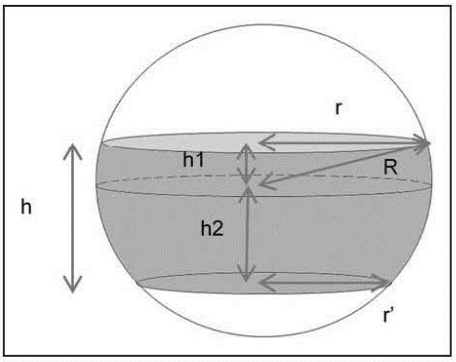

Figure 4. Spherical segment (coloured) of height $h = h1 + h2$.

where r and r' are the radius of the circles resulting from the intersection of the sphere with two planes (Figure 4). Like the radius of the sphere, they are found by optimization. In this case, h is the height of the spherical segment. For the volume before implantation r and r' are calculated from the sphere radii (a minimal and a maximal) and the height with the Pythagoras formula.

The third strategy is totally different, one takes each polygon given by the CMM corresponding to one altitude and the inner area is calculated by the function 'polyarea'. That area is multiplied by the above half height plus the below half height (Figure 5). The volume before implantation is calculated the same way in order to be relevant, using the parametric equation of a circle to reconstruct seven or eight circles for the first mobility. Each radius is

calculated with the Pythagoras formula knowing the height and the radius of the sphere. (This method is called method 3 in the following text.)

For every method, the minimum and maximum volumes of the part of the insert before implantation is calculated by the same way and one made the subtraction to access the total wear. Finally, the total wear is divided by the survival time in years to get the annual volumetric wear. It is the same principle for the second mobility, convex side. Methods are the same and selected according to the investigations of the concave side. Statistical analyses are done to compare the methods, one-way ANOVA (analysis of variance) tests are used and the series are significantly different if the p-value is lower than 0.05.

Surface roughness measurement

In the related study,[9] a campaign of roughness measurement are carried out with a mechanical profilometer SOMICRONIC® on the 12 explants I1–I8, T1–T4 and a blank cup. Filtering processes are detailed in Geringer et al.[9] Five images of 1 mm^2 are taken on a zone at roughly 30° called the no-worn zone, five images of the same size are taken at roughly 60° called the worn zone and a single image is made on the top zone called the apex. That same amount of 11 images are taken for the same 13 cups with the optical profilometer Wyko® NT 9100 (Bruker Nanoscope-Veeco Instruments, Inc.) except that the considered angles are about 40° and 80°. The measurements are performed by zone. Due to the comparison of two different profilometers, it is not possible to find exactly the same area for measuring. However, a particular attention is paid on finding the same area on each cup by marking with a pen. As mentioned in Geringer et al.,[9] zones at 30° or 40° are related to the worn zones and the ones at higher angles are related to no-worn zones. A tilt processing and a spherical filter are applied without any additional filtering process.

The principle of the optical profilometer, a non-contact method, is that an incident white light goes through a semi-reflective splitter to be split into two waves. The first one will be reflected by a mirror and the second one will be reflected by the sample surface. The two rays recombine and it results in constructive and destructive interferences. The resulting pattern of interference fringes is recorded by a charge-coupled device camera. The analysis of a series of interferograms captured during the vertical translation of the system enables to determine the surface height at each pixel, i.e. a roughness profile of the surface. The mechanical profilometer is a contact method using a stylus in diamond. Its vertical position is recorded as it is moved horizontally. Advantages of the mechanical profiling are that it is independent of optical properties of the sample material and the machine is cheaper than the optical machine. However it is much slower, one measurement takes 40 min against 40 s with an optical profilometer. Obviously, the mechanical method can damage the surface and it cannot measure the roughness of every kind of surfaces unlike the optical method. The vertical resolution is lower than 1 nm whereas it is closer to roughly 10 nm for the mechanical technique. For more information on surface measurement techniques and roughness parameters, see Stout and Blunt.[17]

In the already mentioned related study, the most relevant parameters for differentiating the worn zones from the no-worn zones are identified as Sa, Sq, Ssk, St, Srk and Sdr.[9] Geringer et al. and Najjar et al.[9,22] help to understand the meaning of these parameters. Sa, Sq and Ssk are the amplitude parameters, St the spatial parameter, Srk the Abbott–Firestone parameter and Sdr the hybrid parameter. Ssk is the skewness that is the degree of asymmetry of a surface height distribution about a mean plane. It is interesting for wear measurement since a positive Ssk indicates the preponderance of peaks and a negative Ssk the preponderance of valleys. A peak is defined as a point

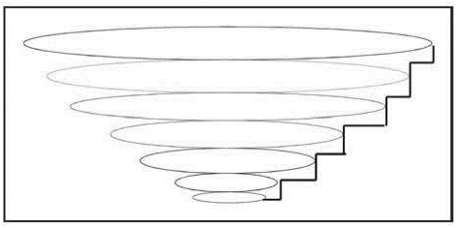

Figure 5. The volume is calculated by addition of each cylinder.

Table 2. Relative errors (%) of the worn volume for the five methods compared to Pro/Engineer®'s results.

Explants	Method 1a	Method 3	Method 1b	Method 1c	Method 2
I2	**0.09**	**0.61**			0.96
I3	**0.18**	**0.67**	0.99	14.88	1.14
I5	**0.64**	**0.85**			5.68
I6					
I7	**0.20**	**0.71**	0.61	0.50	14.61
I4	**0.10**	**0.57**	2.68	1.53	0.34
I8	**0.09**	**0.45**	0.61	0.86	
I1	**0.18**	**0.61**	0.62	1.84	2.10
T4	**0.14**	**0.68**	0.72	1.00	
T3	**0.14**	**0.49**	0.69	0.86	
T2	**0.09**	**0.68**	0.75	0.65	0.85
T1	**0.24**	**0.58**	0.71	0.05	

Bold characters are related to the smallest errors; I6 was not palpated by CMM.
CMM: coordinate measuring machine.

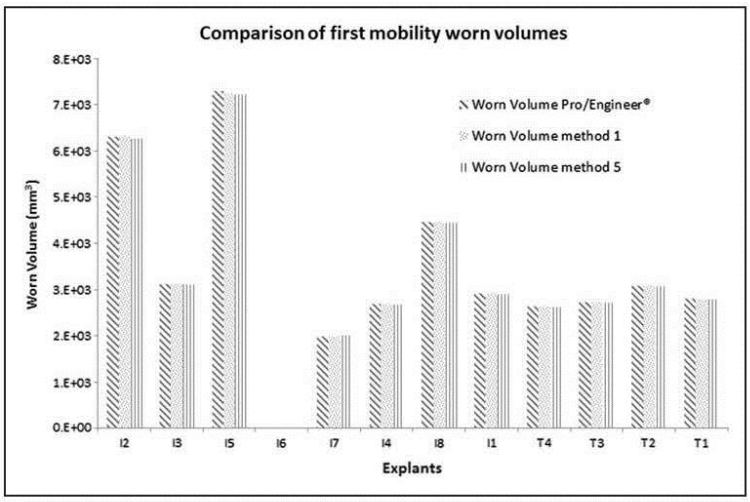

Figure 6. Comparison of first mobility palpated volumes for Pro/Engineer® and the two methods selected.

above its eight nearest neighbours and a valley is defined as a point below its eight nearest neighbours. St is the sum of the largest peaks height and the largest valleys depth; therefore, it is more sensitive to the surface than Sa or Sq. Srk (or Sk) is the depth of the working part of the surface that is the main flat part. Sdr is the developed interfacial area ratio, it is a percentage defining the additional surface area due to the texture compared to the plane surface of the same size. Even though the difference in Sa is small, the difference in Sdr can be large so this parameter enables to differentiate surfaces with similar mean roughness but a difference in texture as Sdr increases with the number of peaks and valleys.

Several comparisons of these parameters are performed to be able to compare the two profiling methods in the type of application carried out in the related study,[9] i.e. wear characterization of hip replacement cups. The first comparison is on the mean of every parameter in each of the three studied zones: the apex, the no-worn and the worn zones. The comparison on the apex zone is direct since there is only one value for each cup, it is not very reliable statistically speaking. It is the reason why for the other comparisons one focused on the other two zones. For them, ANOVA is first used to conclude if the mean values of a particular parameter for a series of 13 cups measured with both techniques are different or not. If there is a significant difference further tests needed to be performed and these multiple comparisons are carried out using the Bonferroni's correction.[23,24] In this method, the significance level for each pair comparison is set to α/n where n is the number of comparisons and α the significance level used for a single comparison test, usually equal to 0.05 (5%). As the null hypothesis (no difference) is rejected when the p-value is lower than the α-level, it will be rejected less often since this level is lower for each comparison. Therefore, the increase in the number of type I errors is avoided preventing saying it is significantly different when it is not. For these statistical tests, the software Origin® is used.

The second comparison is between the worn and no-worn zones for each parameter, each cup and each method to be able to say that for instance the mechanical profilometer can distinguish worn zones from no-worn zone on a particular cup for a particular parameter; the results were expected to be similar for every parameter. Again ANOVA and Bonferroni tests are performed comparing for every cup and every parameter the mean of the five measurements taken on the worn zone with the mean of the five measurements taken on the no-worn zone.

A third comparison is investigated: the cups are ranked from the highest to the lowest mean value for the mechanical method and each parameter. The aim is to see if the ranking is the same for the optical method and to draw some conclusions about wear of the cups. Other series of ANOVA tests with Bonferroni's correction are performed to know if some cups in the ranking could be considered significantly different. Thus, the mean of the five measurements taken on the same zone are compared for each parameter.

Results

Wear calculation

First of all, from CMM measurements, the two best methods are selected among the five detailed previously. Pro/Engineer® has been used a lot in the

Table 3. Results of annual wear given by Pro/Engineer® and the two Matlab®'s methods for the first mobility of series of 12 explants.

MB type	Explants	Implant survival (years)	First mobility 3D wear (mm^3/year) Pro-engineer®	First mobility range/2 (mm^3/year) Pro-engineer®	First mobility 3D wear (mm^3/year) Matlab® method 1a	First mobility range/2 (mm^3/year) Matlab® method 1a	First mobility 3D wear (mm^3/year) Matlab® method 3	First mobility range/2 (mm^3/year) Matlab® method 3
MB SS 316L	I2	11.4	22.4	2.9	22.2	4.8	21.5	4.8
	I3	10.4	41.9	1.9	93.0	2.8	93.0	2.8
	I5	9.3	132.2	3.6	135.1	6.2	138.2	6.2
	I6	9.1	No data	No data	No data	No data	No data	No data
	I7	7.3	−0.4	2.1	22.2	3.8	22.3	3.8
MB SS 316L AF	I4	10.3	0.2	1.1	19.3	2.7	19.1	2.7
	I8	6.3	10.1	4.4	11.9	6.1	11.8	6.1
MB SS 316L high brooker	I1	I2	15.2	1.7	7.0	2.4	7.1	2.4
MB Ti-6Al-4V (AF)	T4	6.2	−7.9	3.2	−8.2	4.6	−8.3	4.6
	T3	7.3	0.5	2.7	−0.3	3.9	−0.3	3.9
MB Ti-6Al-4V	T2	13.9	25.2	1.4	4.2	2.3	4.0	2.3
	T1	15.5	4.0	1.3	3.5	1.8	3.6	1.8

AF: arthrofibrosis.

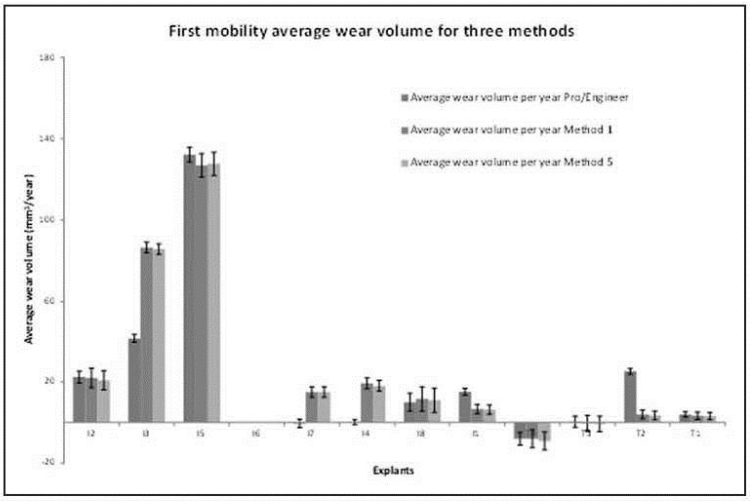

Figure 7. Comparison of the results of first mobility annual wear for the three methods.

industry and is used in the first place in Geringer et al.;[9] therefore, it is considered as the reference in this study. Consequently, all the new methods are compared to Pro/Engineer®. Therefore, the relative errors of worn volumes with the Pro/Engineer® results are compared for all the methods, they are presented in Table 2. The absolute value of the difference between the worn volumes of the method and Pro/Engineer® is divided by the palpated volume given by Pro/Engineer® and multiplied by 100 to calculate this relative error.

The two methods with the smallest errors are methods 1a and 3. Figure 6 shows the worn volumes given by these two methods and Pro/Engineer®.

There are not significant differences, confirmed by ANOVA ($p > 0.05$), between them which enabled to validate these two techniques for the volume calculations from scattered points given by CMM.

These two techniques are used to calculate the average annual wear the way it is described in 'Wear calculation'. The results are presented in Table 3 and Figure 7.

Table 4. Results of annual wear given by Pro/Engineer® and the two Matlab®'s methods for the second mobility of a series of 12 explants.

Characteristics	Explants	Implant survival (years)	Second mobility 3D wear (mm^3/year) Pro-engineer®	Second mobility range/2 (mm^3/year) Pro-engineer®	Second mobility 3D wear (mm^3/year) Matlab® method 1a	Second mobility range/2 (mm^3/year) Matlab® method 1a	Second mobility 3D wear (mm^3/year) Matlab® method 3	Second mobility range/2 (mm^3/year) Matlab® method 3
MB SS 316L	I2	11.4	0.1	8.3	4.3	16.6		
	I3	10.4	74.8	7.1	62.3	14.1		
	I5	9.3	44.1	17.5	27.4	17.5		
	I6	9.1	75.2	8.8	58.2	17.6	59.8	17.8
	I7	7.3	1.2	16.2	−14.6	15.7		
MB SS 316L AF	I4	10.3	24.3	4.7	7.0	9.3		
	I8	6.3						
MB SS 316L high brooker	I1	12.0	32.9	6.0	14.5	11.0		
MB Ti-6Al-4V (AF)	T4	6.2	76.2	15.1	50.2	30.1		
	T3	7.3	46.9	25.7	32.0	25.6		
MB Ti-6Al-4V	T2	13.9	15.0	5.9	12.4	11.8		
	T1	15.5	13.2	2.8	6.3	6.3	6.4	6.3

AF: arthrofibrosis.

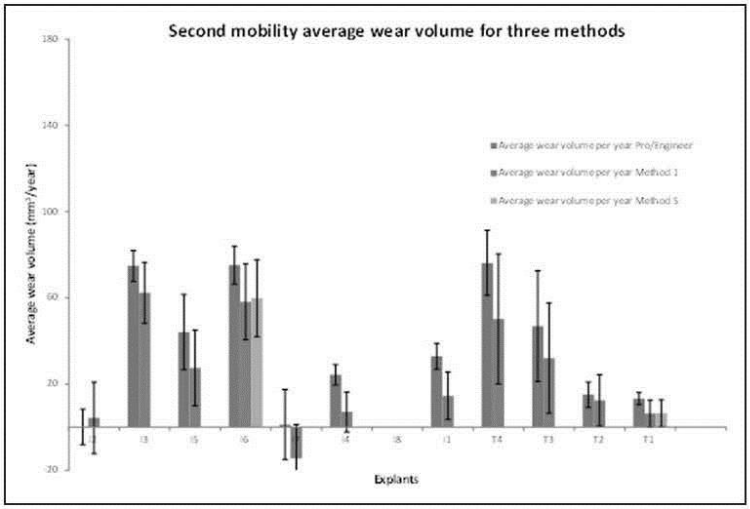

Figure 8. Comparison of the results of second mobility annual wear for two methods and few results from method 5.

First of all the results given by methods 1a and 3 are not significantly different, they could be considered as similar. Compared to the results from Pro/Engineer®, they are significantly different in five cases I3, I7, I4, I1 and T2, approximately half of samples.

About the second mobility, convex side, the method 1a is adapted to calculate the annual wear for the second mobility, the method 3 is not handy to use in that case so it is adapted only twice to confirm the results obtained from method 1a. The results are presented in Table 4 and Figure 8.

Once again the methods 1a and 3 are not significantly different. The comparison with the wear volumes from Pro/Engineer® showed a significant difference in two cases I4 and I1.

Table 5. Results of ANOVA tests ($p = 0.05$) between the worn and no-worn zones to know in what cases the two profilometers distinguish wear.

	Sa	St	Sq	Sdr	Ssk	SRk
Mechanical profilometer	I3, I5, I6	I3, I5, I6	I3, I5, I6	I3, I5, I6	None	I3, I5, I6
Optical profilometer	I3, I5	I5	None	I3, I5	None	I3, I5

ANOVA: analysis of variance.

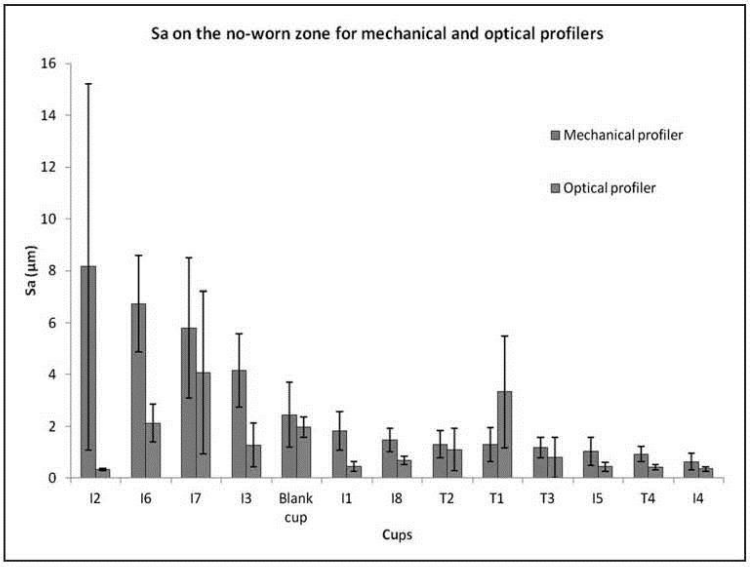

Figure 9. Sa values for every cup and both techniques on the no-worn zone ranked according to the mechanical technique.

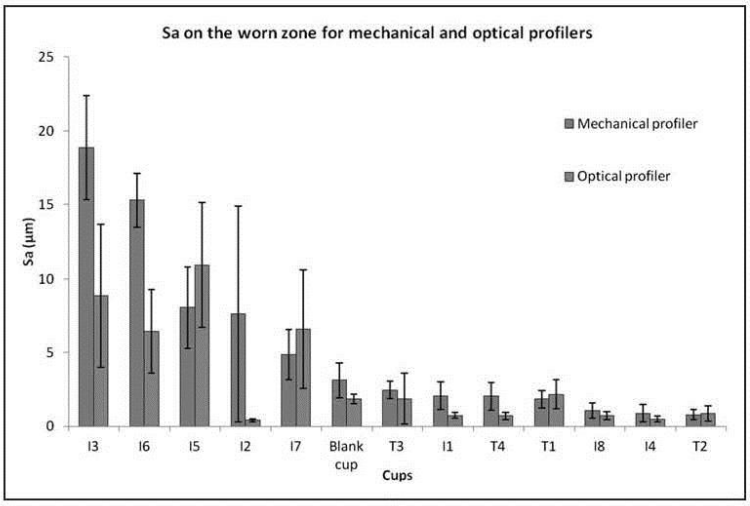

Figure 10. Sa values for every cup and both techniques on the worn zone ranked according to the mechanical technique.

Table 6. ANOVA results ($p = 0.05$) for the mechanical profilometer on the worn zone for the parameter Sa.

	Blank cup	I1	I2	I3	I4	I5	I6	I7	I8	T1	T2	T3	T4
Blank cup													
I1													
I2													
I3													
I4													
I5													
I6													
I7													
I8													
T1													
T2													
T3													
T4													

ANOVA: analysis of variance.
Yellow (pale grey) indicates no significant difference and red (dark grey) a significant difference.

Table 7. ANOVA results ($p = 0.05$) for the optical profilometer on the worn zone for the parameter Sa.

	Blank cup	I1	I2	I3	I4	I5	I6	I7	I8	T1	T2	T3	T4
Blank cup													
I1													
I2													
I3													
I4													
I5													
I6													
I7													
I8													
T1													
T2													
T3													
T4													

ANOVA: analysis of variance.
Yellow (pale grey) indicates no significant difference and red (dark grey) a significant difference.

Surface roughness measurement

ANOVA enables to compare means of two or more series of samples given their distribution is normal, their variance equal and they are independent and random. These last two requirements were fulfilled since the five measures are taken by turning the cup randomly with an approximate angle of 40° and 80° for the worn and no-worn zones, respectively. Besides the ANOVA test is known to be robust regarding the two other assumptions, all the more as the number of measures were equal for all series.

Comparison between optical and mechanical profilometers. The global comparison of the two techniques resulted in only one significant difference which is for the parameter Sdr and for the worn zone. This is the only case the statistical tests concluded the two profilometers gave significantly different results.

Worn/no-worn zone comparison. Other ANOVA tests are performed to know in what cases the mechanical and the optical profilometers are able to distinguish wear. We might think that if two techniques distinguished worn zones the explant would be considered worn. Otherwise we could not be sure wear is significant. Obviously, it is of great interest to know if a zone of an explant is worn or not. The comparison of the results from the two profilometers and the mean comparison tests can give this kind of answer. The results are presented in Table 5.

The mechanical profilometer distinguished wear for three cups I3, I5 and I6 for most parameters. The optical profilometer distinguished wear for I5

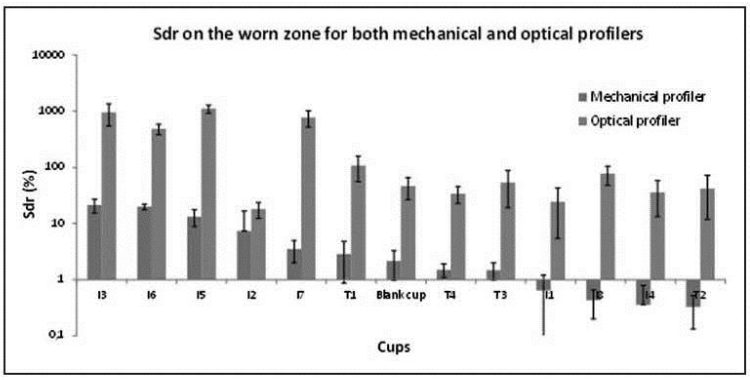

Figure 11. Sdr values for every cup and both techniques on the worn zone ranked according to the mechanical technique.

Table 8. ANOVA results ($p = 0.05$) for the mechanical profilometer on the worn zone for the parameter Sdr.

	Blank cup	I1	I2	I3	I4	I5	I6	I7	I8	T1	T2	T3	T4
Blank cup													
I1													
I2													
I3													
I4													
I5													
I6													
I7													
I8													
T1													
T2													
T3													
T4													

ANOVA: analysis of variance.
Yellow (pale grey) indicates no significant difference and red (dark grey) a significant difference.

only four times for both I3 and I5 for three parameters. The results are very similar except that the optical profilometer seemed to detect wear less often.

We saw similar results for Sa, St, Sdr and Srk and they are less interesting for the two other parameters so one decided to focus on the most relevant parameters Sa and Sdr. Indeed Sa gives general information and it is the most commonly used parameter, Sdr is the most differential parameter in the related study and, unlike Sa, it enables to differentiate a peaked surface from a plane one.

Cups comparison. The last series of ANOVA tests enabled to compare the cups one by one to see if the value of each parameter is significantly different from the others. That is performed for the mechanical and the optical measurements separately. The aim is to adjust the ranking made on the means since one did not know for sure if a cup placed after another one in the ranking is significantly different or could be considered identical. There are a total of 12 rankings but one focused on Sa (Figures 9 and 10 and Tables 6 and 7).

The ANOVA test with the Bonferroni's correction resulted in no significant difference between any of the 13 cups for the optical profilometer. So it could be concluded that no ranking could be established for the optical technique which made the comparison of techniques impossible. However, it is worth noticing that none cup is significantly different from the blank cup for both methods which is reassuring since they are not supposed to be worn in the no-worn zone.

First, the cups ranking (from the highest Sa values to the lowest) is never exactly the same between the mechanical and the optical techniques. However, the same trends are observed. Generally, the highest values measured with the mechanical profilometer corresponded to the highest values measured with the optical one except for a few cases like I2. But the error is so high that it could be said as different

Table 9. ANOVA results ($p = 0.05$) for the optical profilometer on the worn zone for the parameter Sdr.

	Blank cup	I1	I2	I3	I4	I5	I6	I7	I8	T1	T2	T3	T4
Blank cup													
I1													
I2													
I3													
I4													
I5													
I6													
I7													
I8													
T1													
T2													
T3													
T4													

ANOVA: analysis of variance.
Yellow (pale grey) indicates no significant difference and red (dark grey) a significant difference.

Table 10. Rankings given by ANOVA for Sa and Sdr parameters and for both profilometers.

Rankings for (from the highest to the lowest)	Sa	Sdr
Mechanical profilometer	• I3, I6 • I5, I7 • The others (not different from I7 but different from I5)	• I3, I6 • I5 • The others
Optical profilometer	• I5, I3, I7, I6 • T1, T2, T3, blank cup (not different from I7 and I6 but different from I3 and I5) • I1, I2, I4, I8, T4 (not different from blank cup but different from I7)	• I5, I3, I7 • I6 (different from I5 and I3 but not different from I7) • T1 (even though T1 is not different from I6 but different from I7) • The others

ANOVA: analysis of variance.

for sure. This is the reason why statistical test, One-way ANOVA test, is used; it is of interest to know with a high confidence which cups are different from the others. Then, based on these tables from the ANOVA tests it is possible to make a new ranking.

For the mechanical technique this ranking would be:

- I3, I6 // I5, I7 // the others (not different from I7 but different from I5).

For the optical technique it would be:

- I5, I3, I7, I6 // T1, T2, T3, blank cup (not different from I7 and I6 but different from I3 and I5) // I1, I2, I4, I8, T4 (not different from blank cup but different from I7).

These two rankings are quite similar.

The second parameter one focused on in that study is Sdr. It is the most significant parameter when the mechanical profilometer is used. The same conclusion as for Sa could be made for the no-worn zone. For the worn zone, Figure 11 shows the ranking of the Sdr average values according to the mechanical technique and Tables 8 and 9 present the ANOVA results about the cups comparison for each method.

The new ranking for the mechanical profilometer is as follows:

- I3, I6 // I5 // the others.

The ANOVA tests also enable to adjust the ranking for the optical profilometer, it becomes:

- I5, I3, I7 // I6 (different from I5 and I3 but not different from I7) // T1 (even though T1 is not different from I6 but different from I7) // the others.

Again profilometers look similar about the cups comparison. All the rankings are presented in Table 10.

Discussion

Wear calculation by CMM

First of all, the comparison of the relative errors showed that methods 1a and 3 are the most appropriate to calculate worn volumes since they gave the closest volumes compared to Pro/Engineer®. It appeared also that the original number of points from CMM was sufficient to get satisfying results regarding that measured zone. Besides the worn volumes from Pro/Engineer®, and methods 1a and 3 are quite similar since the largest relative errors are, respectively, 0.64% and 0.85%.

However, the average annual wear calculated with these methods gave sometimes results significantly different from the results given by Pro/Engineer®. It is thought to be due to the tolerances, the fact that one had to take them into account to calculate the theoretical volumes added an inaccuracy. Indeed, when an explant is chosen it had already been manufactured so the actual diameter could be known, the error about the tolerances had already been taken into account. A difference between the theoretical volumes is noticed which resulted from three different methods used to calculate it. It raises the question of using different methods to calculate the theoretical volume and the palpated one. However, it might be more consistent to use the same to calculate both. Therefore, a difference in the theoretical volumes added to the even slight difference in palpated volumes can entail large difference in wear volumes since the scale is much smaller for wear volumes (the maximum order of magnitude is $1000\,mm^3$ compared to about $7000\,mm^3$ for the palpated volumes), all the more as if the two differences are not in the same direction. Therefore, it is not sufficient to have the tolerances to calculate accurately the wear volume since these tolerances introduce a quite large error in the results. The ideal situation would be to know the exact volume before implantation in order to be able to calculate wear without taking into account the manufacturing tolerances but only the errors introduced by the CMM. Unfortunately it is not achievable since these measurements should be made after manufacturing and should be kept in the implant file. Blunt et al. preferred another solution. They considered the unworn zone as the reference, i.e. the implant before implantation. They reconstructed the whole unworn volume by interpolating the points measured in the unworn zone with a non-uniform rational B-splines NURB.[1] They obtained wear scar maps showing the deviations from the worn surface in good agreement with observations.

As the methods have been validated, the three results could be considered as valid, hence all of them had to be taken into account to give volumetric wear range. As a result it could be quite large, for instance for the first mobility of the explant named I3, the average annual wear is between 40.0 and $95.8\,mm^3$/year. Nevertheless, the values found are in agreement with the ones from the literature, for example $21.5 \pm 3.2\,mm^3$/Mc (Mc means million of cycles and 1 Mc corresponds to about a year of gait) for a dual mobility prosthesis in a hip simulator,[25] or $21.5\,mm^3$/Mc for a simple mobility implant under smooth conditions in a hip simulator as well-simulating normal walking.[6] Moreover, Affatato et al. compared the wear performance of UHMWPE and cross-linked polyethylene, they measured wear by a gravimetric method. Three acetabular cups of each are run in a simulator during 3 Mc and six control cups are used to correct the soak effect. They calculated a wear rate of $37\,mm^3$/Mc for UHMWPE.[26] It is worth noting that tests with hip walking simulator do not take into account the microseparation and the movement with high angles. Other studies performed explants wear analysis. For instance Hall et al. presented wear measurements of 129 explanted Charnley prosthesis comprised of a stainless steel femoral ball and an UHMWPE socket. The diameter of the head is 22.25 mm and the thickness of the socket is 10 mm. They used a shadowgraph technique to assess wear. They found a wear rate of $55(SE = 5)\,mm^3$/year.[10] It is similar to the values we found. Besides, Jasty et al. studied the volumetric wear for 128 acetabular components in polyethylene retrieved after autopsy or after revision. They used a fluid-displacement method found to be accurate to within 10%. They found values between 8 and $284\,mm^3$/year.[11]

Therefore, the results of this study are in agreement with the values in the literature even though the methods used could be very different. Some techniques are not used anymore and yet they gave similar results. Actually the results range found for a same technique even a same study is so broad that it is difficult to compare the techniques.

The fact that the results from methods 1 a and 3 are similar may mean that the approximation of a spherical segment is not too rough since method 3 did not use this approximation at all. Besides, the largest asymmetrical wear is noticed for the explant I3 and the relative errors are, respectively, 0.18% and 0.67% for methods 1a and 3. Therefore, this approximation might be considered valid even in critical cases but it would require more tests on critical cases to be sure it is always valid.

Limitation remains since the mechanical stylus of the CMM could not palpate the whole surface. Wu et al.[27] already highlighted the probe accessibility difficulty linked to its actual size. A new CMM device should be available for measuring wear volume in the concave side. Small head of the CMM and a moving plateau with fixed cup should be useful for measuring the entire wear volume on the concave total face.

There is an improvement of the CMM machine since an articulating arm is installed. It enables to

palpate a larger surface. However, for weak grooves in the material, the mechanical stylus filters the exact heights of each measured point as it could penetrate the surface a little. Indeed, such a thin tip in diamond is likely to dig into polyethylene. Therefore, the calculated wear is a minimum limit. The true wear is likely to be higher, all the more as the bottom of the insert could not be accessed by the stylus. This assessment could be confirmed by Sutcliffe.[28] Plastic behaviour of asperities could occur under stresses

Surface roughness measurement

Global technique comparison. The fact that the ANOVA test performed for each zone taking the series of 13 cups resulted in only one difference showed that the two methods, mechanical and optical profilometers, give similar results. Indeed, Sdr is the parameter the most inclined to be different since it exacerbates the errors the most. Besides, the worn zone is the most irregular so this difference could be due to the measurement locations instead of the profilometers themselves. Therefore, this only difference allowed concluding that they gave similar results in most cases.

Worn/no-worn zone comparison. First of all, one could conclude from the comparison of worn and no-worn zones: the I3 and I5 cups are worn for sure since both techniques had detected it. Then, it appeared that both techniques could distinguish wear for the same cups I3 and I5. However, the optical profilometer failed to distinguish wear for I6 but it may be due to a digging effect of the stylus from the mechanical method. Consequently, the roughness detected was likely to be a bit exaggerated and it might have considered that there was slight wear whereas the optical profilometer did not detect this error. Or, it could come from the optical profilometer that could see the holes but could not detect them if the slope of patterns was too high, upper than 40°. Therefore, in that particular case the mechanical profilometer, initially thought as less accurate due to the mechanical stylus; it should not be neglected for profilometry analyses related to wear.

The two cups for which both techniques distinguished wear had the stainless steel metal-back. It is not surprising not to detect wear for the cups with the Ti-6Al-4V metal-back since it just slightly rubbed, wear did not occur like the others. Moreover, there are four cases of fibrosis (I4, I8, T3 and T4) the hip mobility was highly limited which explained wear is not detected.[9] The remaining cases which are thought to wear normally and yet the profilometers did not distinguish it are I1 and I2. However, I2 is suspected to have an intermediary state of fibrosis and I1 worn only slightly, as observed in Table 3 compared to the other explants with a stainless steel, 316L, metal-back. Consequently, the results were in agreement with the explants characteristics.

Cups comparison. The ranking and the cups comparison for Sa and Sdr parameters showed that for the no-worn zone the ranking given by both techniques could be the same since there is no significant difference between any of the values measured by the optical technique. Besides, the zone called no-worn zone seemed to be indeed no-worn since the 12 results given by both techniques are not significantly different from the blank cup.

Several conclusions could be made for Sa in the worn zone. First, the cups different from the blank cup are the cups for which the corresponding method is said to distinguish wear. The rankings of the cups according to their Sa values after ANOVA tests for both techniques are very similar so again both techniques could be seen as equivalent. Besides I3, I5, I6 and I7 are on the left of the blank cup in the ordered ranking, thus they must be more striated than the blank cup which would correspond to a wear domain after polishing, i.e. after about 9 years of implantation. Indeed I3, I5 and I6 had a survival time equal or higher than 9 years. Note that it is different for I7 since it is not significantly different from I3, I5 and I6 but not different from the blank cup neither. Hence its roughness must be lower, so must be its survival time. The others are more polished than the blank cup, which corresponded to a wear domain between 0 and 9 years. Other authors noticed a well-polished zone on worn implants.[11] It is the case except for I2, I4, T1 and T2. However T4 had fibrosis, I2 is suspected to have it too and the metal-backs in Ti-6Al-4V follow a particular wear process. Ssk is said to be a parameter of interest for describing the wear process since we know if there are more valleys or more peaks. However, the ANOVA tests highlighted the fact Ssk is not able to detect significant difference between the worn and no-worn zones or between the cups. It could be concluded that due to the too high uncertainty errors Ssk cannot allowed to draw any conclusion about the methods comparison or the wear mechanisms in this case.

The Sdr parameter is interesting for a comparison purpose since it exacerbated the differences. At first, the results given by the mechanical and the optical methods seemed very different. It is possible to explain the general tendency that the mechanical results are lower than the optical ones. Indeed the stylus used in the mechanical machine is thought to squash the surface; moreover, the asperities could be unseen and the developed area is smaller than reality.

As expected, the results are similar to the ones from the Sa analysis. In the worn zone, the cups for which the methods distinguished wear are significantly different from the blank cup so it is relevant. Again the rankings are very similar and allowed to separate the cups between the most altered (I3, I5 and I6) and the cups more polished than the blank cup since the developed area is equal or lower. The optical profilometer seemed to differ from the mechanical one for I6 and I7; it described I6 as less worn and I7 as more

worn. It is confirmed by the fact that the mechanical profilometer gave a higher Ssk value for I6 (0.67 against 0.02). The Ssk value for the I7 cup on the worn zone is more similar (0.28 and 0.20) so one could not be sure about the location of I7 in the wear process.

Therefore, generally for the cups thought to have worn normally (i.e. without fibrosis and with a stainless steel metal-back) the roughness parameters seemed to indicate an abrasive process which is in agreement with the literature. Indeed, Jasty et al. observed some highly polished area in the worn zone separated from the less worn zone by a ridge and some multidirectional scratching.

They concluded to abrasive and adhesive wears. However, they did not separate wear mechanisms of explants according to the implantation time ranging from 1 to 21 years.[11]

Some differences remained between both techniques but they could be explained by the fact that the mechanical method is a contact method unlike the optical one. Besides, the samples could have been deteriorated a little since the mechanical measurements. It cannot be due to the sampling that is good enough in this analysis. The optical profilometer took more points since it had a better resolution which would make it the best method. However, it is limited by the slope inclination of the holes and by the fact that the UHMWPE material absorbed a little which altered the reflection. Therefore, first of all, it can be concluded that one method is not always better than the other but one must choose the more adapted to its issue. Second, both techniques are proved to give similar results in this kind of explants analysis. Finally, in this type of analysis the mechanical profilometer was not less accurate than the optical profilometer, it is of great interest to use the results from both and the ANOVA tests to draw conclusions about the explants wear.

Some limitations can be evoked. First, the measures are not made at the exact same locations and we are not assured to avoid a very particular zone with a very different roughness affecting the results. However, performing five measures all around the cup is a mean to avoid this kind of problem. Another limitation is the fact that the surface roughness measurements are not carried out on the inner surface. Therefore, we could not draw conclusion for the techniques comparison in the particular case of dual mobility but we had to be more general. Nevertheless, this limitation came from the setup not adapted to the inner measurements. Therefore, further measurements will have to be performed using another setup to complete the study.

Conclusion

Wear analysis is crucial in numbers of applications such as the orthopedic implants field. Indeed wear is a major cause for implants failure, so the wear process must be studied to increase the prostheses longevity. The right instrument to use depends a lot on the applications. The purpose of this article is to compare some methods in the particular application of Metal-on-Polymer (MoP-polymer is UHMWPE) dedicated to dual mobility explants analysis. Indeed, they are likely to differ from simple mobility implants in the wear performance.

It could be concluded from this study that CMM together with a software like Pro/Engineer® or Matlab® can be used to calculate wear. Depending on the software used, the range would be different but in agreement with the order of magnitude found in other studies. Besides, if several softwares are used the range was broader but it was also closer to reality. The relevant point was ranking wear of dual mobility cups thank to wear volumes from CMM data. CMM has already been proven to be efficient for wear analysis, our study proved that this efficiency does not depend on the post-treatment since using two different techniques gave similar results. It is already said in other studies that CMM could be adapted for the explants wear analysis; this study makes the same conclusion in the particular case of dual mobility. It is of interest to confirm it is applicable to that particular type of implants since they are used more and more. Besides, it is not deducible from the studies on simple mobility since in the case of dual mobility there are inner and outer surfaces of UHMWPE that wear. Moreover, it is seen that the results are in the same range as in the literature for dual or simple mobility. Consequently, with present designs the benefits of less dislocation seem not to be counterbalanced by a higher wear which is encouraging for further development of this dual mobility concept. Nevertheless, the volumetric wear ranges are so broad that it is difficult to conclude to a similar wear for sure.

Moreover in addition to quantitative information, qualitative information can be obtained from profiling techniques. Basically there are contact and non-contact techniques but the most suitable method depends on the application. In the application mentioned in that paper it has been seen that the mechanical profilometer should not be neglected as it did not give less accurate results. Even though the accuracy of z-axis measurements is better for the non-contact profilometer, i.e. optical, the mechanical one allows providing better measurements especially in the worn zones. Besides, it seems that the same abrasive mechanisms than for simple mobility are involved. Nevertheless, further studies will have to be performed on the inner surface to be sure it is the same for both friction surfaces even if the surface area is different. It suggests that development of new design can pursue the same goals as for simple mobility. Moreover, the same analysis should be investigated for testing in vitro, first, and in vivo, second, of new material as cross-linked and/or melted UHMWPE, for example.

Methods which are presented in this study, should allow improving these new materials.

With the technological progress more and more advanced techniques have been developed, they enable to give more accurate results on a smaller scale because of a better resolution. One might suggest the AFM investigations could be relevant for qualitative analyses. The key issue seems to be the simultaneous rotating plate that is supporting the cup. For optical and mechanical profilometers or AFM, it should be a good way of development.

These new techniques should be used in the particular application of explants analysis to see if they enable to get more information about the wear mechanisms. The final aim is to measure the wear volume of UHMWPE cup as close as possible to the actual value. Thus the study of new materials, cross-linked and/or remelting UHMWPE, for decreasing wear should be relevant for better lifetime of hip prosthesis, especially the couple MoP.

Funding

This work was supported by the Région Rhône-Alpes-France, Explora-Pro grant, and specific research fundings from CHU St-Etienne-France.

Acknowledgements

The authors acknowledge Mr Eric Laisne for technical help about the optical profilometry.

References

1. Blunt L, Bills P, Jiang X, et al. The role of tribology and metrology in the latest development of bio-materials. *Wear* 2009; 266: 424–431.
2. Bevill SL, Bevill GR, Penmetsa JR, et al. Finite element simulation of early creep and wear in total hip arthroplasty. *J Biomech* 2005; 38: 2365–2374.
3. Teoh SH, Chan WH and Thampuran R. An elasto-plastic finite element model for polyethylene wear in total hip arthroplasty. *J Biomech* 2002; 35: 323–330.
4. Wu JSS, Hung JP, Shu CS, et al. The computer simulation of wear behavior appearing in total hip prosthesis. *Comput Meth Prog Biomed* 2003; 70: 81–91.
5. Maxian TA, Brown TD, Pedersen DR, et al. A sliding-distance-coupled finite element formulation for polyethylene wear in total hip arthroplasty. *J Biomech* 1996; 29: 687–692.
6. Bowsher JG and Shelton JC. A hip simulator study of the influence of patient activity level on the wear of crosslinked polyethylene under smooth and roughened femoral conditions. *Wear* 2001; 250: 167–179.
7. González-Mora VA, Hoffmann M, Stroosnijder R, et al. Wear tests in a hip joint simulator of different CoCrMo counterfaces on UHMWPE. *Mater Sci Eng C* 2009; 29: 153–158.
8. Affatato S, Spinelli M, Zavalloni M, et al. Tribology and total hip joint replacement: current concepts in mechanical simulation. *Med Eng Phys* 2008; 30: 1305–1317.
9. Geringer J, Boyer B and Farizon F. Understanding the Dual mobility concept for total hip arthroplasty. Investigations on a multiscale analysis. *Wear* 2011; 271: 2379–2385.
10. Hall RM, Unsworth A, Siney P, et al. Wear in retrieved Charnley acetabular sockets. *Proc Inst Mech Eng* 1996; 210: 197–207.
11. Jasty M, Goetz DD, Bradgon CR, et al. Wear of polyethylene acetabular components in total hip arthroplasty. *J Bone Joint Surg* 1997; 79-A: 349–358.
12. Morris B, Zou L, Royle M, et al. Quantifying the wear of acetabular cups using coordinate metrology. *Wear* 2011; 271: 1086–1092.
13. Tuke M, Taylor A, Roques A, et al. 3D linear and volumetric wear measurement on artificial hip joints-validation of a new methodology. *Precis Eng* 2010; 34: 777–783.
14. Kandpal HC, Mehta DS and Vaishya JS. Simple method for measurement of surface roughness using spectral interferometry. *Opt Laser Eng* 2000; 34: 139–148.
15. Dhanasekar B and Ramamoorthy B. Digital speckle interferometry for assessment of surface roughness. *Opt Laser Eng* 2008; 46: 272–280.
16. Kumar UP, Bhaduri B, Kothiyal MP, et al. Two-wavelength micro-interferometry for 3-D surface profiling. *Opt Laser Eng* 2009; 47: 223–229.
17. Stout KJ and Blunt L. Nanometers to micrometers: three-dimensional surface measurement in bio-engineering. *Surf Coat Technol* 1995; 71: 69–81.
18. Poon CY and Bhushan B. Comparison of surface roughness measurements by stylus profiler, AFM and non-contact optical profiler. *Wear* 1995; 190: 76–88.
19. Yun J-P, Chang S-P, Xie T-B, et al. A novel contact and non-contact hybrid profilometer. *Precis Eng* 2009; 33: 202–208.
20. Taguchi A, Miyoshi T, Takaya Y, et al. Optical 3D profilometer for in-process measurement of microsurface based on phase retrieval technique. *Precis Eng* 2004; 28: 152–163.
21. Badami VG, Smith ST, Raja J, et al. A portable three-dimensional stylus profile measuring instrument. *Precis Eng* 1996; 18: 147–156.
22. Najjar D, Bigerelle M, Migaud H, et al. About the relevance of roughness parameters used for characterizing worn femoral heads. *Tribol Int* 2006; 39: 1527–1537.
23. Brown AM. A new software for carrying out one-way ANOVA post hoc tests. *Comput Meth Prog Biomed* 2005; 79: 89–95.
24. Curtin F and Schulz P. Techniques and methods multiple correlations and Bonferroni's correction. *Biol Psychiatr* 1998; 44: 775–777.
25. Saikko V and Shen M. Wear comparison between a dual mobility total hip prosthesis and a typical modular design using a hip joint simulator. *Wear* 2010; 268: 617–621.
26. Affatato S, Bersaglia G, Rocchi M, et al. Wear behavior of cross-linked polyethylene assessed in vitro under severe conditions. *Biomaterials* 2005; 26: 3259–3267.
27. Wu Y, Liu S and Zhang G. Improvement of coordinate measuring machine probing accessibility. *Precis Eng* 2004; 28: 89–94.
28. Sutcliffe MPF. Surface asperity deformation in metal forming processes. *Int J Mech Sci* 1988; 30: 847–868.

'Computational Modeling of Biomechanics and Biotribology in the Musculoskeletal-Computational modeling of hip implants' Ed. Zhongmin Jin, Woodhead publishing series in Biomaterials, pp. 389-416.

Section 5 Applications of computational modeling for joint replacements

19. Computational modeling of hip implants

Introduction

This chapter considers computational modeling related to joint implants. One will specifically pay attention to hip joint. First reported scientific publications were presented in last decades of 19th century [1-3]. The most relevant was the first hemi-arthroplasty improved by J. Barton [1]. Unfortunately hip replacement problem has not been totally fixed. Nowadays curing this crippling condition should not only be regarded as a way to enhance patients' comfort and life satisfaction. This issue is a health problem. Moreover the economic impact on health policy is widespread. Due to people aging, implants, whatever the joint, are the most reliable solution for restoring mobility of patients.

During last century many new ideas busted in the field of medicine and these novelties have hugely improved the overall clinical well-being of patients [4,6]. 250,000 hip prostheses are implanted, each year, in the US, and approximately the same number in Europe per year [7]. One in every 30 Americans is walking with a hip prosthesis [8]. Therefore developing new solutions that would be more effective for younger patients as well as economic for society is more and more appealing. Thus, the problem of the hip implant is related to the aging people and the economic points. Some innovative materials and designs were launched on the market since 19th century. Unfortunately the implant 'for life' is not nowadays available. The average duration of implants after the first implantation is approximately 15 years, or 80 % of lifespan at 20 years of implantation. Increasing the lifespan of implants, all organs, is a kind of leitmotiv, involving surgeons, researchers and companies associated to implants (manufacturers, distributors, etc.). Younger, heavier, more active, and longer-lived patient population is placing higher and higher demands on the performance of bearings and on the structures. For improving the quality of materials constituting implants, three ways could be investigated:

- Manufacturing implants in collaboration with surgeons, implantation to patients and the following of lifespan allows knowing the efficiency of implants;

- From experimental investigations (hip walking simulator for instance) some research teams could suggest improving implants to surgeons and/or companies, implantation and patients survey allows feedback;
- Research investigations, joining experiments and modeling, are practiced in close collaboration with surgeons and implants companies. Thus implants were extracted by surgeons and they are delivered to research teams for analyses (wear volume, wear mechanisms, etc.) after explantation. A close collaboration between researchers-manufacturers-surgeons allows feedback and come back to the lab for getting better and better implants.

The third way should improve the design, materials, surface treatments, etc., for improving lifetime of implants and, finally, benefits for patients. Unfortunately it needs time.

This chapter is dedicated to focus on benefits of modeling investigations related to artificial hip joint. State of art, related to hip implants, is well described in [4], for instance. The history will not be detailed in this text. To be concise, nowadays, three main couples of materials are available on the market of hip implants and they were improved by time: Metal on Metal (MoM); Metal on Polymer (MoP); and Ceramic on Ceramic (CoC). The couple Ceramic on Polymer is not widely implanted and one cannot consider this one as a major couple. We are going to pay attention on 2 assemblies. The first one is MoP and the other one is CoC. After a presentation of the finite element modeling, a particular MoP assembly is suggested: the dual mobility concept. This mechanism will be described and the first modeling, according to our knowledge, will be suggested. In this case, the scale is the macroscopic one for MoP. Second the CoC couple will be investigated by the way of microscopic scale. The topic will be studying the cohesion between ceramic grains thanks to the approach of the cohesive zone. Finally outlooks of the modeling will be developed specifically to hip implants and different joints.

1- Model and methods

The Figure 1 shows hip prosthesis in the actual case. Different assemblies should be submitted to contact and/or friction issues: it should be about femoral bone- stem / neck-head / head-cup / cup-metal back, etc. This work will be dedicated to study the friction of the contact head and cup. As mentioned previously, two couples are considered: Metal

(head) on Polymer (cup) and Ceramic (head) on Ceramic (cup). Unfortunately, as usually expected, final issue on modeling is not established. However it is a very interesting way for predicting what is the mapping of stresses on the assembly head and cup.

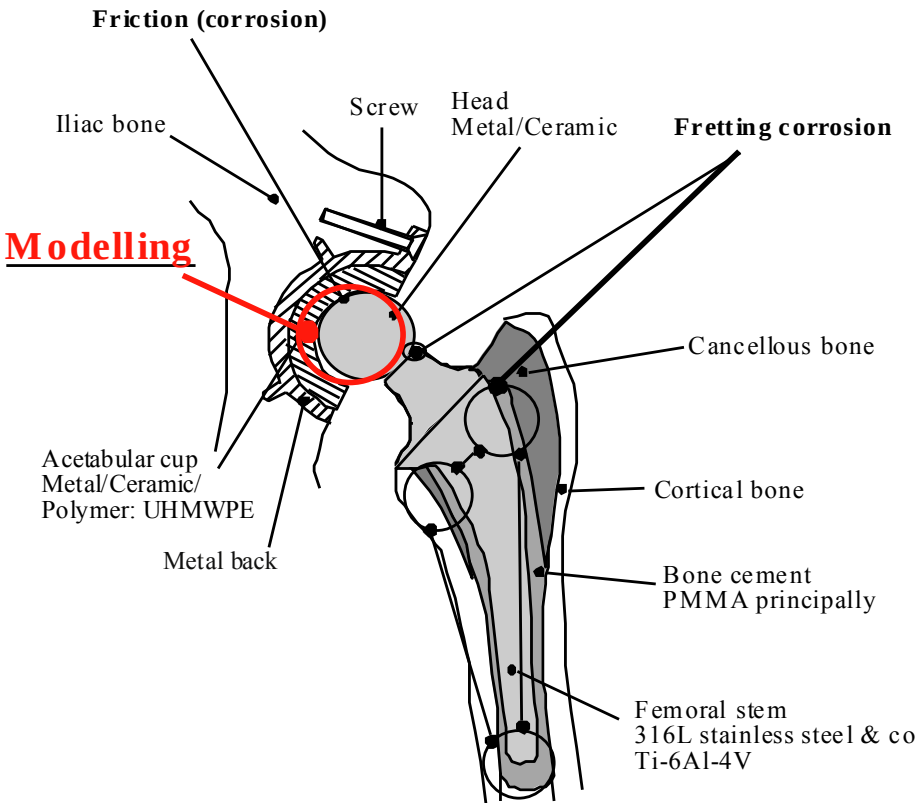

Figure 1: hip prosthesis

a. FEM software

Finite Element method (FEM), a numerical technique for finding an approximate solution to a partial differential equation, was first used for solving complex structural analysis problems in Civil and Aerospace Engineering. FEM has been developed as improved computer environments. Modern FEM packages include thermal, electromagnetic, fluid and structural working environments. In a structural simulation, FEM allows producing stiffness and strength visualization as well as minimizing weight, materials, and manufacturing costs. However, FEM is applied to an approximation of a mathematical model. In order to generate a good finite element model, experience and judgment are needed. In a typical FEM, a complex 3D model may require (so) numerous elements for obtaining accurate results. Consequently, computation time increases with increasing total number of elements. Thus, a powerful computer is needed for reducing computation time. Some research labs

have invested in calculation clusters for performing big calculations. Fortunately, computing speed of a modern computer has been greatly improved. For this reason, most engineers and scientists agree that FEM is an almost essential tool.

There are numerous commercial software packages including Abaqus®, Adina®, Ansys®, LS-Dyna®, Nastran ®, etc. Each commercial software package maintains its own advantages. For instance, Abaqus® shows strong ability in contact problems or structural problems. Thus, contact problems in hip prosthesis or other joints have been solved with Abaqus®.

A modern FE analysis consists of three distinct stages: pre-processing, processing, and post-processing. Each step will be described below:

1) Pre-processing

This is the task that should be completed before processing the analysis. The pre-processing includes the generation of model geometry, the preparation of information such as nodal coordinates, connectivity, loading and boundary conditions as well as materials. Model generation may be handled manually or done by importing the geometry built by another drawing program such as AutoCAD®. Because meshing the model is very important, it is necessary to spend much effort in complete the accurate and efficient meshing.

2) Processing

The system equations are formed using the data as described in the pre-processing stage. And the equations were solved in the processing stage. This stage usually requires huge computational resources (computing time and memory space). If some equations are not solved, pre-processing should be employed again. The loop should be under survey during the calculation time.

3) Post-processing

If the equations are solved successfully, results are presented in the post-processing stage. Usually, (even users could define what to calculate), the deformed configuration, mode shapes, temperature, stress/strain distribution are computed and displayed. Of course, useful data can be extracted directly.

These three stages are usual and common to all cases. Notwithstanding they have to be adapted to each specific case. The step of adaptation, the third one, should be analyzed with attention and it has to be validated by the modeler, especially depending on design: possible area of

discontinuities, chamfers, etc. This powerful tool will be used in this chapter for two topics: the micro modeling of ceramic material and the macroscopic modeling of UHMWPE cup against a metallic head. About both scales, finite element modeling is a key tool to investigate the wear issue. On the macroscopic scale it gives hints on the design changes that could be achieved in order to decrease wear.

b. Meshing strategies about multi scales analysis

In a typical hip replacement model, both the femoral and the acetabular parts are represented and meshed, Figure 1. Depending on what authors are interested in, the femoral part may be fully or partially included, i.e. only the femoral head or both the femoral head and stem will be considered. For instance, if one is interested in the stresses in the femoral neck, one will model this part and mesh it more finely to obtain more accurate results. Therefore meshing must be adapted to the objectives of the study. Obviously the number of elements is critical to obtain useful information. However if the elements number increases; thus the simulation takes more time. The best compromise has to be found by the modeler. Obviously the number of elements is critical to obtain useful information. However the more elements the longer the simulation takes. As a consequence, that number of elements must be optimal as a compromise between the accuracy and the computational time.

Most of the time, one determines that optimal number by performing a convergence study. It is time consuming since a lot of numbers of elements are tested while the appropriate parameters are observed. When increasing the number of elements the parameters values may change a lot at first. Then they should reach a quite constant value. The corresponding number of elements is considered optimal since fewer elements would give a less accurate result and more elements would increase the computational time considerably compared to the benefit in accuracy.

Sometimes such a thorough convergence study is not required, if the model is not complete yet for instance it would be useless to perform the convergence study at this point. However useful results are expected, therefore a simple study could be used instead, as it was done for the dual mobility implant example mentioned previously.

One may look at different number of elements for the insert and the metallic parts, then eliminating the responses considered non-physical. The number of elements may be chosen by deciding the "global seeds" in Abaqus® for instance. Obviously the notion "non-physical" should be defined precisely for each study, depending on what one is interested in. For instance if one is interested in the stresses resulting from a contact between the femoral head and the insert, one may look at the contact status of nodes, the contact area, the maximal stresses and so forth. An example of a non-

physical situation could be the fact that there are several non-contacting nodes within an area of contacting nodes. It could be all the cases different from what is expected, for instance several maxima on the insert surface whereas only one is expected at the center. Another non-physical situation is a local maximum corresponding to a stress concentration due to the finite elements. After this condition is clearly established regarding the study, one should choose a situation in the range of the physically acceptable solutions. Obviously it may not be the optimal number but the response is ensured to be physical and accurate enough in a short enough period of time.

To sum up the mesh must be adapted to the objectives of the study; there is an optimal number of elements to choose. Besides mesh refinement is possible locally to improve the accuracy without impairing the computational time too much. Finally it is worth mentioning that the scale used must be adapted to the objectives of the study as well. For example a whole implant model cannot be used to study the roughness or lubrication issues given it would require a too elevated number of elements to model properly these phenomenon. At that time studying materials, lubrication and roughness issues is not a realistic issue on FEM investigations. This aim is reachable with not refined meshing process, i.e. simple geometry. The computation efficiency (number of computer cores, quality of computer processor, etc.) increases, each year, step by step and these kinds of investigations should be probably investigated next decades.

c. Hip joint model, focus on head and cup assembly

It is known that several types of implants are used, particularly three main types: metal on polyethylene (Ultra High Molecular Weight PolyEthylene UHMWPE), MoP, and ceramic on ceramic, CoC, and metal on metal, MoM, implants. Obviously the model will be adapted to the kind of implant investigated. In this work, one will pay attention specifically to MoP and CoC couples. MoP will be focused on at first sight since they constitute the “gold standard” from Sir J. Charnley. Then the promising ceramic-on-ceramic case will be detailed.

i. Metal on Polymer

A study performed on a commercial dual mobility product, from SERF-Dedienne Santé in France, to investigate the feasibility of a design change to decrease wear and improve the implant longevity. This study will be used as an example to illustrate the modeling of MoP hip replacement. The initial spherical design was known to entail a mobility blocking due to the deformation of the insert in UHMWPE. Typically the equator thickened and the insert became thinner at the location of

applied load. Therefore we thought that an ellipsoidal shape could compensate that deformation and prevent blocking stage. The femoral stem, head and the acetabular part are metallic in MoP implants. As a consequence they are very often considered to be rigid bodies [9-13], indeed the Young's modulus of CoCr is about 210,000 MPa, that is much more than the Young's modulus of UHMWPE (about 900 MPa) [9,13,14]. Regarding the insert in UHMWPE, it can be modeled as a deformable homogeneous solid part. Consequently only this part will deform significantly, which is consistent with what happens.

The properties are adapted to the implant as well. For a MoP implant the insert might be considered elastic, i.e. only the Young's modulus E of about 900 MPa and thePoisson ratio ν of about 0.4 are taken into account [9,14].

Then the parts are put in position one regarding the other. Often an angle of 45° for all parts is used to be closer to the anatomical situation [10,14], even though it is still debatable if it has a significant influence or not . It may be advised to define a first step to make the head and the acetabular part come in contact by imposing a displacement found in a prior simulation. It is not part of the simulation but it aims at ensuring convergence since contact is a problematic situation all the more as the parts are spherical. Then a step of load application should be defined if one is interested in what happen during gait. The common load used is about 3-4 times the body weight [9, 15] given it corresponds to what is supported by the hip during walk. The ISO 14242 was established in order to reproduce the normal load during gait. One may consider that the damageable load is the maximum load and it is equal to 3000N in the UHMWPE case and between 50 and 500 MPa. It is oriented at 12° as an average direction of the load resultant in reality since it is known not to be constant [15].

The contact definition is a critical step in order to achieve convergence on one hand and to obtain consistent results on the other hand. A normal and tangential behavior could be defined. A "hard contact" and frictionless contact may be used given the joint was considered well-lubricated [14,16]. Others set a penalty friction coefficient of 0.038 to ensure a unique solution. Several authors used such a low friction coefficient [11, 14]. A surface-to-surface interaction [17] can be used with metallic surfaces as master surfaces. Then, in implicit Abaqus® model, several parameters could be adjusted to help convergence, hence a slave adjustment surface and a contact control with an automatic stabilization factor of 0.001 were added for each step except the initial step. The stabilization factor was chosen to help convergence without having a significant influence on the physics of the process, indeed it is only a numerical tool.

ii. Ceramic on Ceramic

About modeling the degradation of bio-ceramics, ceramics dedicated to implants is a challenge. Ceramics are constituted by grains; the bulk structure is at the scale of micrometers. The mechanical specimen related to the micro-structure is, in this study, a femoral head of 28 mm of diameter. Two ceramic materials are used for manufacturing elements of hip implants: pure alumina and a composite based on alumina mixed with zirconia. This study will be dedicated on the composite. It will be modeled thanks to Abaqus® software. A specific approach will be suggested in order to model the microscopic scale. The strategy is described as following. An algorithm from model generation to mechanical analysis is investigated. In the field of ceramics, some issues on the mechanical behavior are related to the grain boundaries. In order to describe the fracture behavior, a cohesive zone law was considered (time-independent). These elements are submitted to stresses and the grain boundaries are removed when their failure criterion is satisfied. Thus, under cyclic loading, cracks are produced around grains. They reproduce the fracture phenomenon by applying stresses. For example the Figure 2 shows two-dimensional finite element modeling for investigating fracture and fatigue behaviors of Al_2O_3-ZrO_2 ceramic composite at the microscopic level (i.e. ceramic grain scale). On Figure 2 the structure contains a void related to a defect of structure.

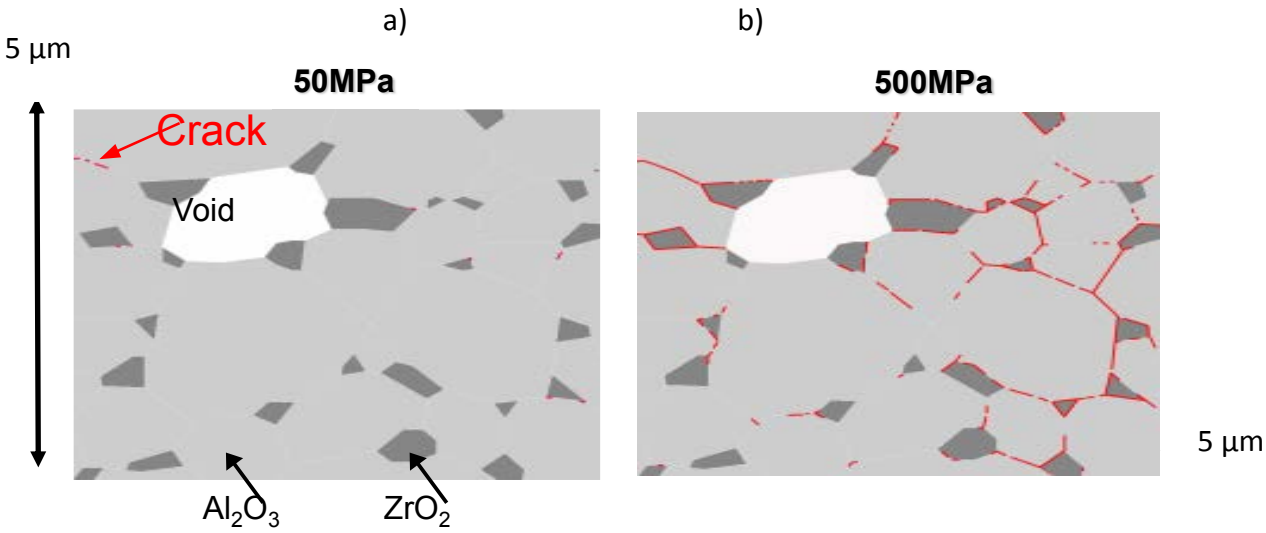

Figure 2: alumina zirconia structure with void; red line are cracks after applying normal load of a) 50 MPa and b) 500 MPa

2- Results

a. Contact mechanics on cup, MoP

i. Dual mobility concept

The concept of dual mobility was invented in 1975 by Pr. Gilles Bousquet, a French orthopaedic surgeon, and André Rambert, a French engineer. Pr. Gilles Bousquet wanted to mix the “low friction” principle of Charnley, introduced in the 60s, with the stability due to a large head used in the Mac Kee Farrar implants. Therefore they made a three-part implant. Indeed there is still a metallic acetabular cup fixed in the acetabulum like for simple mobility implant. There is a metallic head of 22.2 mm in diameter, which is the head size introduced by Charnley to decrease wear. The third part is an insert in UHMWPE between the head and the metal back. There are indeed two mobilities since the head is moving within the insert, itself moving within the metal back. With a 35 years overview it has been proved to increase stability reducing the number of dislocations particularly due to its great range of motion [18,19]. The benefit of the dual mobility implants were found for primary or revision prosthesis [20-27]. Besides, wear seems similar to what one has with a simple mobility prosthesis [28,29] even though it was thought to be higher because of two articulating surfaces. Therefore so far the dual mobility implants seem to be promising but are mostly used for old people to prevent dislocation. Even though there is not a consensus on the friction couple to use, young people are likely to have ceramic-on-ceramic prosthesis known to have almost no wear and particles release. Indeed particle release is the main drawback of the “gold standard” MoP since polyethylene particles have been proved to enhance osteolysis [30,31]. The number of particles released might be linked to the stresses applied on the polyethylene insert, consequently it is of interest to avoid stress concentration that might promote the particle release.

ii. Stresses map

It is of interest to look at the stresses on the insert surfaces (inner and outer) since it gives several types of information (on the deformation, on the location of this deformation, on the mechanics of the contact). All these enable to get a better understanding of the working principle, on the location of high stresses. Possibly one might have some insights on the wear phenomenon occurring during the implant lifetime. Particularly wear is the main issue regarding implants since it reduces their longevity and entails particle releasing, a phenomenon whose consequences are still not fully understood. The modeling from Abaqus® allows establishing the stresses map. In Abaqus® one may look at the stress called S calculated at the integration points, thus at every other points it is interpolated. One may pay attention on the meshing procedure. Indeed, results depend on the quality of the mesh, i.e. the appropriate number and the type of elements. A coarse mesh and linear tetrahedral elements C3D4 proposed by Abaqus® together with the free technique were used for the model construction. Meshing was a very important issue since all the results depended on the quality of the mesh so it was important to think of the appropriate number and type of elements. To get reliable results mesh refinement was necessary. It resulted in an insert with hexahedral (C3D8R) and wedge (C3D6) elements and the head with both hexahedral (C3D8R) and tetragonal (C3D4) elements. Therefore the stress maps are not true at every point and one should remain critical regarding thesemaps. In a dual mobility implant the two insert surfaces are investigated because they can deform a lot. As a reminder the normal load is of 2500N and the applying direction is the vertical one from up to down on the top of the metal back. First the inner surface corresponds to the contact between the insert and the femoral head. Figure 3 highlights stresses map in this inner part of the dual mobility cup, UHMWPE, in contact with the metallic head. On this figure one can see that the head seems to keep one central contact point corresponding to the maximum in S (in red) and the other circles may represent the contact occurring alternatively during motion, depending on the rotation direction of the head. The maximum stress is around 20 MPa. They are located on the top of the inner part of the cup. It is worth noting that these results are presented without any friction. As the maximum stress is lower than the one related to the yield strength of UHMWPE (around 60 MPa) normally the material is safe. However roughness of the material could exhibit some grooves (association of peaks and valleys) that involve small contact surfaces and obviously high stresses. Thus these high stresses could be the point for passing over the yield strength and they can promote wear.

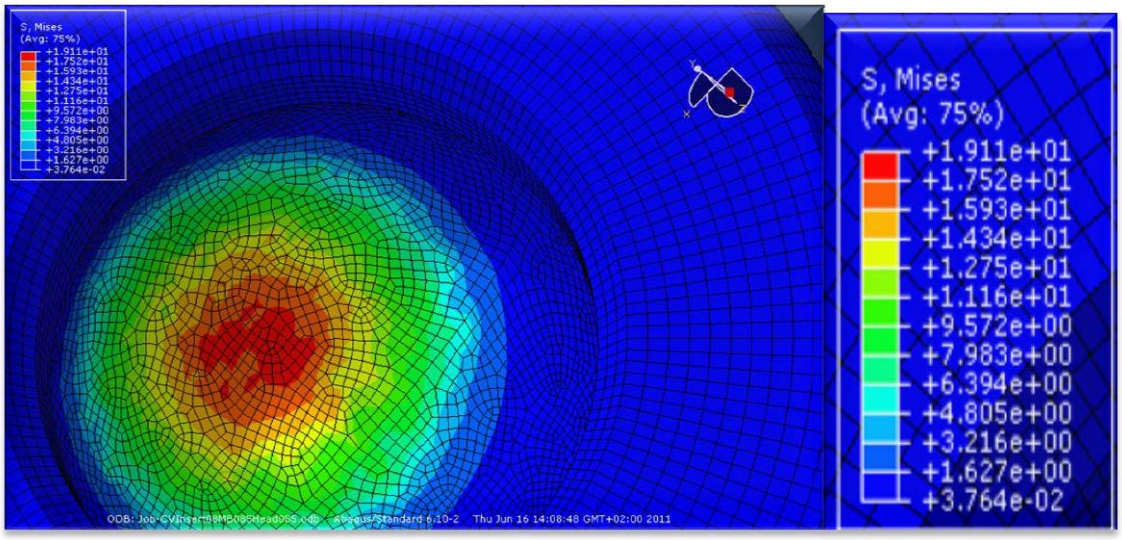

Figure 3: stresses map (von Mises stresses, MPa) inside the dual mobility cup, normal load of 2500N.

Secondly Figure 4 shows the outer surface that corresponds to the contact between the insert and the metal back. The maximum stress is 3-4 MPa. It is approximately 6-5 times lower than the one corresponding to the inner mobility. Thus one might suggest that the exterior face should be less solicited than the inner face related to the first mobility. The cross section, Figure 5, indicates the location of maximum stresses in the dual mobility cup. The meshing process allows describing zones thatare the most solicited. This statement is useful for predicting wear on the cup. One may look at the stresses in a section and see that the colors are oriented in the loading direction. As a conclusion, one can say that the stress maps, even though they are plotted by Abaqus® extrapolated the data obtained at the integration points, they might give useful information regarding the deformation and the physics of the contact. Then, this information could be used to perform the design optimization of the implant. Moreover investigations in progress will consider the influence of friction on the wear for correlating, for example, the wear track from hip walking simulator and modeling works. This point will be detailed in the third part.

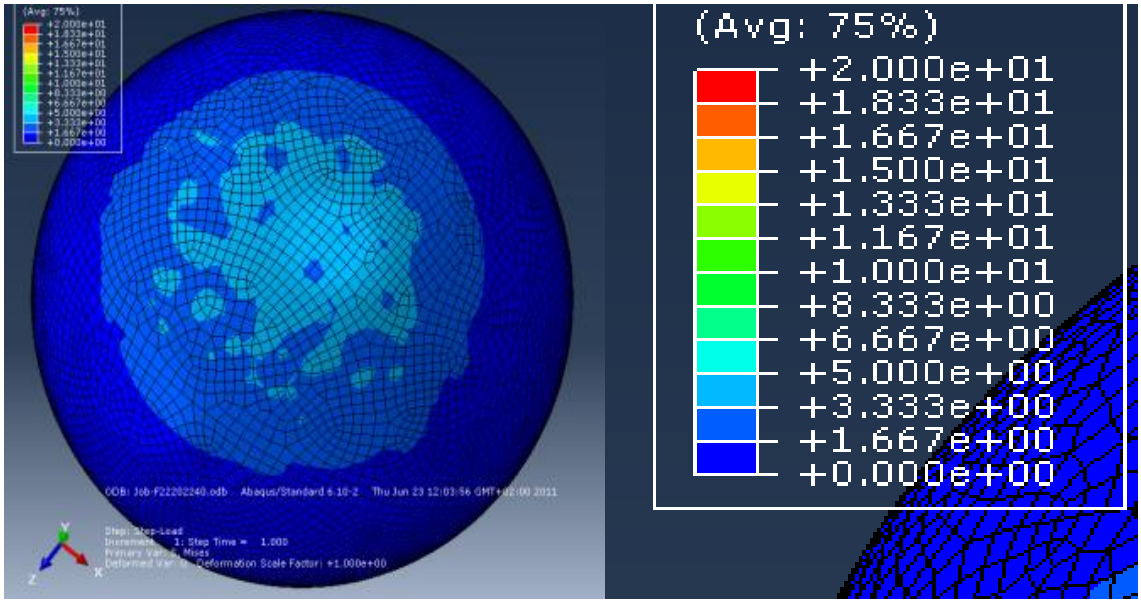

Figure 4: stresses map (von Mises stresses, MPa) outside the dual mobility cup, normal load of 3000 N.

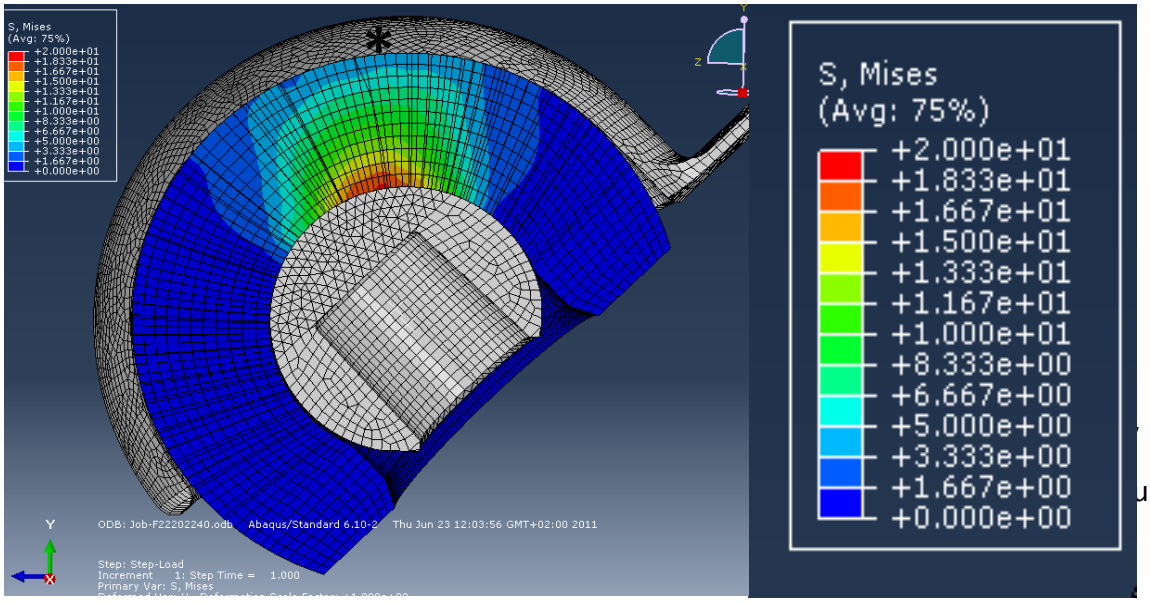

is as

ual to

b. Micro modelling thanks to FEM, CoC

i. Materials, constitution and properties

Ceramics such as alumina, zirconia, zirconia toughened alumina (ZTA) are significantly considered for hip implants. Particularly, alumina is the primary successful material in total hip prosthesis so far. Alumina (Al_2O_3) maintains advantages including good biocompatibility, high mechanical strength, great fracture resistance, and so on. However, the ceramic might have drawbacks such as the body reaction around the implants. In addition, wear debris occurred at contact surfaces leads to bone resorption, consequent inflammatory reaction and implant loosening. Bone resorption and aseptic loosening are the main causes limiting the lifetime of current implants. Alumina ceramics are available in various purities and their mechanical properties depend on the purity. In a biomedical field, high purity, greater than 99.5 percent, is used. Alumina particle size varies from a few microns to tens ones [32,33].

Zirconia (ZrO_2) has good material properties like Alumina. Zirconia maintains low corrosion, good chemical stability, good mechanical strength, etc. In addition, Young's modulus of zirconia lays in the same order of magnitude of stainless steel alloys. Thus, this ceramic has been considered as a good biomaterial.

Zirconia toughened alumina (ZTA or Al_2O_3-x % vol ZrO_2) is one of promising materials for hip implants nowadays. ZTA maintains a variety of advantages such as high mechanical properties of Yttria-stabilized zirconia, high inertness of alumina without any of their respective drawbacks, great wear resistance, high fracture toughness, high chemical inertness for long durability, etc. [34]. ZTA is made with various contents of zirconia particles (e.g. 1.5%, 3% or 10%). Mechanical properties of ZTA are various depending on the content of zirconia. Zirconia particles are placed among alumina particles. That is, some voids among alumina particles disappear and they are filled with zirconia particles. Voids in a ceramic could lead to reduction of strength and increase possibility of cracking. Table 1 shows the mechanical properties of pure alumina, zirconia and ZTA.

Table 1: Mechanical properties of ceramic biomaterials.

	Modulus of elasticity, MPa	Poisson's ratio
Alumina	374,000	0.21-0.23
Zirconia (monoclinic)[35]	92,000~244,000	0.22
Zirconia toughened alumina	360,000	0.23

Poisson's ratios of three biomaterials are similar, whereas moduli of elasticity are different. For micro-modeling; these material properties should be understood.

ii. Cohesive zone law, back ground and case study related to CoC implants

For the purpose of investigating failure behavior of ceramics, various methods including fracture mechanics, continuum damage mechanics have been considered. Particularly, a method using cohesive zone law is remarkable. The method enables interfacial fracture between physical parts, and the characterization of post yield softening with bilinear, exponential, power-law, polynomial or trapezoidal form. Moreover, a conventional cohesive zone law contains stiffness degradation when reloading is imposed. The stiffness degradation allows fatigue modeling. Total number of fatigue cycles sometimes requires long computation time and sufficient storage space in implicit analysis [36].

Originally, a cohesive zone law was proposed for interfacial fracture of concrete and cement composites [37]. Nowadays, powerful computers and better knowledge of material properties allows extension of the cohesive zone law to other areas. As a result, various applications with the development of a cohesive zone law are being introduced. Fatigue crack propagation of polymers was simulated with a cohesive failure model [38]. The classical Paris failure curve between the crack advance per cycle and the range of applied stress intensity factor was used. A cohesive zone law was developed for predicting fatigue damage of adhesively bonded joints [39]. Mixed-mode bilinear traction-separation law was considered for joints between thick sheets of 7075-T6 aluminum alloys. The sheets were bonded each other with toughened epoxy film adhesive. The failure behavior of the epoxy film adhesive was described with a cohesive zone law. Intergranular fatigue damage in

rolling contacts was described with a cohesive zone law [40]. The low-cycle fatigue life of solder joints plastically deformed was investigated with the cohesive zone law [41]. That is, a damage evolution law was expressed as a function of accumulated plastic strain accounted for gradual loss of stiffness and strength of solder materials under cyclic loading. Creep-fatigue crack growth of single crystal supper-alloys was described with a cohesive zone law [42]. Crack growth processes were described in pure fatigue regime and creep-fatigue regime. Exponential cohesive zone behavior was taken into account for energy dissipation.

These cohesive zone laws described above are implemented in finite element framework. In finite element analysis, computation time depends on total number of elements as mentioned above. Particularly, in implicit analysis, calculation time increases as the number of steps increases. Thus, a conventional cohesive zone law is sometimes ineffective for high-cycle fatigue modeling. For high-cycle fatigue modeling, some strategies including degradation process were proposed [43,44]. A cycle jump strategy was implemented for such degradation process in a finite element model. That is, fatigue damage was determined by calculating the damage variable after certain number of cycles with the quasi-static constitutive equations [43]. The extraction strategy of strain energy release rate from a cohesive zone was proposed for analyzing crack propagation under cyclic loading [44]. A fatigue damage model using Paris type crack growth laws was developed with explicit finite element codes. In the model, strain energy of interface elements was released during cyclic loading without stiffness degradation. Meanwhile, in implicit finite element analysis, a method using experimental data (S-N curves) was proposed for describing degradation [45]. The high-cycle fatigue bending of aluminum alloys was reproduced and compared with experimental results. In the method, stiffness degradation and reduction of fracture energy were used in the cycle jump strategy.

A cohesive zone law is being used for modeling of hip prosthesis. A two-dimensional finite element model was developed for interfacial fracture of alumina microstructures using a bilinear cohesive zone law [36]. Mechanical behavior of a grain boundary was described with a bilinear, time-independent cohesive zone law. The mechanical properties of grain boundaries were defined on the basis of experimental data. Table 2 shows the mechanical properties of a cohesive layer inserted between alumina grain boundaries.

Table 2: Mechanical properties of the cohesive layer for alumina

Nominal normal stress	Nominal shear stress	Displacement at failure
1000 MPa	400 MPa	0.002 µm

It is necessary to understand traction-separation response in a cohesive zone law. Figure 6 illustrates traction-separation response in a conventional bilinear cohesive zone law. Normal and shear displacements are usually considered in the cohesive law. Figure 6 b) shows cohesive behavior under pure tensile deformation. This plot is useful for understanding the relationship between normal stress and displacement during loading. Initial normal stress of a cohesive zone linearly increases on line (1) when external loads are imposed to the cohesive zone. If the stress remains below the maximum strength value (T_n^{max}), unloading leads to stress decrease on line 1 (toward the origin of the normal stress-displacement plane). If the stress reaches T_n^{max} and then decreases along line (3), unloading subsequent to damage initiation occurs linearly toward the origin of the stress-displacement plane (line (2)). Reloading subsequent to unloading also occurs along the same linear path until the softening envelope (line (3)) is reached. Once the normal displacement of an element reaches pre-described failure magnitude (δ_n^f), normal stress in the element become fully released. Cohesive behaviour in the shear direction is similar to that in the normal direction.

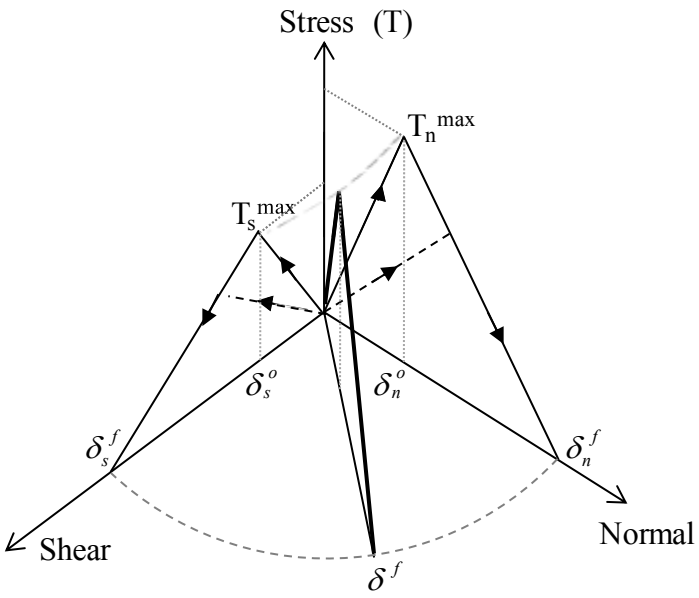

(a)

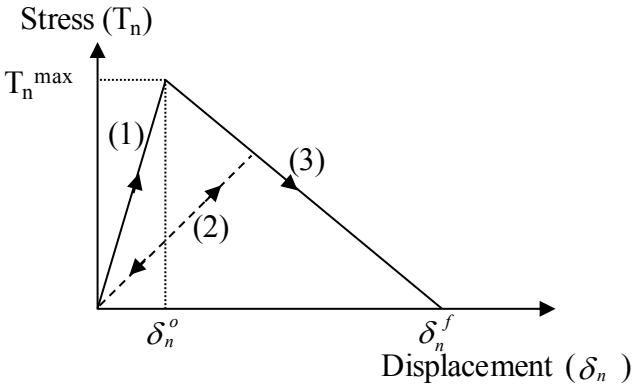

(b)

Figure 6: Conventional bilinear cohesive zone law

Ceramic microstructures used for hip prostheses are subjected to normal and shear deformation. The maximum value of a displacement in a cohesive element can be defined as:

$$\delta^{\max} = \sqrt{\left\langle \delta_n^{\max} \right\rangle^2 + \left(\delta_s^{\max}\right)^2} \tag{1}$$

where δ_n^{max} and δ_s^{max} are maximum values of normal and shear displacements attained during the loading history, respectively. The symbol $\langle\ \rangle$ denotes that a pure tensile

deformation initiates damage. In order to quantify the damage of a cohesive element [15], a damage variable (*D*) is used and defined as

$$D = \frac{\delta^f (\delta^{max} - \delta^0)}{\delta^{max} (\delta^f - \delta^0)} \tag{2}$$

where δ^f denotes the effective displacement at complete failure, and δ^0 is the effective displacement when normal stress (T_n) and shear stress (T_s) of a cohesive element satisfy the following equation.

$$\left(\frac{\langle T_n \rangle}{T_n^{max}} \right)^2 + \left(\frac{T_s}{T_s^{max}} \right)^2 = 1 \tag{3}$$

where T_n^{max} and T_s^{max} are maximum values of the nominal normal stress and the nominal shear stress, respectively.

In equation 2, if *D* of a cohesive element is equal to unity, the cohesive element is fully damaged and removed from a model. Whereas, *D* is zero, it means that the cohesive element is non-damaged.

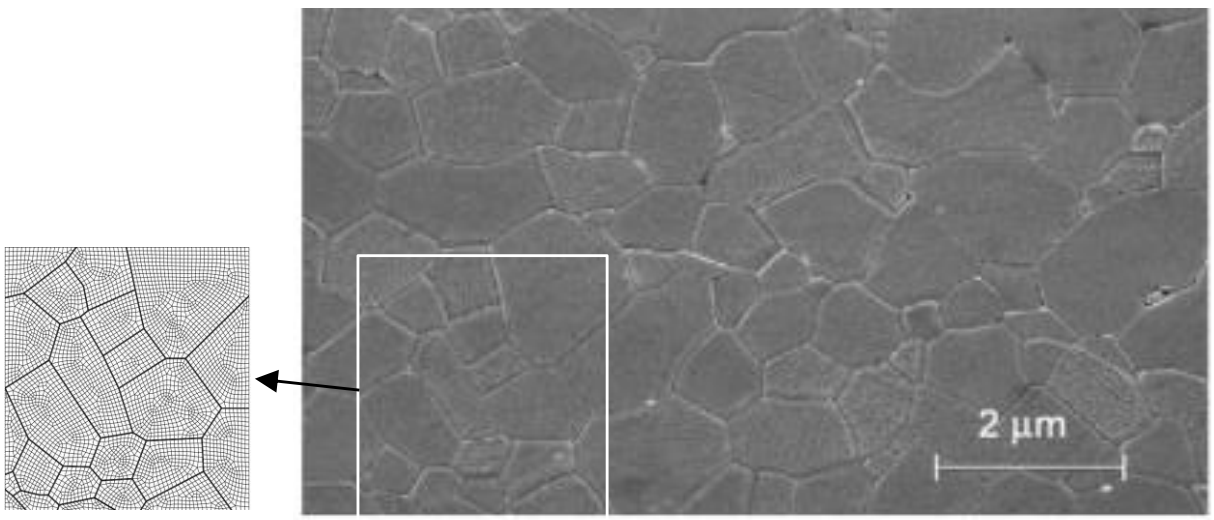

Figure 7: Al_2O_3 microstructure (right) [47] and a finite element model (left)

Figure 7 presents Al_2O_3 microstructure and a finite element model for white rectangular area. The number of grains may be increased so as to generate a bigger model. However, computation time will increase with respect to total number of grains. The FE model consists of two parts: grains and cohesive layers. In the FE model, a dark line denotes a cohesive layer and polygons are grains. Grains only behave elastically under loading. The mechanical behavior of the cohesive layer is governed by a pre-described cohesive law described above. Once the cohesive elements meet pre-described failure criterion, Figure 8, they are removed. It can be suggested that deleted elements are cracks.

In a hip prosthesis, small parts at contact surface undergo compressive and shear deformation. In the generated FE model, such deformation can be made by applying compressive and shear loads to the top of the model and by fixing the bottom surface. Triangular load wave was applied, ranging from zero to 70 MPa for normal stress (28 MPa for shear stress).

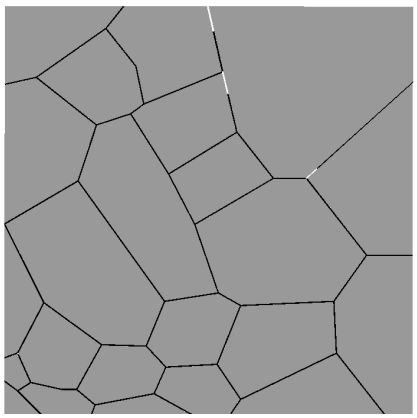

(a)

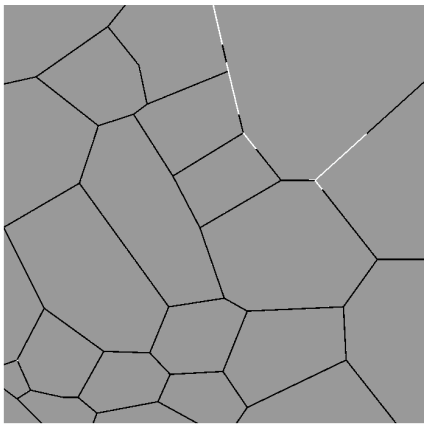

(b)

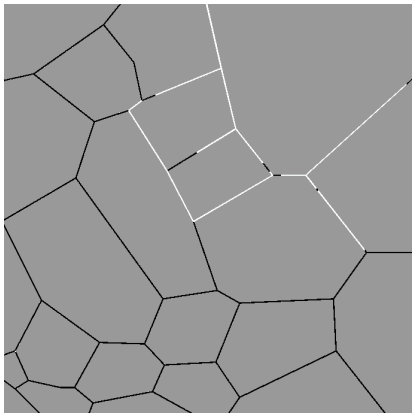

(c)

Figure 8: Crack distribution with respect to number of fatigue cycles: (a) after the first cycle, (b) after the 10^{th} cycle, and (c) after the 25^{th} cycle. Grey areas are Al_2O_3, black lines denote cohesive layers, and white ones denote cracks. Triangular load wave was applied, ranging from zero to 70 MPa for normal stress (28 MPa for shear stress).

Figure 8 shows crack distribution after various cycles. A single cycle contains loading and unloading steps. Commercial software, Abaqus® was used for simulating the model. In the plots, grey areas are Al_2O_3, black lines denote cohesive layers, and white ones denote cracks. It is apparent that three small cracks are generated after the initial cycle, and these cracks are propagated with increasing number of cycles. After the 15^{th} cycle, many cohesive elements in the upper-right side disappeared. One may consider that three grains are almost separated from a model. The plot is a good example for application of a cohesive zone law to a biomaterial. In the simulation, 15 cycles were conducted. This is not sufficient for high-cycle fatigue, since alumina in a hip prosthesis is subjected to ten thousand cycles. Cycle

jump strategies described above may be used for simulating high-cycle fatigue of alumina microstructures.

iii. Crack growth rate

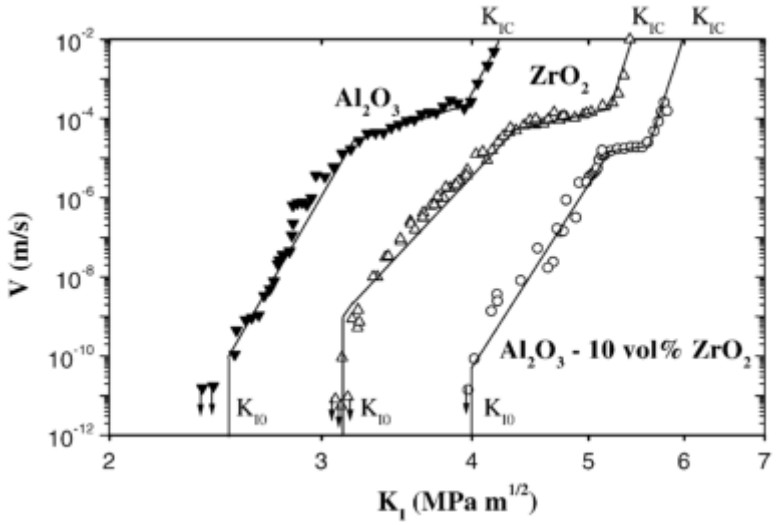

Figure 9: Relation between crack velocity (V) and stress intensity factor (K_I) for biomaterials [3]. K_{IO} denotes fracture threshold and K_{IC} is fracture toughness.

For designing a head and a cup of hip prosthesis, crack growth rate of a material should be understood. Crack growth rate is typically measured with pre-existing tensile tests. During a test, crack size and applied stress are recorded. Fig. 4 is a notable plot showing crack velocity versus stress intensity of Al_2O_3, ZrO_2, and Al_2O_3-10 % vol ZrO_2 [3]. Table 2 shows fracture toughness (KIC) of the materials. Fracture toughness of Al_2O_3-10 % vol ZrO_2 is 5.9 MPa $m^{1/2}$. That is, the magnitude is 1.4 times higher than that of Al_2O_3.

Table 3: Fracture toughness of biomaterials. MPa $m^{1/2}$

Alumina Al_2O_3	Zirconia ZrO_2	Zirconia toughened alumina Al_2O_3-10 % vol ZrO_2
4.2	5.5	5.9

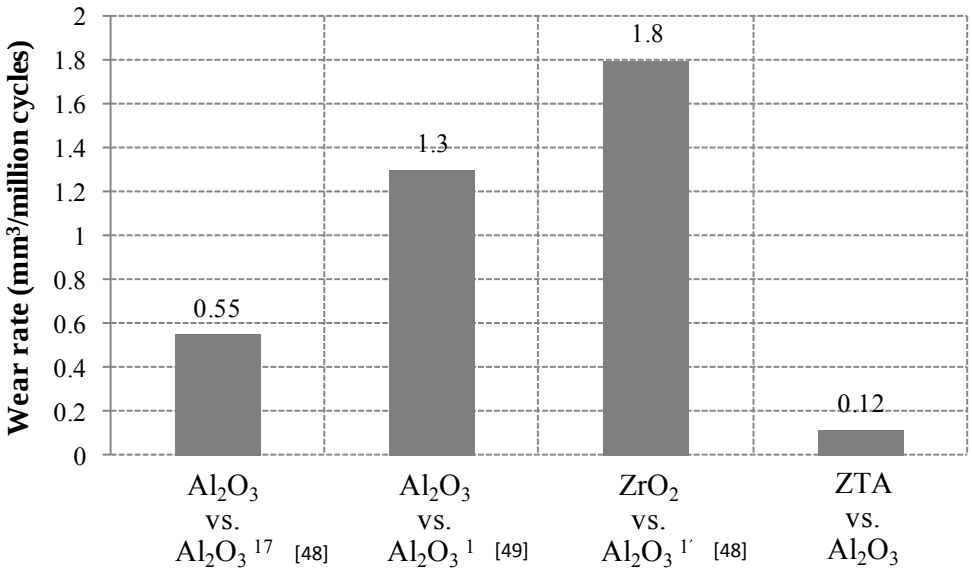

Figure 10: Wear rates of biomaterials. [48]: Steward et al., 2003, [49]: Nevelos et al., 2001.

Wear resistance is also important for selecting the material of hip prosthesis, since wear occurs between a head and a cup. Approximately every ten years, hip prostheses inserted into the human body are replaced. Thus, material showing low wear rate is critical for prolonging the durability of hip prosthesis. Figure 10 shows wear rates of biomedical materials. Wear rate varies according to experimental conditions. In the experimental condition similar to those found at hip prosthesis, wear rate is determined after interrupting a variety of wear tests at different cycles. It is identified from the plot that zirconia toughened alumina maintains lower wear rate than others. Thanks to low wear rate, Figure 10, and high fracture toughness of zirconia toughened alumina, Figure 9, ZTA is proven to be the most promising material of a head or a cup in hip prosthesis. Nevertheless, ZTA has not been practically used for the material of a head and a cup, in this study. For reminder, head was ZTA and cup was alumina. Manufacturing cost of ZTA is somewhat higher than those of pure alumina and zirconia. Specially, surface finishing of ZTA is expensive, affecting wear resistance. In order for ZTA to be practically used, the cost of surface finishing should be decreased.

3- Discussion

a. Problems of convergence

Every people which manipulates FEM software was confronted in front of problems of convergence. We are going to present some elements part of the strategy for decreasing crash modeling. Severe problems should occur during the computing time with a high number of nodes as “excessive distortion of elements”, “negative eigenvalues” or “numerical singularities”. While running Abaqus® the whole job suffers from severe discontinuities, they were due to openings and over-closures. The modeler has to understand warnings and errors and he has to improve a strategy in order to solve the problems. The contact is a no-negligible part of the work presented in this study. First of all some notions have to be applied related to the mechanical contact: convert SDI, decrease time increment, use C3D10M elements, check surface normals, use asymmetric solver, use contact controls. Surface adjustment is helpful when using contact and a complex geometry. The option “surface adjustment tolerance of zero” to remove penetration was also the one adopted for the investigation of the dry contact in the study [50]. On the Figure 5, different interfaces, principally metal back-cup and cup head, are submitted to the problem of contact. At the beginning the fact that the contact characteristics appeared at the first attempt of the first increment meant that there was already contact between the two surfaces. The strategy was then to translate the insert outwards and make a simulation to measure exactly when the contact occurred, this displacement would be used in a first step to establish the contact. It was also a common practice to add stabilization that is a non-physical damping helping for convergence. The choice of the damping factor was a tradeoff between the number of increments required for job completion (time cost) and sufficiently small ratios ALLSD (energy dissipated by viscous damping)/ALLFD (frictional energy). Indeed it was important to check that this artificial damping was negligible; it means that the damping factor has no influence on stresses mapping.

The second main source of problems was the “rigid body” definition. Indeed the job aborted with many warnings “numerical singularities” typical of rigid body motion, another warning was “zero pivots” indicating over-constrained problem. Moreover the head went through the insert without “seeing” it. It was also due to the rigid body definition. The solution was to constrain all the degrees of freedom and to import the head as deformable and then use a rigid body constraint. The boundary conditions and loads must be applied to the reference points in order to avoid the over-constraints. A contact control was added for each step to help prevent rigid body motion and enhance convergence as it is commonly suggested for contact problems instead of the stabilization in the step definition. However

one has to check it does not have an incidence on the results by checking that the energy due to this stabilization is well below the frictional energy.

A field of convergence is the optimal number of elements, i.e. the number of elements that give the most accurate results in the least time. On the hip joint, as the model was constituted of three parts and not much time was left, the study has usually to be simplified. It was decided to look at different number of elements in the spherical case for the insert and also for the metallic shell and head (the same number was taken for both), eliminate those that did not give a physical response and choose a situation in the physically acceptable range. This number would not be the real optimal number but it would give a physical response, accurate enough in a short enough time. With Abaqus®, the size of mesh, i.e. the number of elements, was defined by the "global seeds" chosen during meshing; there were 9 different "global seeds" for the insert and for each of them several "global seeds" for the pair metallic shell/head. For each simulation one looked at seven parameters thought to be appropriate for this contact analysis, the contact area ( ) at the end of the load application, the mean contact pressure (CPRESS), the mean von Mises equivalent stress (S) and their maximum on the inner and outer surfaces of the insert. It is worth noting that the von Mises equivalent stress must be measured at the integration point of the element whereas the contact pressure is measured at the nodes. Finally according to these investigations, an appropriate number of elements is each time fixed with the aim of gaining time. Furthermore after fixing this essential step, the macroscopic investigations of finite element modeling are focused on the design optimization.

b. Design effect on stresses mapping

The usual design of the cup is spherical. However some advantages should be provided by working on the cup design, i.e. an aspherical shape. This topic concerns both MoP and CoC assemblies. Meng et al. [50] paid attention on the aspherical design of Metal on Metal. Some benefits were highlighted: the lubricant film thickness increased and the hydrodynamic pressure decreases with these modifications of geometric parameters in comparison with spherical surface. Ceramic on Ceramic assembly was too investigated with a specific attention on the cup rim and chamfer design [51]. Especially the radius chamfer has a consequence on reducing the maximum tensile stress. Stresses mapping is widely studied and a case study will be suggested on the dual mobility cup. The Figure 11 illustrates a rough illustration of the modification of design related to a dual mobility cup.

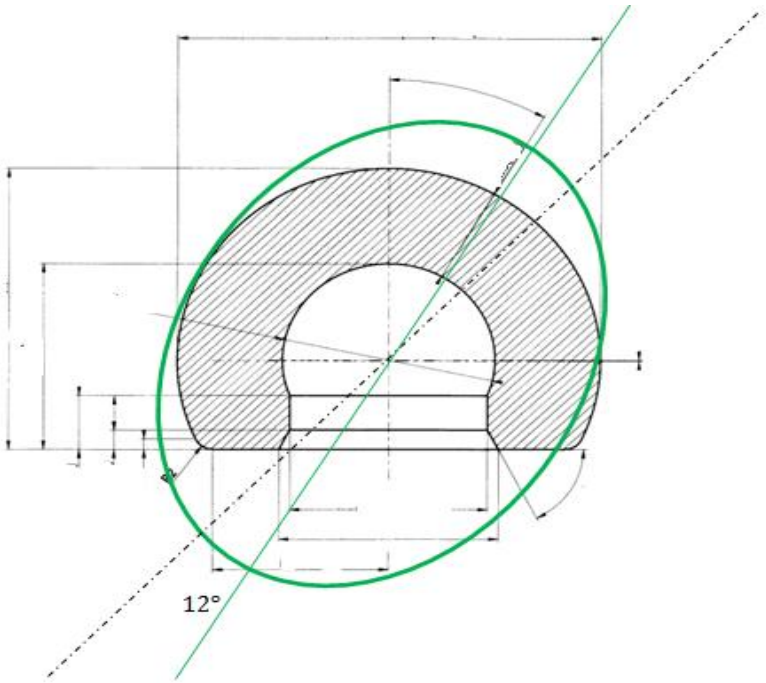

Figure 11: Sketch of the spherical insert; the ellipsoïdal shape illustrates the modification of design.

As mentioned in [51], the clearance is a key parameter, i.e. the space between the cup and the metal back. Besides by reducing the clearance, identified as a key parameter [51], at this point the contact area was increased so the maximum pressure was expected to decrease and also not to be concentrated at the center of the contact zone like it was observe for another aspherical cup [51], a more uniform pressure distribution was observed as well. Obviously without any deformation the contact area is larger for the spherical implant at equal clearance but it might be less obvious if the clearance is decreased. Anyway one might have thought that since the clearance was smaller and the insert thicker, it would deform more and the contact area after deformation would be larger. This would result in a lower contact pressure and a reduced wear. It was also of interest to avoid the blocking in the equatorial region due to the deformation of the insert. The general idea was that the insert would be compressed the most where the load was applied that was at 45°-12°=33° since it was positioned at 45° and the load was applied with an angle of 12°. At this location the insert was thicker. Hence the outer surface was made ellipsoidal where the inner surface

was kept spherical. One may cite a typical case study related to these investigations. The spherical insert had the dimensions 22.30 mm for the external diameter which induced a clearance of 0.20 mm between the cup and the metal back. For the others the minimal radius for the external ellipsoid was chosen to be 22.20, 22.25 and 22.30 mm to see the effect of increasing the clearance at the equator where the blocking happened. The major radius was 22.305, 22.32, 22.35, 22.40, 22.45, 22.457, 22.46, 22.49 mm which corresponded to a clearance of respectively 0.195, 0.18, 0.15, 0.10, 0.05, 0.043, 0.04, 0.01. Jin et al. said this clearance must be in the range 0.025mm and 0.14mm when they identified the parameters to reduce the peak contact stress in polyethylene [52]. In this chapter one might suggest an overview on 2 points: the number of elements and the effect of the excentricity (the ellipsoïdal shape of the insert, i.e. the cup). First of all, the number of elements is essential. The Table 4 highlights the influence of the number of elements on the time calculation and the values of the mechanical parameters at the inner and the outer parts. When the number of elements is multiplied by 4.5 the time is multiplied by 12. From few 1,000 to 77,000 elements, values are quite constant; the system reaches a plateau. Either the meshing refinement is so accurate and the time is so long or one should choose a compromise for the best efficiency. One can see that the mean pressure contact is around 30 MPa, in the inner part, and around 12 MPa, in the outer part. It is worth noting that no surface roughness is considered in this study. The maximum stress is clearly under the ultimate strength of pristine UHMWPE. Notwithstanding, considering the roughness should involve to get stresses beyond the ultimate strength. Consequently, UHMWPE should easily be submitted to wear. Usually the the number of elements, concerning the insert, is fixed around 15,000.

Table 4: Time consuming on the modeling and mechanical parameters extracted from Abaqus® modeling; S: von Mises stresses.

Nb elements Insert	CAREA MB/Insert final (U.A)	CPRESS ext max (MPa)	CPRESS int max (MPa)	S ext max (aver. 75%) (MPa)	S int max (aver. 75%) (MPa)	Time hh:min:sec

77,924	587	12	25	5.65	21.27	00:19:39
124,111	596	11	29	6.64	20.88 21.68	00:39:01
194,085	591	12	34	8.90	22.82 23.27	01:17:17
281,160	589	12	31	6.79	25.89	02:30:27
352,431	578	12	35	9.38	25.89	04:00:32

The effect of the excentricity is evocated in Figure 12. The mean contact pressure of the exterior side, Cpress, is represented with a maximum around 12 MPa. 22.30/22.30 is the regular sphere: the maximum contact pressure is located on the top of the cup, near the '*' mark in the Figure 5. 22.30/22.49 seems to decrease the maximum of stresses of 1-2 MPa. The benefit of the aspherical shape is minor concerning UHMWPE cup. On the contrary, the benefit on MoM seems to be proved. The aspherical shape and the clearance are relevant for decreasing the pressure and for increasing the lubricant film thickness. Unfortunately the clearance of the UHWMPE cup, the one investigated in this study, is not delivered by the manufacturer. Because UHMWPE is smooth, the repartition of stresses is not significant without taking into account the roughness. It could be an interesting perspect

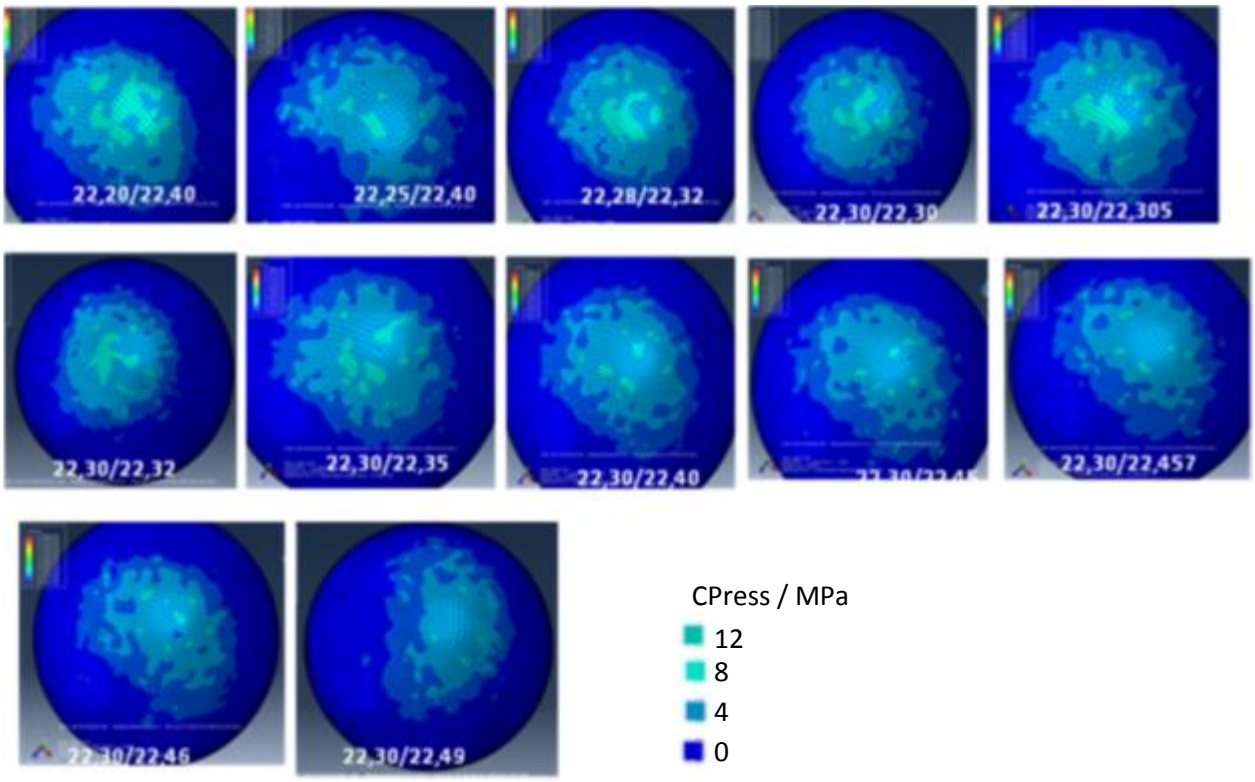

Figure 12: CPress values for all modeling related to the aspherical shape; X/Y: X is semi minor axis; Y: Y is semi-major axis.

c) Future developments

According to the results presented in this chapter, some investigations could be planned for taking into account the benefits of Finite Element modeling on lifetime of hip implants. First of all experimental results from hip walking simulator, for example, seem to be the reference results. The point is that these experimental investigations have to be as close as possible to the live conditions, i.e. the conditions of the hip implants in the patients. In vitro tests are managed, most of the time, according to ISO standards that have to be modified with feedback results and comparison with explants. Hip walking simulators are in constant evolution in order to be as close as possible to human gait. One might cite the evolution of the actual applied load during human gait. Thus analyzing the explants from in vitro tests should be useful for adjusting results from modeling. It is a kind of basic requirement for improving the modeling of prosthetic elements.

Results that are presented in this study are focused on the macro scale for UHMWPE cup and micro scale for ceramic, few microns. Obviously the link from micro scale to macro scales (ceramic) is a lack and vice versa from macro to micro scales (UHMWPE). Due to the scale difference, planning the wear behavior at the micro scale cannot be converted to the macroscopic scale. For instance, 10,000 elements are necessary at the micro scale related to ceramic, i.e. 5 x 5 μm^2. For 1 x1 cm^2, a factor of 10^8 related to the number of elements is approximate but realistic. Obviously it is impossible to manage finite element modeling with 10^{12} elements.

About the modeling process related to ceramic, one might have an idea on the wear rate, with the suggested modeling [36], at the microscopic scale. One might extrapolate to the macroscopic scale. The order of magnitude is not excessive but many hypotheses involve being far from the physical reality. Taking into account wear is a specific challenge in the finite elements modeling. Bevill et al. [53] suggested a FEM model for taking into account the creep and wear on UHMWPE. These physical phenomena have a joint effect. However the microscopic behavior of polymer cannot be part of the modeling, as suggested previously. In [53] and [54], the clearance seems to be a significant factor. One of the strategies for linking the micro to the macro scale should be the Russian dolls. This work is far to be achieved [55]. Benefits of this approach seem to be on the poroelasticity. Notwithstanding this concept might be used for joining the modeling to the micro to the macro scale.

4- Conclusion.

The modeling is frequently used for investigating the mechanical behavior of materials involved in hip prostheses. Some finite element modeling software's were launched on the market. In this work, a specific attention was paid on Abaqus®. The first part was dedicated on the ways for using as best as possible the software, i.e. for having the best efficiency and stability of the calculations at both scales (micro and macro).

Modeling composite ceramic is in progress from the micro-scale. Some part of progresses should be about linking from micro to macro. The expected benefit should be predicting the wear rate of this kind of material. A good outlook might be using the concept of Russian dolls.

Stresses mapping on UHMWPE dual mobility cups highlight the most solicited area of this typical implant, concave and convex sides of the cup. Highest stresses location are related to the most worn area. The relation seems to be complicated but the link between stresses and wear is based on the Archard's law and Bowden et al. [56,57]. Anyway stresses will be the first results and thanks to these ones wear should be predicted in a second time.

As evocated, optimization of the dual mobility showed that an aspherical shape could have benefits in terms of stresses and contact area. Benefits are not huge but the aspherical shape should help in terms of lifetime of this promising implant, the dual mobility concept. On FEM of UHMWPE cup, some investigations were achieved from parametric analyses and experiments with hip walking simulator to FEM for predicting the influence of design and dislocation [58-62].

On the CoC implant, creep is not relevant on the contrary to UHMWPE. However cup abduction angle and micro-separation are relevant for Ceramic on Ceramic hip implants [63]. From a micro-separation of 100 µm, the maximum contact pressure is approximately constant. It is worth noting that the usual micro-separation is beyond 1 mm. The link from micro to macro should allow taking into account the material characteristics (grains and the intergranular zones) and the mechanical stresses. The final aim is to improve the association materials-design and the lifetime of implants for getting more and more benefits.

References

[1] S.J.E. Matthews, V.S. Nikolaou, P.V. Giannoudis “Innovations in osteosynthesis and fracture care” Injury 39 (2008) 827-838

[2] L. Blunt, P. Bills, X. Jiang, C. Hardaker, G. Chakrabarty “The role of tribology and metrology in the latest development of bio-materials” Wear 266 (2008) 424-431

[3] M. Viceconti, S. Affatato, M. Baleani, B. Bordini, L. Cristofolini, F. Taddei “Pre-clinical validation of joint prostheses: A systematic approach” Journal of the mechanical behaviour of biomedical materials 2 (2009) 120-127

[4] P. Hernigou, A. Poignard, O. Manicom “The history of total hip arthroplasty”, Prothèse totale de hanche: Les choix J. Puget, Paris, Elsevier, 5-9

[5] S. Pramanik, A. K. Agarwal, K. N. Rai “Chronology of Total Hip Joint Replacement and Materials Development” Trends Biomater. Artif. Organs 19 (2005) 15-26

[6] J.J Callaghan, A.G. Rosenberg, H.E. Rubash “The adult hip”, Philadelphia PA, Eds Wolters Kluwer Health Lippincott Williams & Wilkins, 7-14

[7] Bozic K J, Kurtz S M, Lau E, Ong K, Vail T P, Berry D J (2009) ‘The epidemiology of revision total hip arthroplasty in the United States.’ Journal of Bone and Joint Surgery American, 91, 128-133.

[8] http://www. 600bn.com/?tag=orthopedic-implants

[9] Z.M. Jin, D. Dowson, J. Fisher, A parametric analysis of the contact stress in ultra-high molecular weight polyethylene acetabular cups, Med. Eng. Phys. 16 (1994) 398-405

[10] S.L. Bevill, G.R. Bevill, J.R. Penmetsa, A.J. Petrella, P.J. Rullkoetter, Finite element simulation of early creep and wear in total hip arthroplasty, Journal of Biomechanics 38 (2005) 2365-2374

[11] K.J. Stewart, D.R. Pedersen, J.J. Callaghan, T.D. Brown, Implementing capsule representation in a total hip dislocation finite element model, The Iowa Orthopaedic Journal 24 (2004) 1-8

[12] S.H. Teoh, W.H. Chan, R. Thampuran, An elasto-plastic finite element model for polyethylene wear in total hip arthroplasty, Journal of Biomechanics 35 (2002) 323-330

[13] C.F. Scifert, T.D. Brown, J.D. Lipman, Finite element analysis of a novel design approach to resisting total hip dislocation, Clinical Biomechanics 14 (1999) 697-703

[14] T.A. Maxian, T.D. Brown, D.R. Pedersen, J.J. Callaghan, A sliding-distance-coupled finite element formulation for polyethylene wear in total hip arthroplasty, J. Biomechanics 29 (1996) 687-692

[15] D.R. Pedersen, R.A. Brand, D.T. Davy, Pelvic muscle and acetabular contact forces during gait, Journal of Biomechanics 30 (1997) 959-965

[16] M. Mak, Z. Jin, J. Fisher, T.D. Stewart, Influence of acetabular cup rim design on the contact stress during edge loading in ceramic-on-ceramic hip prostheses, The Journal of Arthroplasty 26 (2011) 131-136

[17] Q. Meng, L. Gao, F. Liu, P. Yang, J. Fisher, Z. Jin, Contact mechanics and elastohydrodynamic lubrication in a novel metal-on-metal hip implant with an aspherical bearing surface, Journal of Biomechanics 43 (2010) 849–857

[18] O. Guyen, Q.S. Chen, J.P. Carret, F. Schultz, J. Bejui-Hugues, D.J. Berry, K.N. An, A tripolar hip implant range of motion simulation, 50th Annual Meeting of the Orthopaedic Research Society Poster 1343

[19] O. Guyen, P.P. Prabhakar, F. Schultz, J.P. Carret, J. Bejui-Hugues, D.J. Berry, K.N. An, Tripolar versus conventional total hip implants range of motion to impingement test, 51st Annual Meeting of the Orthopaedic Research Society Poster 1191

[20] F. Farizon, R. de Lavison, J.J. Azoulai, G. Bousquet, Results with a cementless alumina-coated cup with dual mobility A twelve-year follow-up study, International Orthopaedics (SICOT) 22 (1998) 219–224

[21] C. Vielpeau, B. Lebel, L. Ardouin, G. Burdin, C. Lautridou, The dual mobility socket concept: experience with 668 cases, International Orthopaedics (SICOT) (2010)

[22] R. Philippot, J-P.Camilleri, B. Boyer, P. Adam, F. Farizon, The use of a dual-articulation acetabular cup system to prevent dislocation after primary total hip arthroplasty: analysis of 384 cases at a mean follow-up of 15 years, International Orthopaedics (SICOT) 33 (2009) 927–932

[23] O. Guyen, V. Pibarot, G. Vaz, C. Chevillotte, J.-P Carret, J. Béjui-Hugues, Unconstrained tripolar implants for primary total hip arthroplasty in patients at risk for dislocation, The Journal of Arthroplasty 22 (2007) 1-10

[24] F.L. Langlais, M. Ropars, F. Gaucher, T. Musset, O. Chaix, Dual mobility cemented cups have low dislocation rates in THA revisions, Clinical Orthopaedics and Related Research 466 (2008) 389–395

[25] R. Philippot, P. Adam, M. Reckhaus, F. Delangle, F.-X.Verdot, G. Curvale, F. Farizon, Prevention of dislocation in total hip revision surgery using a dual mobility design, Orthopaedics& Traumatology: Surgery & Research 95 (2009) 407-413

[26] P. Massin, L. Besnier, Acetabular revision of total hip arthroplasty using a press-fit dual mobility cup, Orthopaedics & Traumatology: Surgery & Research 96 (2010) 9-13

[27] M. Hamadouche, D.J. Biau, D. Huten, T. Musset, F. Gaucher, The use of a cemented dual mobility socket to treat recurrent dislocation, Clinical Orthopaedics and Related research 468 (2010) 3248–3254

[28] M.H. Fessy, La double mobilité, Maîtrise Orthopédique 152 (2006)

[29] J. Geringer, B. Boyer, F. Farizon, Understanding the Dual mobility concept for total hip arthroplasty. Investigations on a multiscale analysis, Wear, 271 (2011) 2379-2385

[30] M. Stilling, Polyethylene wear analysis experimental and clinical studies in total hip replacement, Acta Orthopaedica 80 (2009) 1-74

[31] M.T. Manley, K. Sutton, Bearings of the future for total hip arthroplasty, The Journal of Arthroplasty 23 (2008) 47-50e.1

[32] International Organization for Standardization ISO) Implants for surgery – ceramic materials, EN ISO 6474-1,2010 (ISO, Geneva).

[33] Bizot P. and Sedel L. Alumina bearings in hip replacement: theoretical and practical aspects, Operative Techniques in Orthopaedics, 2001, 11(4), 263–269.

[34] De Aza A.H., Chevalier J., Fantozzi G., Schehl M. and Torrecillas R. Crack growth resistance of alumina, zirconia and zirconia toughened alumina ceramics for joint prostheses, Biomaterials, 2002, 23, 937–945.

[35] Eichler J., Eisele U. and Rodel J. Mechanical properties of monoclinic zirconia, Journal of the American Ceramic Society, 2004, 87[7], 1401–1403.

[36] Kim K., Forest B. and Geringer J. Two-dimensional finite element simulation of fracture and fatigue behaviours of alumina microstructures for hip prosthesis, Proceedings of the Institution of Mechanical Engineers, Part H: Journal of Engineering in Medicine, 2011, 225, 1158–1168.

[37] Elices M., Guinea G.V., Gomez J. and Planas J. The cohesive zone model: advantages, Limitations and challenges, Engineering Fracture Mechanics, 2002, 69, 137–163.

[38] Maiti S. and Geubelle P.H. A cohesive model for fatigue failure of polymers, Engineering Fracture Mechanics, 2005, 72, 691–708.

[39] Khoramishad H., Crocombe A.D., Katnam K.B. and Ashcroft I.A. Predicting fatigue damage in adhesively bonded joints using a cohesive zone model. International Journal of Fatigue, 2010, 32, 1146–1158.

[40] Slack T. and Sadeghi F. Cohesive zone modelling of intergranular fatigue damage in rolling contacts, Tribology International, 2011, 44, 797–804.
[41] Yang Q.D., Shim D.J. and Spearing S.M. A cohesive zone model for low cycle fatigue life prediction of solder joints, Microelectronic Engineering, 2004, 75, 85–95.
[42] Bouvard J.L., Chaboche J.L., Feyel F. and Gallerneau F. A cohesive zone model for fatigue and creep–fatigue crack growth in single crystal superalloys, International Journal of Fatigue, 2009, 31, 868–879.
[43] Turon A., Costa J., Camanho P.P. and Davila C.G. Simulation of delamination propagation in composites under high-cycle fatigue by means of cohesive-zone Models, NASA/TM-2006-214532.
[44] Harper P.W. and Hallett S.R. A fatigue degradation law for cohesive interface elements – Development and application to composite materials. International Journal of Fatigue, 2010, 32, 1774–1787.
[45] Kim K. High-cycle fatigue simulation for aluminium alloy using cohesive zone law, Proceedings of the Institution of Mechanical Engineers, Part C: Journal of Mechanical Engineering Science, 2012, doi: 10.1177/0954406212454626.
[46] Camanho P.P. and Davila C.G. Mixed-mode decohesion finite elements for the simulation of delamination in composite materials, NASA/TM-2002-211737, 2002.
[47] Guimaraes F.A.T, Silva K.L., Trombini V., Pierri J., Rodrigues J.A., Tomasi R., Pallone E.M.J.A. Correlation between microstructure and mechanical properties of Al2O3/ZrO2 nanocomposites, Ceramics International, 2009, 741–745.
[48] Stewart T.D., Tipper J.L., Insley G., Streicher R.M., Ingham E. and Fisher, J. 'Severe wear and fracture of zirconia heads against alumina inserts in hip simulator studies with microseparation', Journal of Arthroplasty, 2003, 18(6), 726–734.
[49] Nevelos J.E., Ingham E., Doyle C., Nevelos A.B. and Fisher, J. 'Wear of HIPed and non-HIPed alumina–alumina hip joints under standard and severe simulator testing conditions', Biomaterials, 2001, 22(61), 2191–2197.
[50] Meng Q., Gao L., Liu F., Yang P., Fisher J., Jin Z. Contact mechanics and elastohydrodynamic lubrication in a novel metal-on-metal hip implant with an aspherical bearing surface', Journal of Biomechanics 43 (2010) 849–857
[51] Mak M., Jin Z., Fisher J., Stewart T.D. 'Influence of acetabular cup rim design on the contact stress during edge loading in ceramic-on-ceramic hip prostheses', The Journal of Arthroplasty, 2011, 26(1), 131-136
[52] Jin Z.M., Dowson D., Fisher J. 'A parametric analysis of the contact stress in ultra-high molecular weight polyethylene acetabular cups', Med. Eng. Phys., 1994, 16 398-405
[53] Bevill S.L., Bevill G.R., Penmetsa J.R., Petrella A.J., Rullkoetter P.J. 'Finite element simulation of early creep and wear in total hip arthroplasty', Journal of Biomechanics 38 (2005) 2365-2374
[54] Teoh S.H., Chan W.H., Thampuran R. 'An elasto-plastic finite element model for polyethylene wear in total hip arthroplasty', Journal of Biomechanics 35 (2002) 323-330
[55] Gailani G., Cowin S. 'Russian doll poroelasticity; a model for fluid transport in bone tissues'. Proceedings of the fourth Biot conference in Poromechanics, 2009, Columbia University, New York. pp121 - 126.
[56] Archard J.F. 'Contact and rubbing of flat surfaces', J. Appl. Phys. 24 (1953) 981–988.
[57] Bowden F.P. Tabor D., 'Friction and Lubrication of Solids, Parts I and II', Oxford University Press, Oxford, 1954.
[58] Jin Z.M., Dowson D., Fisher J. 'A parametric analysis of the contact stress in ultra-high molecular weight polyethylene acetabular cups', Medical Engineering & Physics 16 (1994), 398-405
[59] Bigsby R.J.A, Auger D.D., Jin Z.M., Dowson D., Hardaker C.S., Fisher J. 'A comparative tribological study of the wear of composite cushion cups in a physiological hip joint simulator', Journal of Biomechanics 31 (1998), 363-369
[60] Scifert C.F., Brown T.D., Lipman J.D. 'Finite element analysis of a novel design approach to resisting total hip dislocation', Clinical Biomechanics 14 (1999) 697-703
[61] Stewart K.J., Pedersen D.R., Callaghan J.J., Brown T.D. 'Implementing capsule representation in a total hip dislocation finite element model', The Iowa Orthopaedic Journal 24 (2004) 1-8

[62] Leslie I., Williams S., Anderson J., Isaac G., Ingham E., Fisher J. 'Increased wear of hip surface replacements with high cup angle and head lateralization in vitro', Journal of Biomechanics 41 (2008) S6
[63] Sariali E., Stewart T., Jin Z., Fisher J. 'Effect of cup abduction angle and head lateral microseparation on contact stresses in ceramic-on-ceramic total hip arthroplasty', Journal of Biomechanics 45 (2012) 390-393